DESIGN AND IMPLEMENTATION OF A THERMOELECTRIC COGENERATION UNIT

SHAVEEN MAHARAJ

Student Number :20101167

A thesis submitted in fulfilment of the requirements for the
Master of Engineering Degree
in the
Faculty of Engineering and the Built Environment
Department of Electronic Engineering
Durban University of Technology

I undertake that all material presented in this thesis is my own work and has not been written for me, in whole or in part by any other person. I undertake that any quotation or paraphrase from the published or unpublished work of another person has been duly acknowledged in the work which I now present for examination.

_____

Shaveen Maharaj

Approved for Final Submission

_____

Supervisor: Dr. Poobalan Govender

Durban, 29 July 2016

ACKNOWLEDGEMENTS

Firstly, and foremost I would like to start by acknowledging my supervisor Dr. Poobalan Govender. This master's research paper is made possible through his continuous motivation, patience and enormous knowledge he has given to me in the process.

Secondly, I would like to thank the management and my previous colleagues at Illovo Sugar Eston Mill for their enormous assistance in providing their technical services, equipment and materials towards the development and testing of the co-generation unit used in this research.

Finally, and prominently I would like to thank my wife and parents who have sacrificed, supported and encouraged me throughout the progression of the master's thesis. This thesis would truly be unattainable without all of them.

.

DEDICATION

This study is dedicated to my wife and my parents, for their patience and support.

ABSTRACT

Industrial plants are excellent sources of waste heat and provide many opportunities for energy harvesting using thermo-electric principles. A thermoelectric generator (TEG) is utilized in this study for harvesting expended heat from various sources. The main challenge associated with this type of technology lies in the creation of a sufficient thermal gradient between the hot side and the cold side of the TEG device. This is necessary for the module to generate an appreciable quantity of electrical energy.

The performance of the TEG generator is tested using different configurations, different heat sources and different cooling methods. Heat sources included electrically driven devices, gas, biomass and gel fuel. Expended heat from different sites within an industrial environment was also chosen for operating the TEG device. The power produced by the generator is sufficient to operate low power LED lights, a DC radio receiver and a cellular phone charger.

TABLE OF CONTENTS

CHAPTER 4: THERMOELECTRIC MODULE CONFIGURATION

CHAPTER 5: PROTOTYPE

CHAPTER 6: ANALYSIS OF EXPERIMENTS

LIST OF FIGURES

LIST OF TABLES

NOMENCLATURE

A	Cross sectional area[m^2]
cf	Refer to
Cu	Electrical Conductor
CSP	Concentrating Solar Power
D	Distance[m]
DC	Direct current
DT	Differential Temperature[^oC]
E	Energy [J]
EMF	Electromotive Force
GHG	Green House Gas
HP	High Pressure[KPa]
HSR	Heat-sink Resistance
I	Current[A]
K_P	Thermal conductivity[WK^{-1}]
K_n	Thermal conductivity[WK^{-1}]
LP	Low Pressure[KPa]
LPG	Liquid Petroleum Gas
MCC	Motor Control Centre
MTBF	Mean Time Between Failure's
N	Number of PN junctions of the module
N-Type	Negative semiconductor material

P	Power[W]
P_{IN}	Power input
P_{OUT}	Power output
P-Type	Positive semiconductor material
PV	Photovoltaic
Q	Heat energy
Qh	Heat Energy[W]
Qc	Heat Dissipated[W]
R	Resistance[Ω]
REFIT	Renewable Energy Feed in Tariff
R_M	Total resistance of the module[Ω]
SWH	Solar Water Heat
ΔT	Differential Temperature[^oC]
Ta	Ambient Temperature[^oC]
Tc	Temperature cold side
TE	Thermoelectric
Th	Temperature hot side
TEG	Thermoelectric generator
V	Voltage[V]
VDC	Volts direct current
α_p	Seebeck Coefficient (P-Type thermoelectric leg)
α_n	Seebeck Coefficient (N-Type thermoelectric leg)
W/mK	Watts per milli Kelvin

CHAPTER 1

INTRODUCTION

1.1 BACKGROUND

The industrial revolution of the late 18th and 19th century has resulted in massive large scale industrialization of Europe and North America. This typical scenario existed till the end of World War 2. The late 1940's, 1950's and 1960's saw many countries gain independence from their colonial masters. Countries on the Asian continent such as India and China pursued mass industrialization programs as far back as the early 1950's. The stuttering economies of African nations were mainly agrarian and mining based. Growing and developing economies like those in Eastern Europe and Asia were focused mainly on developing strong manufacturing infrastructures, with the objective of large scale production. The cumulative effect of pollution from the world's economies has resulted in the depletion of the ozone layer, leading to global warming and hence climate change. Today the world is more aware of the harmful effects of pollution and various mitigating programs have been designed to reduce pollution.

South Africa is a signatory to programs that focus on reducing pollution and greenhouse gases. South Africa also follows a program making electricity available to all its peoples. However, with large scale industrialization and an increase in consumer demand for energy, the countries national electricity grid is currently struggling to meet the nation's demands for electrical energy. As at

January 2015, the country is facing an energy crisis, and several national load shedding programs are currently being implemented in an attempt to minimize the burden on the grid so as to prevent a national shutdown or 'blackout'. The country also has a program to provide more power through the construction of more power stations, with Medupi being one of them. But power stations are long term expensive capital projects, and alternatives are being sought to reduce the burden on the grid. At the national level, there is also a huge drive by government to introduce more energy sources into the nation's energy mix. Pollution free infinite resources such as solar, wind and hydro are currently being considered. The South African government has also considered the options of introducing more nuclear power stations (we currently have 1 at Koeberg) but there has generally been resistance to this idea mainly due to the dangerous nature of nuclear energy and the monetary costs of building nuclear power stations.

Growing pressure due to global warming and the advancements in environmental-friendly green technology have become subjects of urgent discussion to establish a solution to the energy crisis facing the world (Kajitani *et al.*, 2010). Technologies have been developed to generate low levels of electricity from waste heat by converting temperature differences into electrical energy (Rosi, 1968). Electrical energy can be generated from traditional sources of fuels such as wood, coal and gas. These energy sources are relatively inexpensive but emit greenhouse gases that have a negative impact on the environment.

Industrial applications emit vast quantities of thermal energy in the form of wasted heat energy. The waste heat emitted from large or small equipment is usually dissipated into the atmosphere. Given this scenario, the objective of this research is to trap unused waste heat and convert it back into electrical energy. Electrical energy generation from the waste heat can be realized with

thermoelectric devices to convert some of the waste heat into useful electricity (Kajitani *et al*., 2010). Optimizing thermoelectric technology have the benefit of reducing both operating costs as well as the environmental impact in the process (Vieira da Rosa, 2009).

Thermoelectricity is based on the basic research of thermoelectric energy conversion effects and their use for the creation of static electric energy (Anatychuk, 1975 and Anatychuk *et al*., 1986). The thermoelectric effect refers to the direct conversion of temperature differences to an electric voltage, and vice versa. Temperature differences can be exploited to generate power (Crane *et al*., 2011). A thermoelectric device creates a voltage when there is a different temperature on each side or junction of the materials.

Thermoelectric phenomena result from the diffusion of electrons and photons along a temperature gradient in electrically conducting solids (Vining, 1993). Thermo-electric power is generated by devices known as thermocouples which are made up of two dissimilar materials such as iron and constantan, and a hot and a cold junction. The ability of the thermocouple to generate a voltage when there is a temperature difference between the junctions makes it suitable for producing electricity (Anatychuk, 1979). These devices operate on the Seebeck principle which states that any temperature gradient between the hot and cold junctions will result in an output voltage. The efficiency of the thermoelectric conversion is directly proportional to the temperature difference between the hot and cold junctions (Buryak and Karpova, 1988, Fleurial, 1993, and Markowski *et al*., 2005).

1.2 RESEARCH PROBLEM

This study focuses on the application of semiconductor type thermoelectric generators (TEG) as a sustainable energy resource. These TEG modules can only function optimally if a substantial temperature gradient exists across their hot and cold junctions. To this end, an efficient and effective cooling system needs to be designed, tested and implemented for a TEG module to efficiently and robustly operate in a harsh industrial environment.

1.3 AIM OF THE RESEARCH

The objective of this research is to design a simple TEG cogeneration system to convert the expended thermal energy into useful electrical energy. The study focuses on the design and development of a cogeneration system that would utilize the principles of thermoelectrics to generate sufficient electrical energy to power a certain class of device. Different cooling systems and module configurations are to be designed and tested in this study, and a prototype TEG unit for an industrial application will be designed, developed and tested.

1.4 SCOPE OF THE RESEARCH

The scope of the study involves an investigation into alternative green energy solutions and the design and development of a thermoelectric co-generation system.

1.5 RESEARCH METHODS

The quantitative methodology will be followed during the research of the thermoelectric cogeneration system (Leedy and Ormrod, 2014). The thermoelectric phenomenon shall be tested

under various conditions. Data from the tests are measured using various standardized instruments and then objectively analyzed.

1.6 CONTRIBUTION OF THE STUDY

The research focuses on applying thermoelectric principles to recycle waste thermal energy into reusable electrical energy. The study will provide valuable information on the design and development of an industrial based thermoelectric unit driven with recycled waste thermal energy.

1.7 STRUCTURE OF THE THESIS

This document is arranged as follows:

Chapter 2 is a study on the various wasted thermal energy sources available within industry. It highlights different equipment in different applicants within a plant. Thermography is used to identify and investigate possible wasted thermal energy sources in various plant applications.

Chapter 3 describes the background principles to thermoelectric devices. It focuses on the basic theory and configuration of a modern semiconductor thermoelectric generator, as well as the different components required to assemble a simple functioning TEG unit.

Chapter 4 describes the thermoelectric module configuration and optimization, and focuses on the cooling system and module configuration of the thermoelectric unit from various tests. This chapter also investigates thermoelectric application fuels in the domestic and rural sector.

Chapter 5 describes the prototype of the thermoelectric unit for an industrial application. The prototype thermoelectric unit is tested and implemented in a live industrial application.

Chapter 6 analyses the results of the research. Future recommendations are discussed for further investigation. Chapter 7 briefly discusses the cost of a TEG unit.

CHAPTER 2

INDUSTRIAL THERMAL ENERGY SOURCES

2.1 BACKGROUND

Electrical usage within South Africa has grown considerably since the 1990's (Donev *et al.*, 2012). South Africa has great natural energy resources such as solar and wind but unfortunately advances in exploiting these resources have been rather slow. The majority of South Africa's power is produced from the vast coal supplies within the country. Eskom has 27 operational power stations in South Africa which produce 40.7 GW of power (Welty *et al.*, 2008). Given the current energy demand trends, the national grid is unable to cope with the energy demand during peak periods.

Renewable energy, along with energy efficiency, are twin pillars of an ecological energy policy. Consuming energy efficiently reduces the demand on the national grid and hence contributes towards reducing carbon emissions. Renewable energy is sourced from infinite natural resources such as sunlight, wind, tidal currents and geothermal heat. These natural resources are naturally replenished but are not always readily available. South Africa is currently experiencing an electricity deficiency. Now more than ever the country needs to exploit its abundant renewable

energy resources (Donev *et al.*, 2012). Only about 1% of this country's energy demand is supplied from renewable resources such as hydro, wind or solar (Renewable Solutions & Reduced Demand, 2013). This scenario is gradually changing as renewed attempts are being made to increase the production of clean energy.

2.2 WASTE HEAT AS A SOURCE FOR RENEWABLE ENERGY WITHIN INDUSTRY

There is an international drive towards making renewable energy sources the provider of up to 35% of the worldwide energy supply requirements, and virtually half of the electricity generated by 2050 (Destouni and Frank, 2010). Renewable energy sources are embraced within the environmentally friendly industries and they are the future, particularly where biofuels are used as combustible energy sources of fuels (Umar and Abubakar, 2014). In the sugar processing industry, it is not uncommon to find boilers being fueled by waste by-products such as bagasse. The greatest substantial pollutant emitted by bagasse-fired boilers is particulate matter which is caused by the turbulent movement of combustion gases with respect to the burning bagasse. Emissions of sulphur dioxide (SO_2) and nitrogen oxides (NOx) are much lesser than traditional fossil fuels due to the characteristically low levels of sulfur and nitrogen associated with bagasse. Figure 2.1 illustrates the usage of bagasse at the Illovo Sugar Mill as its primary source of fuel energy.

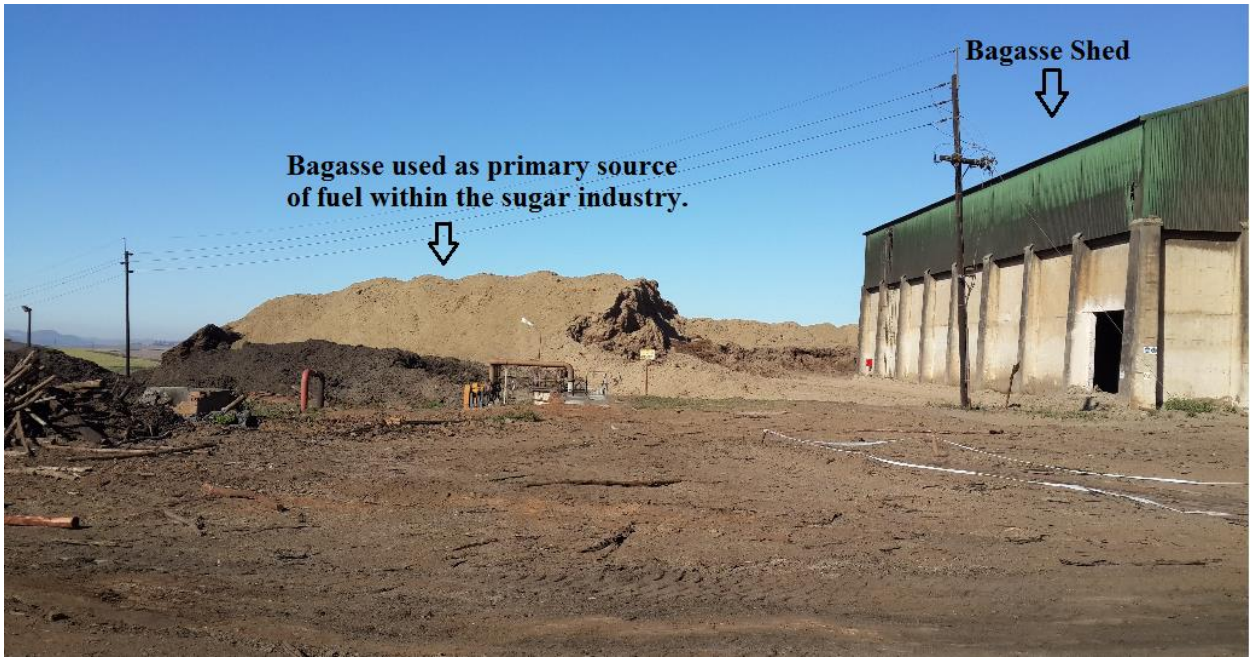

Figure 2.1. Bagasse fuel.

Industrial plants and processes that generate waste heat include the saw and sugar mills, oil refineries, smelters and furnaces and numerous other plants. These industrial plants emit hot exhaust gases, smoke and waste streams that can be utilized with proven modern technologies to generate considerable electrical energy that would otherwise be lost to the atmosphere.

2.3 OPPORTUNITIES TO RECOVER WASTED HEAT ENERGY

'Topping cycle' systems produce electricity and then recover any excess thermal energy for heating or cooling purposes. Conversely, during a 'bottoming cycle' waste heat streams from a process can be used to produce electrical energy. Combined topping and bottoming cycle systems are referred to as cogeneration systems (Conservation of Power and Water Resources, 1978). Fuel driven systems such as furnaces and boilers utilize topping and bottoming cycles to produce heat. The waste heat from a furnace or boiler can be used to generate power. The key benefit of

converting waste heat to electrical power systems is that they exploit heat from the existing thermal processes within the plant, which would otherwise be wasted and lost to the atmosphere. The waste heat would be used to produce electrical energy for use within the plant, instead of consuming additional fuel for the boiler for this function.

Waste heat to electrical power generation has a great potential within the industrial sector where large sources of energy is discharged as thermal losses directly into the atmosphere or into cooling systems (Hendricks, 2006). These thermal losses are the result of process and equipment inefficiencies, and the failure of present process systems to recapture and utilize the excess energy sources (Hendricks, 2006). The majority of this waste heat is of low quality and is available in waste sources at temperatures below 149ºC, or is dissipated as radiation heat energy losses.

The proficiency of generating electrical power from waste heat sources is dependent on the temperature of the waste heat source. The waste heat source characteristics that must be considered to determine the economic feasibility of power generation will include the waste heat source, availability, load factor, temperature, flow rates, pressure, composition and nature of contaminants. (Thekdi, 2009).

Figure 2.2. Surplus process steam vented from plant equipment.

Figure 2.2 illustrates the waste heat losses in the form of exhaust steam being vented to the atmosphere from evaporators and various process vessels. Steam ventilation occurs in Figure 2.2 to stabilize and control the vacuum pressure setpoint within a range of 60kpa to 80kpa at a temperature of 100ºC to 150ºC. This is crucial for the optimal operation of the process and safety of the workers and the plant equipment. These are a few examples of the numerous energy losses that occur on the plant during process production where steam is the key component of a manufacturing process, and waste heat is unavoidable.

Figure 2.3 and Figure 2.4 focuses on the boiler house energy losses with excessive exhaust steam being drained to the feedwater recovery system, but large portions of the steam are still vented into the atmosphere. The feedwater system in Figure 2.3 has an abundance of pipes at

Figure 2.3. Surplus process steam vented at the boiler house.

temperature between 90ºC to 100ºC that are bare and without thermal lagging (insulation), leaving them exposed to the atmosphere where heat energy is lost.

The steam drain pipes shown in Figure 2.4 emits excessive exhaust steam given off by the power house steam turbines. The drain pipe surface temperatures vary from 120ºC to 150ºC depending on the steam take off points of the turbine and the inlet and outlet steam pipes. Most of the waste heat is lost to the atmosphere, while the condensed steam within the pipe is recovered in the drain and routed to the feedwater system in Figure 2.5. Figure 2.5 shows the feedwater control valve with the pipes not completely insulated. These pipes supply the boiler water drum directly with hot water. They are partially exposed to the atmosphere and generate waste heat which is lost to the atmosphere within the boiler house.

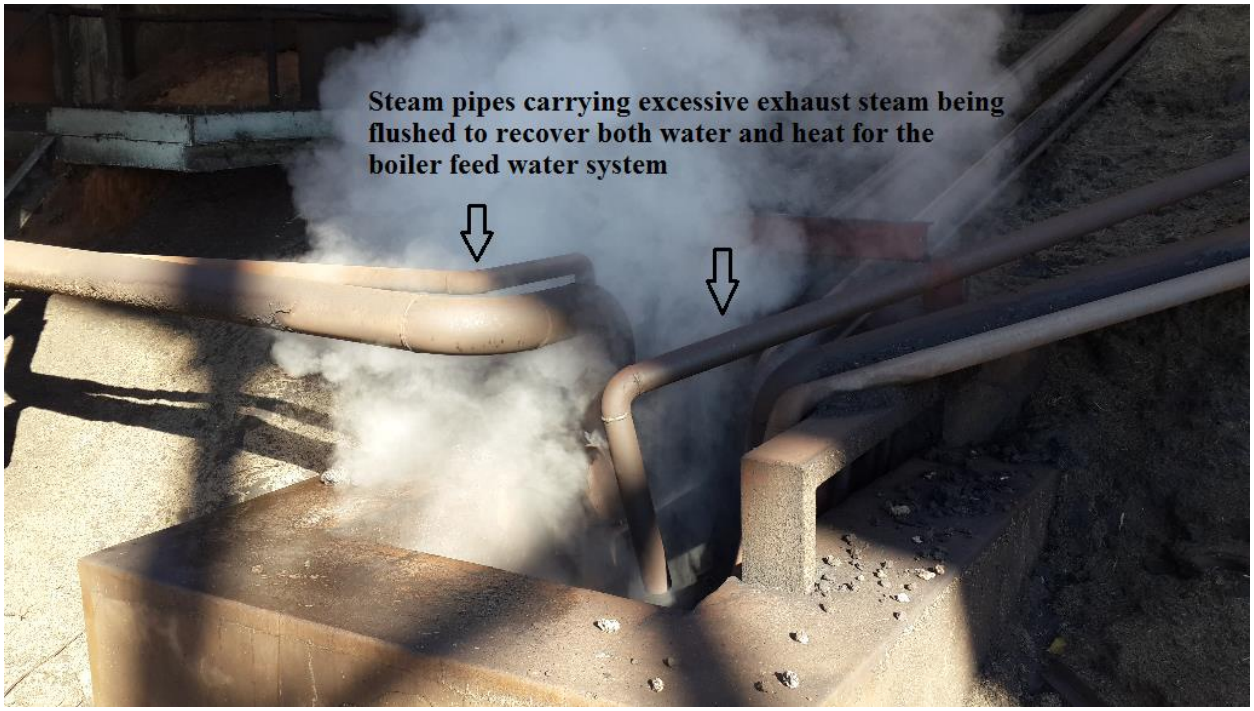

Figure 2.4. Steam drain pipes from the steam turbines.

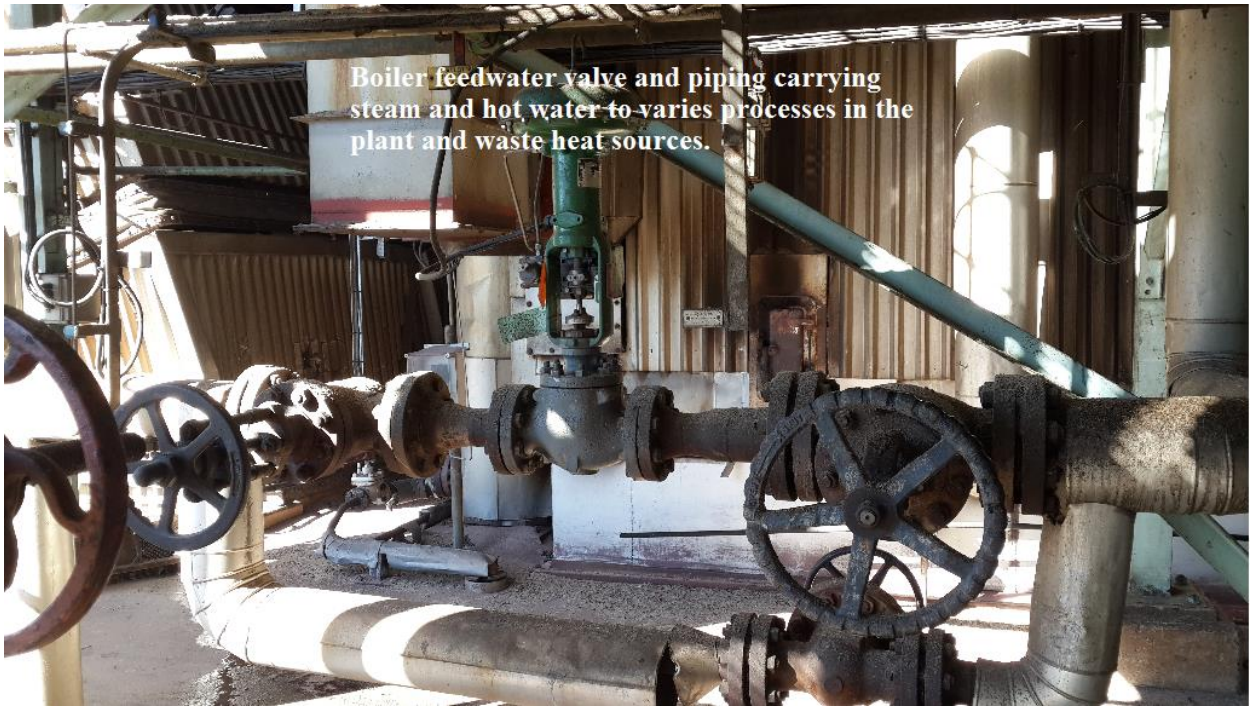

Figure 2.5. Pipes carrying steam and hot water within the boiler house.

Figure 2.6 shows two temperature indicators. The one indicator displays the temperature of the high pressure steam inlet pipes at approximately 390ºC, which feeds steam to the AEG turbine in Figure 2.7. The second indicator displays the exhaust steam temperature at the turbine outlet of approximately 150ºC. The exhaust steam is utilized by the process portion of the plant by equipment such as evaporators and process pressure vessels.

Figure 2.7 shows the steam inlet pipes with thermal lagging to trap the heat energy within and maintain steam temperatures in order to reduce waste heat losses before the steam enters the turbine rotor for efficient safe turbine operation. The waste heat sources on the AEG steam turbine and its steam pipes are considered a continuous waste heat source since the AEG turbine is in constant operation to supply electrical energy to the entire plant.

Figure 2.6. Inlet and exhaust steam temperatures used by the steam turbine.

Figure 2.8 shows one of the numerous smaller steam turbines used to operate a mill. The steam pipes feeding the turbine is thermally lagged (insulated) up to the emergency shut-off valve. Between the turbine inlet and the emergency shut-off is a pipe that carries steam at temperatures of 150ºC to 390ºC. This temperature is dependent on turbine speed and varies with the load demand of the mill.

Figure 2.7. AEG steam turbine.

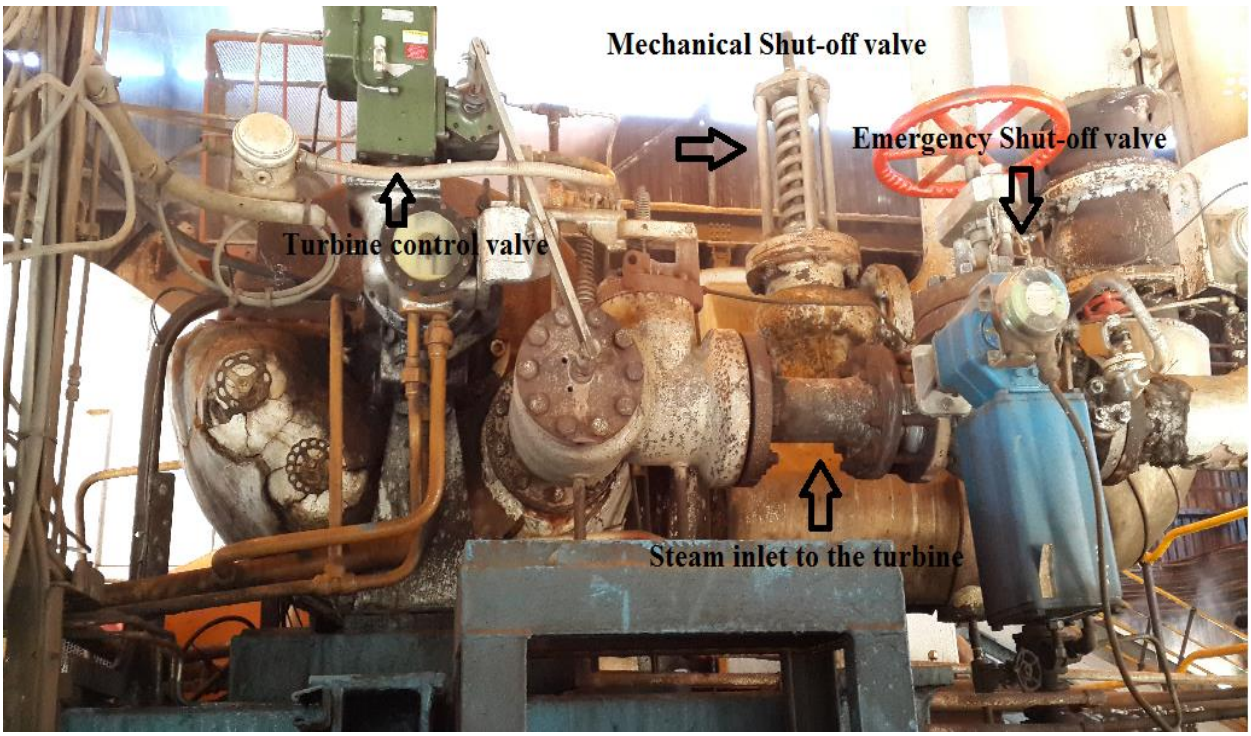

Figure 2.8. Mill steam turbine.

Figure 2.9 shows the boiler stack (or boiler chimney) from where flue gases and smoke from the boiler combustion process is vented into the atmosphere. The flue gas temperature within the boiler stack is approximately 140ºC and may experience small variations in temperature due to fluctuations in the boiler's operating conditions.

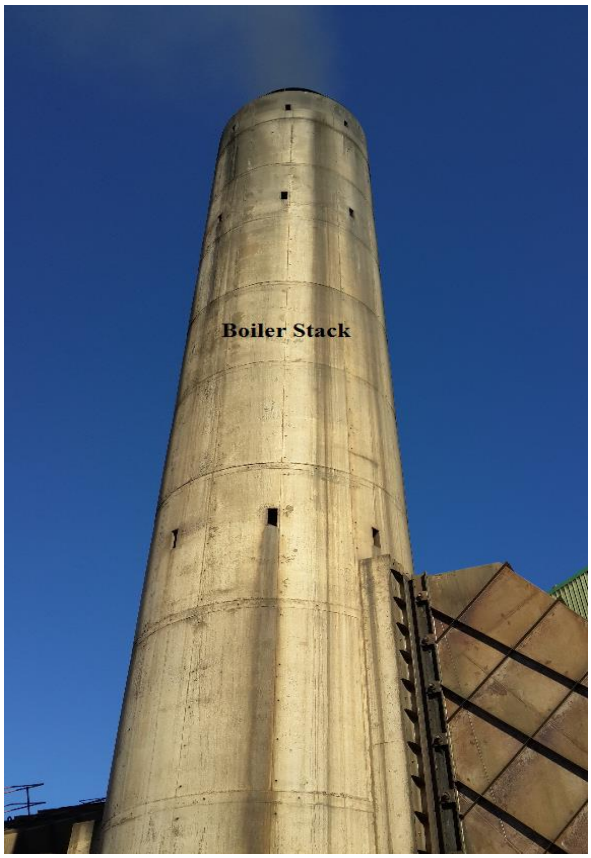

Figure 2.9. Boiler stack.

Figure 2.10 and Figure 2.11 represents another form of waste heat in the form of 'off-gas' (emitted as a by-product) being emitted during the smelting process from smelters and furnaces. Figure 2.10 shows an off-gas converter chamber where gases are scrubbed for treatment of hazardous gases prior to being vented into the atmospheric as smoke. Before the off-gas is passed into the converter for scrubbing, it is maintained at a temperature of between 300ºC to 550ºC for the platinum smelter. Keeping the gases above its dew point prevents condensation of the gases and hazardous corrosive liquids forming, such as sulphuric acid which initiates damages to plant equipment. Hazardous gases are washed down in the scrubber and various converter chambers according to the nature of the chemicals. These gases normally enter into the environment as smoke

at temperatures below 100ºC. Figure 2.11 shows a smelting process where the temperature can rise above 1500ºC for platinum smelters, generating vast amounts of waste heat within its surrounding region (Westcott, 2007).

Figure 2.10. Smelter Off-Gas (Electric Smelting Furnace Off-Gas System Design, 2014).

Figure 2.11. Platinum Smelter (Smelter upgrade- addressing improved air quality, 2009).

Biomass plants that use bagasse as fuel for their high pressure boilers produce efficient steam for various processes in the factory (Hendricks and Choate, 2006). Biomass is generally considered as an energy source completely CO_2-neutral with minimal damage to the environment (Rowe and Min, 2007). The key function of the steam boiler is to transfer heat energy generated from the combustion process to the boiler feed water to produce steam. A standard boiler is designed to absorb the greatest amount of heat energy released in the process during the combustion.

The high pressure steam boiler combustion chamber is an excellent waste heat source area to setup the TEG flat surface unit for testing. Figure 2.12 shows a boiler combustion chamber at Illovo Sugar Eston Mill, with doors that allow access into the furnace during combustion. The furnace temperature of the boiler combustion chamber is approximately 400°C

Figure 2.12. Boiler combustion chamber of a biomass boiler at Illovo Sugar Eston Mill.

within the boiler and the external boiler wall temperature is approximately 160°C, while the actual flame temperature is approximately 1200ºC during full load capacity of the boiler.

Currently common practice in the sugar industry is to have high pressure steam at 31 bar and a temperature 390°C between the boiler and the high pressure steam turbines. Figure 2.13 and Figure 2.14 illustrate high pressure steams pipes that can vary between 3/8" to 14" in size within the boiler house and turbine house in the Illovo Sugar Eston Mill process plant. Thermoelectric heat energy harvesting offers remote power for numerous instrumentation across the manufacturing industries. This energy harvesting design is modified to install onto any pipe diameter and pipe orientation. The existing pipeline infrastructure doesn't have to be altered in any way. A prototype design of a steam pipe thermoelectric co-generation unit configuration will be discussed later in this thesis.

Figure 2.13. High pressure steam piping at the Boiler House at Illovo Sugar Eston Mill.

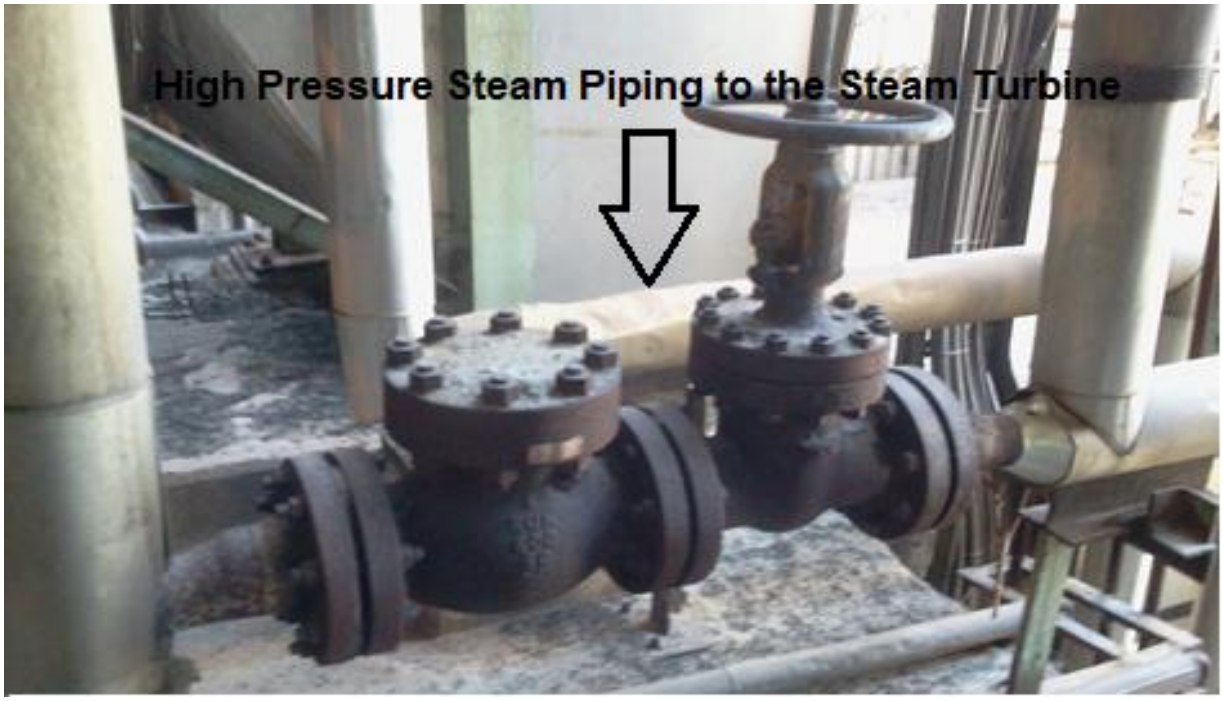

Figure 2.14. High pressure steam piping at the Turbine House at Illovo Sugar Eston Mill.

2.4 THERMOGRAPHY OF INDUSTRIAL APPLICATIONS

Thermographic imaging is a non-contact method of providing diagnostics information about the thermal states of critical equipment. Thermography provides a two dimensional visual of the thermal pattern of heat generated by the equipment. A thermography device records the intensity of radiation in the infrared part of the electromagnetic spectrum and translates it to a visible image for the human eye. Using this technology, we can identify hot areas on industrial equipment within the plant. Figure 2.15 and Figure 2.16 are thermography images of the outer furnace shell of a manganese smelter. The thermal images illustrate the waste heat radiated by the smelter at various portions of the outer shell. The temperature of waste heat generated is displayed alongside the image with graphic colors corresponding to the temperature scale. The temperature scale on Figure 2.15 and Figure 2.16 ranges from 25ºC to 350ºC and represents the waste heat present within the smelter.

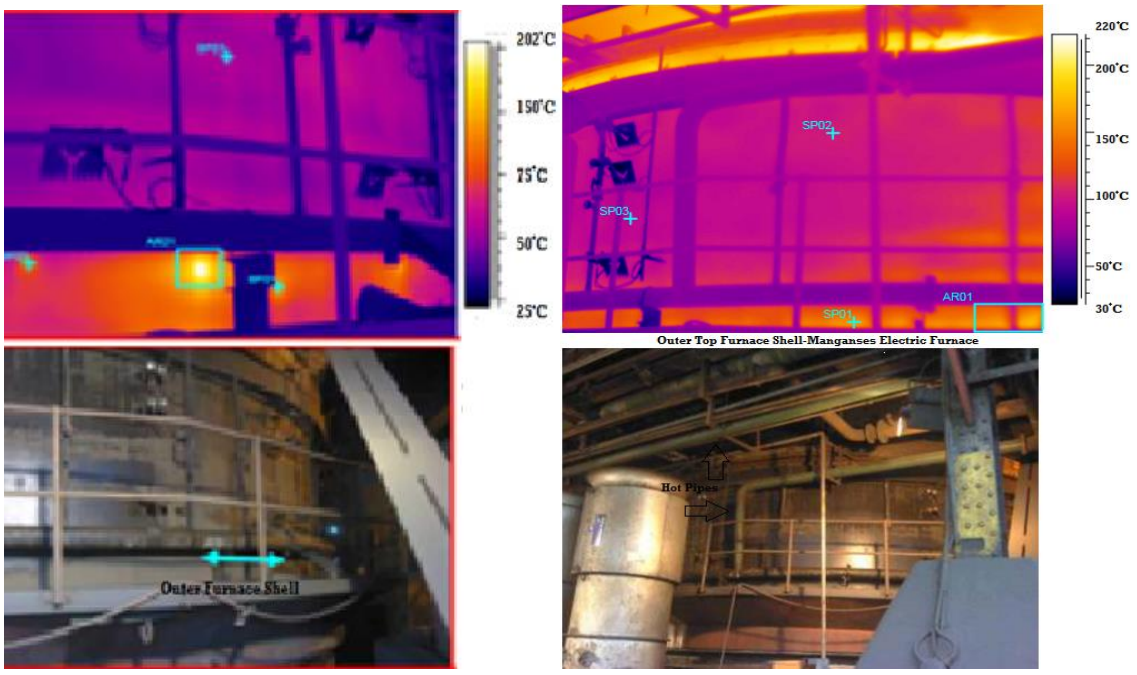

Figure 2.15. Thermography images of an outer furnace shell of a manganese smelter.

Figure 2.17 illustrates the thermography image of an electric motor within a plant. Electric motors generate a substantial amount of waste heat. The amount of waste heat generated depends on various components of the motor and its corresponding load demand within its operation. Figure 2.17 provides an indication of the expected waste heat given off by numerous electric

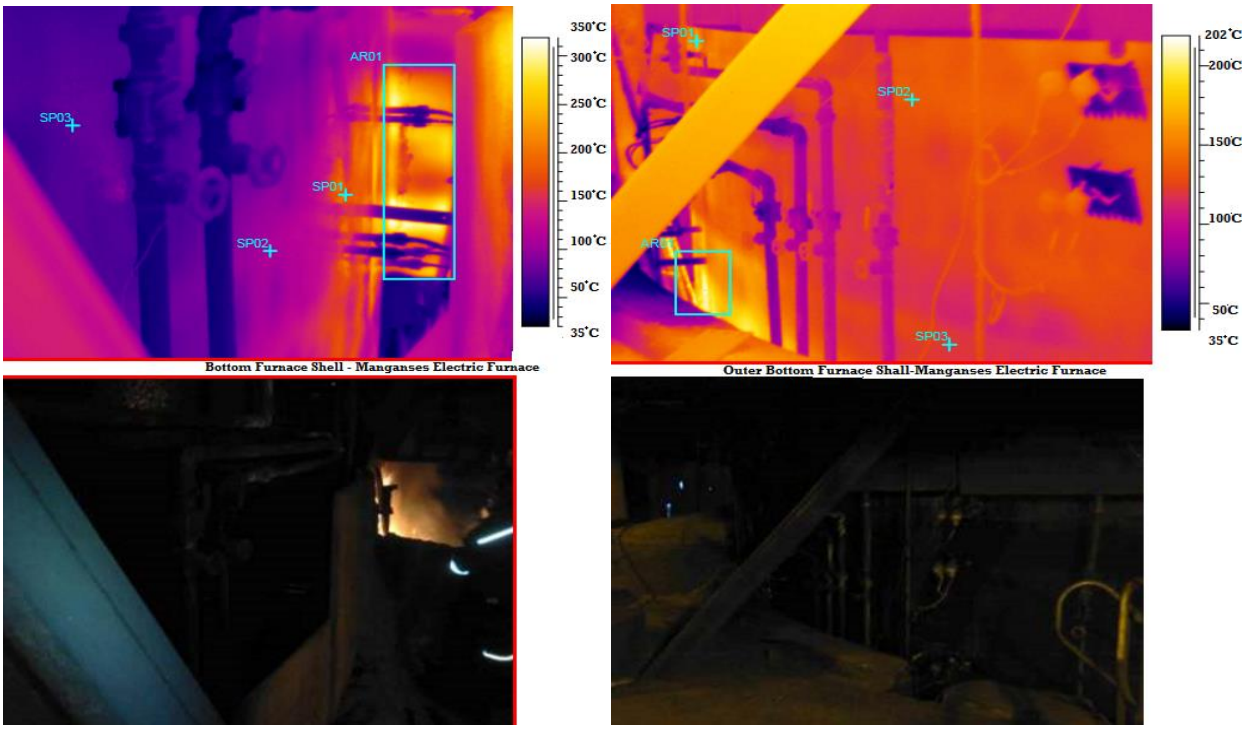

Figure 2.16. Thermography images of an outer bottom furnace shell of a manganese smelter.

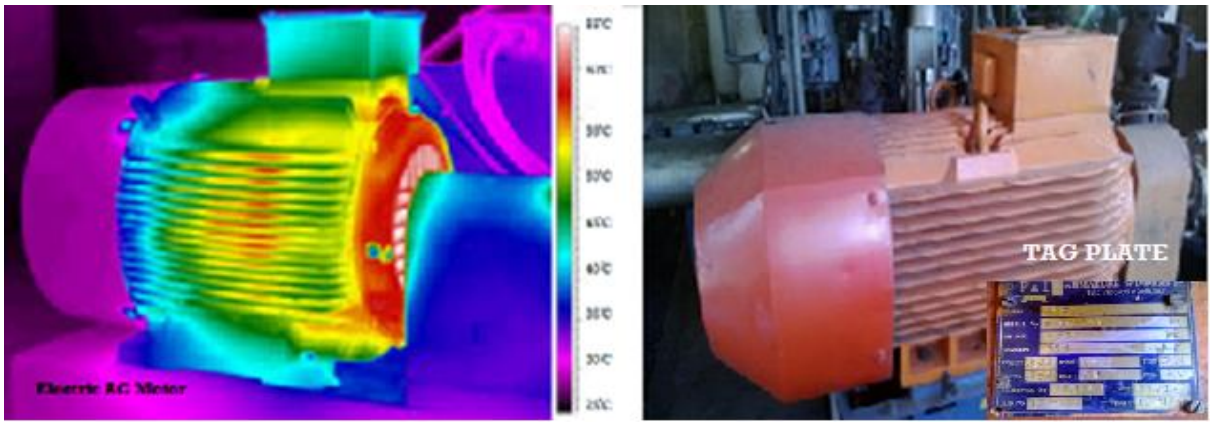

Figure 2.17. Thermography image of an electric motor on the plant.

motors during their operation within an industrial environment. The electric motor in Figure 2.17 rated for 525V at 354A, producing 275 kW, and generates 65ºC of waste heat at its highest hot spot as indicated on the red temperature.

Figure 2.18 represents a common distillation column used in various refineries. It is evident from the thermography image in Figure 2.18 that there is excessive waste heat generated throughout the rectification and stripping sections of the vertical shell of the distillation tower. The waste heat radiated from the vertical shell is determined by the chemical properties of the product being distilled within the vessel. In Figure 2.18 the temperature scale indicates a maximum of 200ºC of waste heat being radiated across the tower shell.

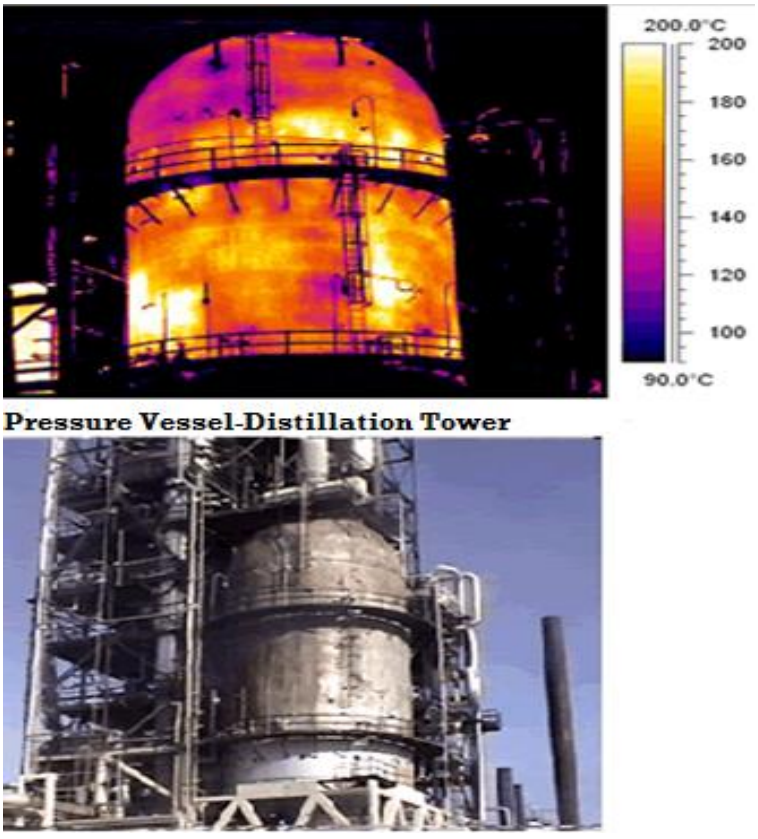

Figure 2.18. Thermography image of a distillation tower at refinery.

Figure 2.19 shows the thermography image of a furnace chamber of a high pressure steam boiler burning fossil fuel for combustion. The maximum temperature radiated from the furnace chamber is 352ºC as is indicated on the adjacent color temperature scale given on Figure 2.19.

Figure 2.20 and Figure 2.21 illustrates the heat energy that is generated in the form of electromagnetic radiation from electrical equipment such as circuit breakers, isolators and motor starters. Thermography technology facilitates the detection and correction of potential electrical hazards in the plant. These hazards could result in major damages to the equipment and process, and injuries to operational staff within the area. From the thermography temperature scale in Figure 2.20, the vacuum pump motor MCC connections radiate 93.9ºC of heat energy. The thermography temperature scale in Figure 2.21 of the MCC connections reaches a temperature of 120.4ºC which represents a substantial amount of waste heat dissipated into the surrounding environment.

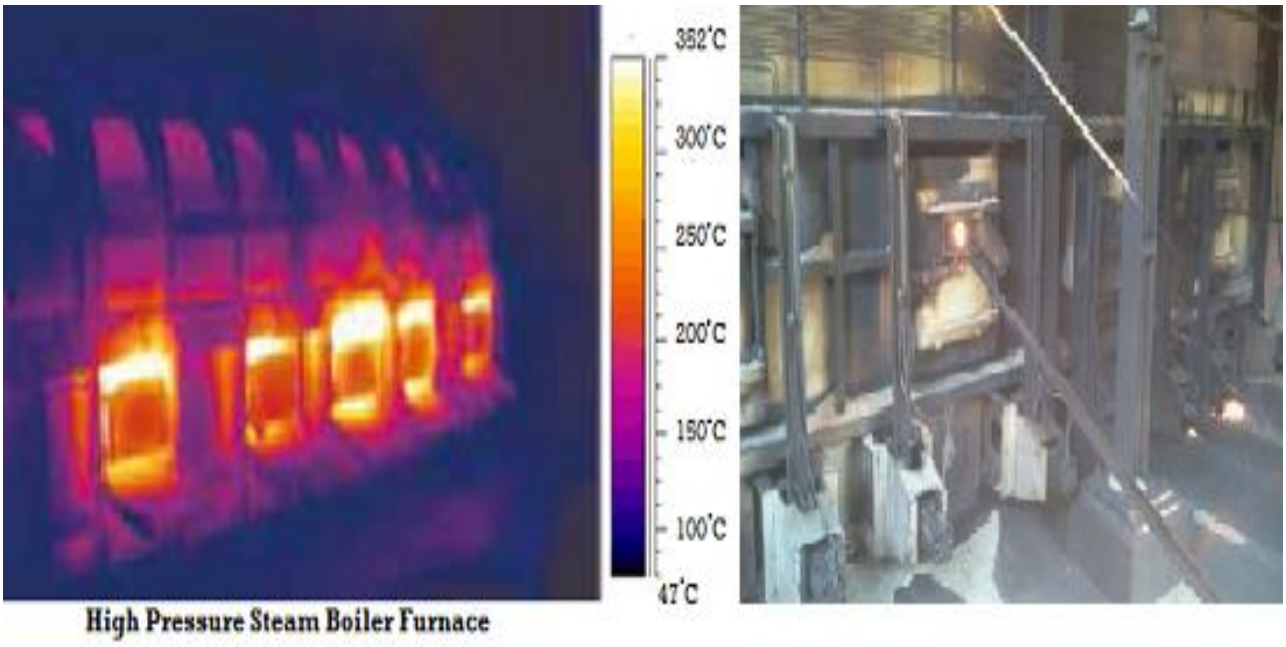

Figure 2.19. Thermography image of the combustion chamber of a steam boiler.

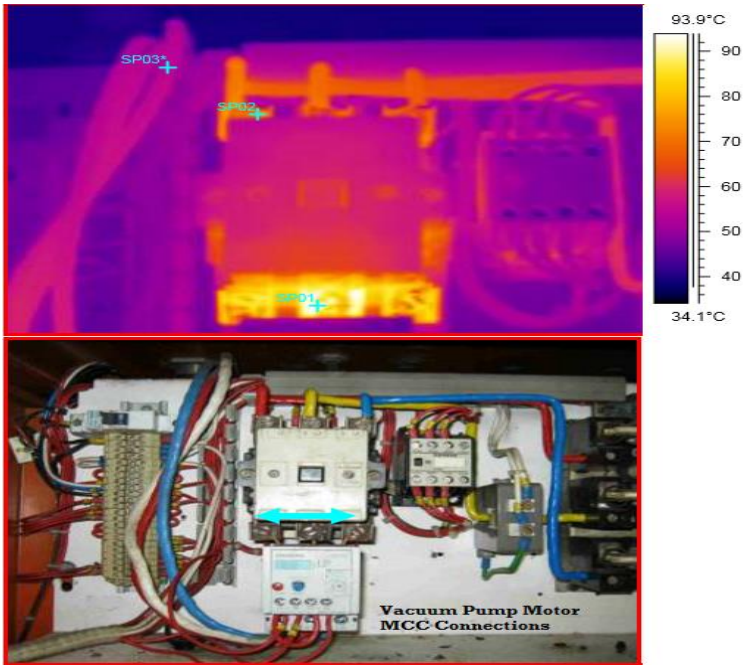

Figure 2.20. A vacuum pump motor's MCC connections.

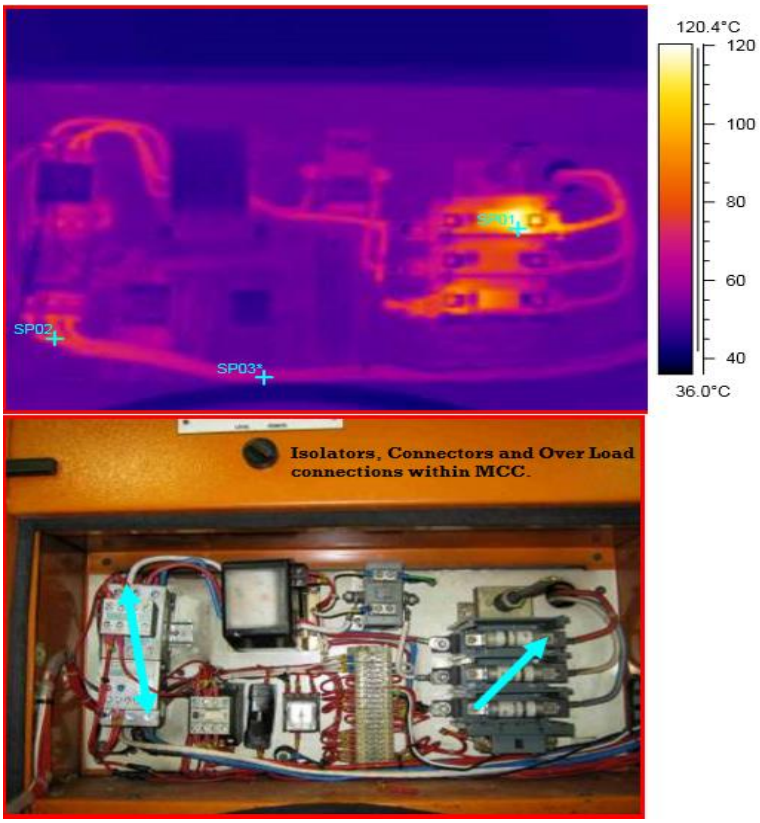

Figure 2.21. Isolators, connectors and over load connections within a MCC unit.

2.5 SUMMARY AND CONCLUSION

The waste heat dissipated into the environment adds no economic value to a plant. Rather, in some circumstances it may have a negative impact on the environment. Even though industry has numerous options for capturing and utilizing waste heat, the traditional heat energy recovery technologies may not be economically feasible. For example, in some situations a plant may not have a need for recapturing wasted heat energy for uses such as preheating of the water in boiler feed-water systems, processing of raw materials and combustion air within a boiler's air draft system. Under these circumstance, thermoelectricity may provide a prospective means of adding benefit to the industrial process by employing the waste energy to produce electrical power (Hendricks and Choate, 2006).

CHAPTER 3

THERMOELECTRICS

3.1 INTRODUCTION

Environmental concerns have enforced the improvement of energy conversion efficiency of both conventional energy sources and new energy sources known as power technologies, which refer to electrical energy sources based on thermoelectric effect (Jaworski, 2015). Thermoelectric systems provide a green and flexible source of electricity and have the potential to meet a wide range of small scale power requirements. Keen interest has been shown in alternative renewable energy technologies as a sustainable source of electrical power (Rowe, 1999). From the literature, new developments in thermoelectric materials are starting to provide promising new prospects for widespread applications of thermoelectric powered systems (Rowe, 1999; Da-Jeng *et al*., 2009). The cost of thermoelectric devices is also becoming affordable and good prospects exist for merging this new technology into a plant's energy mix requirements (Allen *et al*., 2003).

3.2 THERMOELECTRIC DEVICES

Thermoelectric systems are solid-state devices that operate according to the Seebeck effect. They consist of a hot junction and a cold junction and transform heat energy into electrical energy when a temperature gradient exists between the hot and the cold junction. Solid-state thermoelectric devices can function under the Peltier effect where, depending on the direction of the current flow,

electrical energy is converted into thermal energy for cooling or heating. Thermoelectric devices do not use refrigerants or working fluids and generate negligible emissions of greenhouse gases in their life cycle (Chen, 2015). This is a key benefit for industries that aim to decrease their carbon foot print.

In spite of its global recognition, thermoelectric energy is a new and innovative technology for South Africa (Edkins *et al*., 2010). The technology is so new to the country that it has still not been incorporated within the South African Renewable Energy Policy 2009 (Edkins *et al*., 2010). South Africa needs to embrace thermoelectric converters as an apparatus to operate an efficient energy arrangement by removing and harvesting small amounts of heat energy from otherwise wasted heat energy (Elsheikh *et al*., 2013). Thermoelectric devices present numerous advantages over other modern technologies (Riffat and Ma, 2002):

- Thermoelectric devices encompass no moving parts; hence less maintenance is required.
- Analysis of thermoelectric devices show them to surpass 100 000 hours of operation (www.Tellerex.com, Accessed Jan. 2014).
- Thermoelectric devices comprise of no chlorofluorocarbons and additional materials that may necessitate intermittent replenishment.
- Meticulous temperature control to within ±0.1ºC operating thermoelectric devices that has proper circuitry.
- Thermoelectric devices may be positioned in various locations.

Thermoelectric modules are manufactured from semiconductor materials. Semiconductor materials are ‘grown’ into the crystalline structures. The quality of the impurities or dopants determine the conductive properties of semiconductor materials used in thermoelectric modules.

The type of impurities inserted into the semiconductors determines whether they will be classified as either negative (N)-type semiconductor material or positive (P)–type semiconductor material. Electrons are the charge carriers in N-type semiconductor material, and 'holes' are responsible for current flow in P-type semiconductors.

3.3 THERMOELECTRIC MODULES (TEG) AND MATERIALS

Examples of thermoelectric materials include bismuth telluride (BiTe), skutterudite (CeFeSb), zinc–beryllium (ZnBe), silicon–germanium (SiGE) and nanocrystalline thermoelectric materials. The major challenge facing the development of large scale thermoelectric power generation is the minimal heat-to-electricity conversion efficiency (Rowe and Min, 1997), and several studies are ongoing to advance the natural conversion efficiency of thermoelectric materials (Rowe and Min, 1997). BiTe based bulk thermoelectric material is utilized for waste heat recovery. It is readily available and inexpensive to purchase. Hi-Z Technology has developed the HZ-14 modules based on Bi2Te3 (bismuth telluride). These HZ-14 modules have a hypothetical and experimental efficiency of 5% (Rowe and Min, 1997). The operating temperature scale for a commercially produced bismuth telluride module ranges from ambient to 250ºC. These modules are suitable for applications that offer low temperature waste heat recovery. Companies that produce these thermoelectric devices and modules, commonly known as TEG's, provide information on the performance of the individual modules. The datasheets provide the user crucial information such as the performance curves, maximum output voltage (V_{max}), maximum output current (I_{max}), maximum absorbed heat energy (Q_{max}), and maximum output power (P_{max}), at several test conditions (Hsu *et al.*, 2011).

An elementary thermoelectric element comprises of a basic thermocouple that converts heat into an electrical signal for temperature observation (Slaton and Zeegers, 2003). Based on the Seebeck effect, a thermocouple, thermopile or generator can be established by joining the hot ends of two dissimilar conductors at a junction, and closing the cold ends with a load. A higher temperature at the hot junction results in an electric current movement in the circuit and electric energy being supplied to the load. Conventional thermocouples are manufactured from metal/metal compounds such as platinum/platinum rhodium which generates tens of microvolts per degree temperature gradient. Modern semiconductor thermocouples generate hundreds of microvolts per degree temperature difference and have the potential to provide useful amounts of electrical power (Li *et al*., 2014).

Semiconductor materials have been optimized and designed around the operating theory of the Seebeck effect. Figure 3.1 illustrates an individual N-type semiconductor with a voltmeter connected across. We can observe that the heat flows from the hot side to the cold side of the pellet. The electrons are transported from the dopants with the heat. The electrons are affected by the heat in the return direction. Heat transfer conveys more electrons in the pellet than in the circuit's return direction. Thus a significant Seebeck voltage is created (www.Tellurex.com, Accessed Jan. 2013).

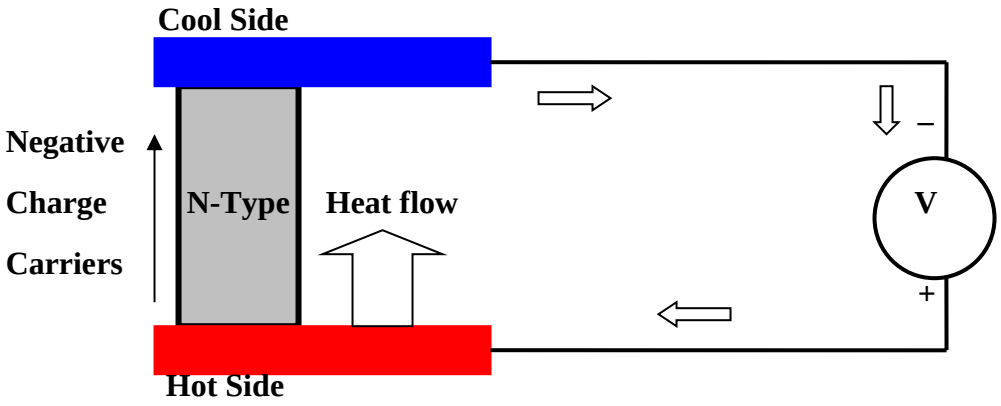

Figure 3.1. N- Type semiconductor pellet connected across a voltmeter.

Figure 3.2 shows the P-type semiconductor pellet connection with the movement of electrons shifting in a direction contrary to that of the hole movement. To optimize the Seebeck effect we use both the N-type and P-type materials in thermoelectric modules by coupling them together thermally in parallel while they are electrically connected in series (cf. Figure 3.3) (www.Tellurex.com, Accessed Jan. 2014).

Thermoelectric modules consist of semiconductors type thermos-elements. A pair of thermoelements is generally acknowledged as a thermocouple. Numerous N-type and P-type semiconductor pairs form thermocouples that are connected electrically in series between 2 ceramic plates to form a module as shown in Figure 3.4 (Riffat and Ma, 2002). There have been numerous attempts to obtain a high-performance ceramic thermoelectric material for application in energy conversion (Elsheikh *et al.*, 2013). The ceramic pellets are the base in forming the electrical insulation for the N-type and P-type bismuth telluride. Common thermoelectric modules are $3mm^2$ by 4mm thickness to $60mm^2$ by 5mm thickness (www.everredtronics.com, Accessed Jan. 2013) Thermoelectric modules may have a range from 3 to 127 thermocouples connected within a single module.

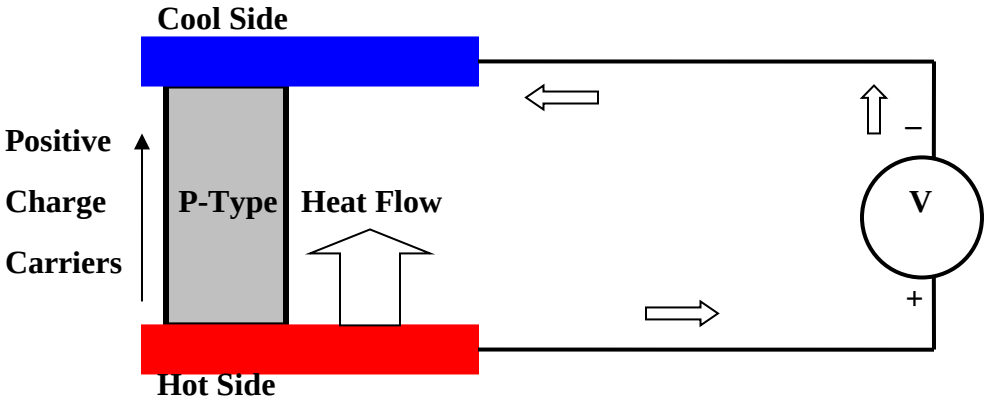

Figure 3.2. P-Type semiconductor pellet connected across a voltmeter source.

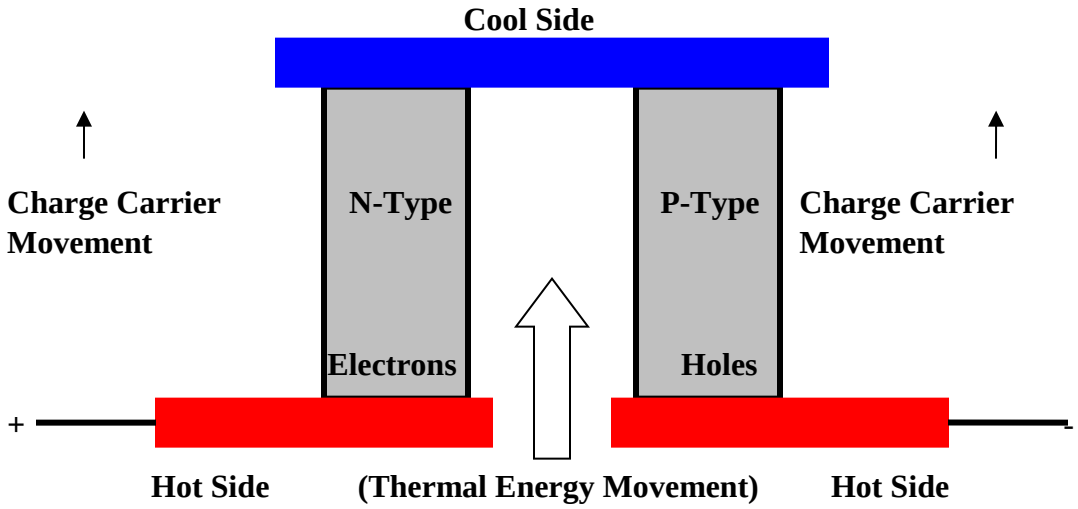

Figure 3.3. N-Type and P-Type material configuration.

The cold side ceramic plate of the thermoelectric module contracts while the hot side ceramic plate expands during operation (Riffat and Ma, 2002).

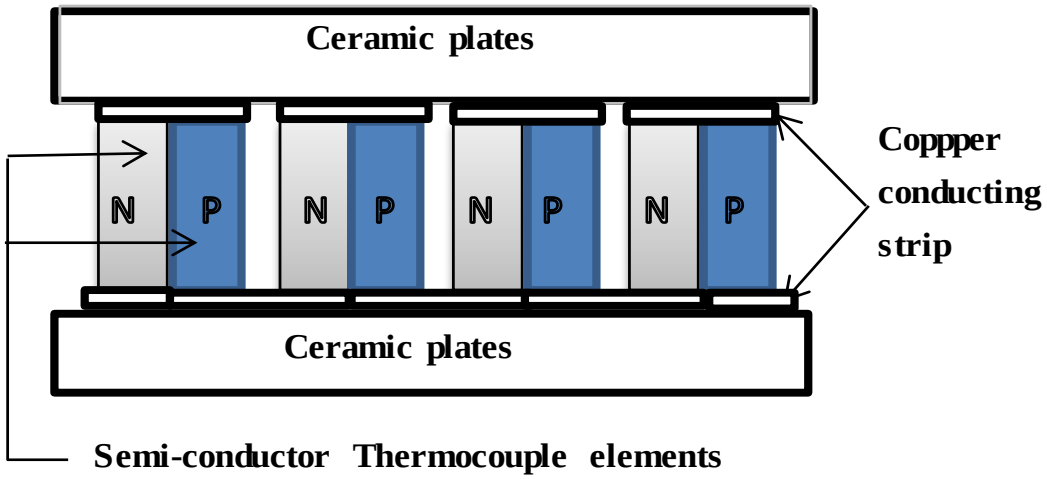

Figure 3.4. N-type and P-type semiconductors between ceramic plates.

A commercially available thermoelectric module is shown in Figure 3.5. This thermoelectric device has been developed for electrical power generation under the Seebeck effect and is densely constructed with very small inter-thermoelement separation to increase the power-per-area. The conducting metal strips in the device is insulated and the module can be coupled directly to electrical conductors such as cooling heat-sinks. Thermoelectric devices are connected to heat exchangers to dissipate heat. The heat energy is dissipated using small heat pumps based on the Peltier effect (Riffat and Ma, 2002).

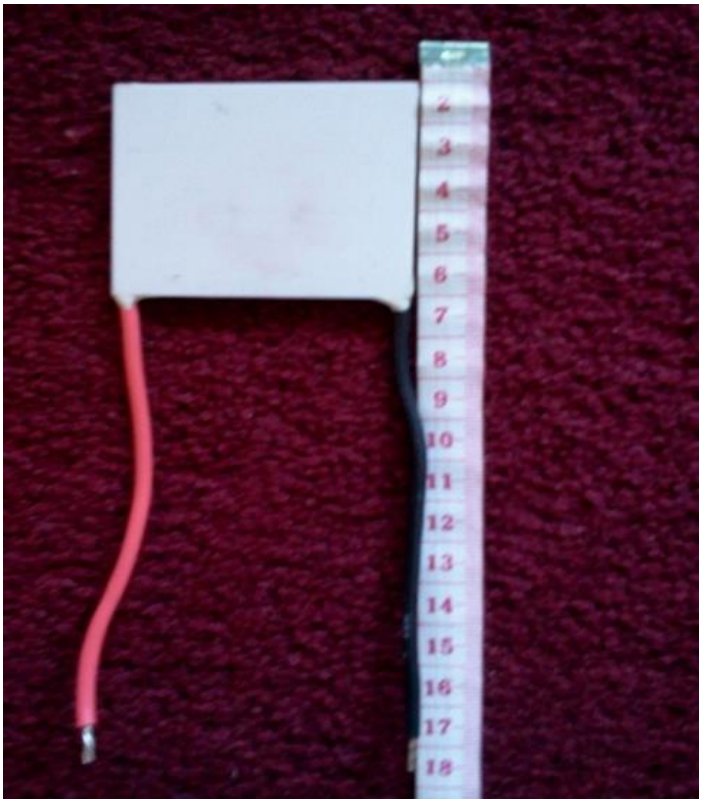

Figure 3.5. A commercially manufactured thermoelectric module.

3.3.1 Operation Principle of Thermoelectric Modules

The operation of TEG modules are based on 3 thermoelectric effects, namely the Seebeck effect, the conduction effect and the Joule effect.

Seebeck effect: In a particular thermoelectric configuration, the heat source applies heat energy, (*Qh (W)*), to produce a temperature difference (ΔT) between the hot side and the cold side of the module. An electrical current *I (A)* is induced within the TEG circuit.

Conduction effect: The conduction effect is the amount of power that is proportional to the thermal conductivity, ($k\ (W\ K^{-1})$). ΔT represents the temperature difference between the hotside (T_H) and coldside (T_C).

Joule effect: As an electrical current passes through the thermoelectric leg, Joule heat is generated internally. The heat generated is proportional to the power produced by the thermoelectric module. The hot side and cold side are heated equally by the heat effect (Hsu *et al*., 2011).

Figure 3.4 illustrates the formation of induced electrical current within the TEG model that is composed of a P-type and N-type thermoelectric pair, electrical conductor (Cu) and ceramic plates. Internal material properties are theoretically stable while independent of temperature and there are no heat losses. The source heat 'Q_h' and the dissipated heat 'Q_c' are approximated at both junctions (Hsu *et al*., 2011). The equations for Q_c and Q_h are given in equation 3-1 and equation 3-2, respectively.

$$Q_h = \left(K_p + K_n(T_h - T_c)\right) + \left(\alpha_p - \alpha_n\right)IT_n - I^2R/2 \tag{3-1}$$

$$Q_C = (K_{P+}\, K_n)(T_{h-}\, T_c) + \left(\alpha_{p-}\, \alpha_n\right)IT_{C-}\, I^2\, R/2 \tag{3-2}$$

With regards to equation 3-1 and equations 3-2, K_p and K_n are the thermal conductivity of the P-type and N-type thermoelectric leg, respectively; $T_h$and *Tc* represent the hot junction and cold junction temperatures of the module, respectively; α_p and α_n denote the Seebeck coefficient of the P-type and N-type thermoelectric legs, respectively.

According to the power balance equations, electrical power can be obtained as follows (Hsu *et al*., 2011):

$$P_{out} = V_{out}.I_{out} = (Q_h - Q_c) \tag{3-3}$$

Rearranging Equations (3-1) to (3-3)

$$\left(\alpha_p - \alpha_n\right) I(T_h - T_c) - I^2 R = V.I \tag{3-4}$$

Divide both sides of Equation (3-4) by Equation (3-1)

$$V = \left(\alpha_p - \alpha_n\right)(T_h - T_c) - I.R \tag{3-5}$$

Simplifying Equation (3-5) and let $\alpha = \left(\alpha_p - \alpha_n\right)$ and $\Delta T = (T_h - T_c)$:

$$V = \alpha\Delta T - IR = A\Delta T - BI \tag{3-6}$$

The value of *B* would be the slope that signifies the matching load of the TEG module. *A* represents the cross sectional area of the module. Equation (3-6) suggests the output voltage is a function of the current for the generated temperature differences between both sides of the thermoelectric module. For the open circuit voltage, $I = 0$ in Equation (3-6); $\alpha\Delta T$ has a maximum value in which α is defined as the effective Seebeck coefficient given as:

$$\alpha = \frac{V}{\Delta T} \tag{3-7}$$

With regards to (3-7), *V* is the open circuit voltage when $I = 0$. Hence the value of α articulates the performance of the TEG module functioning under stipulated conditions. Equation (3-6) becomes the significant indicator to characterize the performance of a TEG module or a system is composed of TEG modules (Hsu *et al.*, 2011).

Thermoelectric power generators obey the laws of thermodynamics for heat engines and are constrained by a heat source and heat-sink system (Allen and Kushch, 2003). It is challenging to

attain the adequate temperatures without a heat-sink attached to the cold side of the thermoelectric module (cf. Figure 3.6).

Thermoelectric generation (TEG) operation is governed by the following physical processes (Sergent and Krum, 1998; Kordyban, 1998):

Thermal convection is described as the physical constant and is determined by the thermal conductivity *k (W K^{-1})* of the module and the geometry of the pellets within. Joule heating is the physical process of heat dissipation in the resistive elements. The total resistance (R_m) of the TEG module is;

$$R_m = R.N \tag{3-8}$$

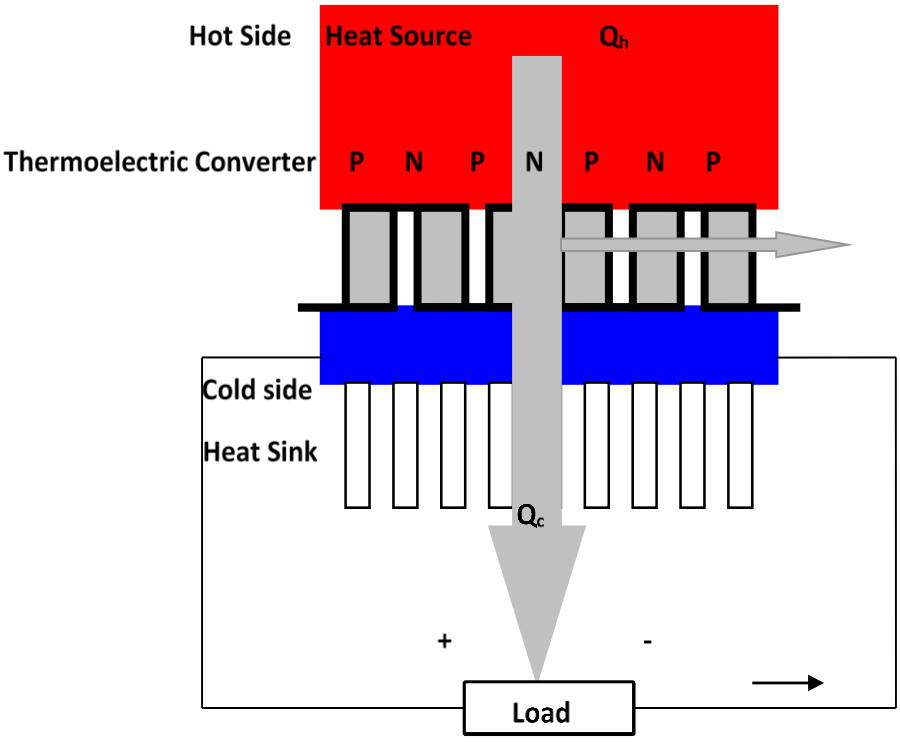

Figure 3.6. Conventional layout for thermoelectric power generation.

With regards to equation (3.8), *R* represents the resistance of the TEG module and *N* refers to the number of PN junction pairs.

Seebeck Effect: Seebeck power generation occurs when the heating of the junctions of two dissimilar materials generate an electrical potential across the junction. The Seebeck coefficient (α_m) for the TEG127-50D module used in this study is calculated as:

$$\alpha_m = \alpha.N = \alpha.127 \tag{3-9}$$

With regards to equation (3-9), α_m is the Seebeck coefficient corresponding to the thermocouple materials and *N* refers to the number of PN junction pairs (Slaton and Zeegers, 2005).

Peltier Effect: The Peltier Effect occurs in a thermocouple when the heat is absorbed by a junction and it is dependent on the direction of current stream through the junction. The amount of heat energy absorbed is:

$$\textit{Heat absorbed} = (P_b - P_a)I \tag{3-10}$$

where P_b and P_a denote the Peltier coefficients of the thermocouple materials, and *I* represents the junction current.

Thompson Effect: The Thompson effect (*T*) relates to the *EMF* generated by a single wire to the temperature difference existing between the ends of the wire and differs for different metals. $T\ (V/K_2)$ is determined by:

$$T = \Delta\alpha/\Delta\mathrm{T} \tag{3-11}$$

The power produced in the module from Equation (3-3):

$$P_{out} = V_{out}.I_{out} = Q_h - Q_c \tag{3-12}$$

where Q_h is the heat energy stream at the modules' hot side and Q_c is the heat emitted at the cold side. The rate at which heat is conducted within a material is proportional to the area normal to the heat stream as well as proportional to the temperature gradient of the heat stream route. At steady state, the heat energy stream can be established from:

$$Q = k.A(\Delta T/D) \tag{3-13}$$

where *k, Q, A, D* and *ΔT* represent the thermal conductance, rate of heat flow, contact area, distance of heat flow and temperature difference, respectively. The relationship between the thermal conductivity (*k*) and the resistance can be expressed in the following equation:

$$k = D/R \tag{3-14}$$

The characteristics of the TEG 127-50D module used in this study (cf. Figure 3.5) have been summarized in Table 3.1. The module's thermal, physical and electrical parameters have been documented. This information provides guidelines on the expected electrical outputs from the module while being operated within the modules thermal parameters.

The heat-sinks performance on the cold side of the thermoelectric module can be enhanced with a fan to ensure proper air movement. An axial-flow fan mounted on the heat-sink will help improve the ventilation and achieve a larger ΔT_{sink} (Rowe and Min, 1997).

Table 3.1. TEG127-50D modules operating parameters.

PARAMETERS	CHARACTERISTICS	VALUE
THERMAL PARAMETERS	Operational hot side temperature of the TEG module	200ºC
	Operational cold side temperature of the TEG module	50ºC
	Operational differential temperature of the TEG module	150ºC
PHYSICAL PARAMETERS	Length of the TEG module	50mm
	Width of the TEG module	50mm
	Height of the TEG module	5mm
ELECTRICAL PARAMETERS	Seebeck coefficient	0.035V/K
	Open circuit voltage	5.20V
	Matched load resistance	1.1Ω
	Matched output voltage	2.5V
	Matched output current	2.15A
	Matched output power	5.4W
	Heat flow through the module	120.3W
	Module efficiency	4.49%

3.4 POWER OUTPUT AND CONVERSION EFFICIENCY OF THERMOELECTRIC MODULES

Thermoelectric Output Power:

Thermoelectric modules are designed and manufactured for power generation and are densely constructed with minor inter-thermoelement separation (Hsu *et al.*, 2011). Maximum power is generated by the thermoelectric module when the module's resistance approaches that of the load. Figure 3.7 illustrates a circuit that enables an accurate measurement of the thermoelectric modules maximum power output (www.Tellurex.com, Accessed Jan. 2014). This circuit minimizes the drawbacks associated with the low thermoelectric module resistance and fluctuations in signal

measurements due to the Peltier effect. With regards to Figure 3.7, a voltage is developed at terminal *a* and terminal *b* when a temperature difference is established across the module. The maximum power delivered by the module and its resistance is determined from equation (3-15) and equation (3-16), respectively:

$$P_{MAX} = \frac{V_1^2}{4R_{L(V_1/V_2-1)}} \tag{3-15}$$

$$R_{M=}R_L\,(V_1/V_2 - 1) \tag{3-16}$$

With regards to equation (3-16), R_M is the modules resistance, $R_L$denotes the load resistance and V_1 and V_2 represent the voltage developed across terminals *a* and terminal *b*, respectively.

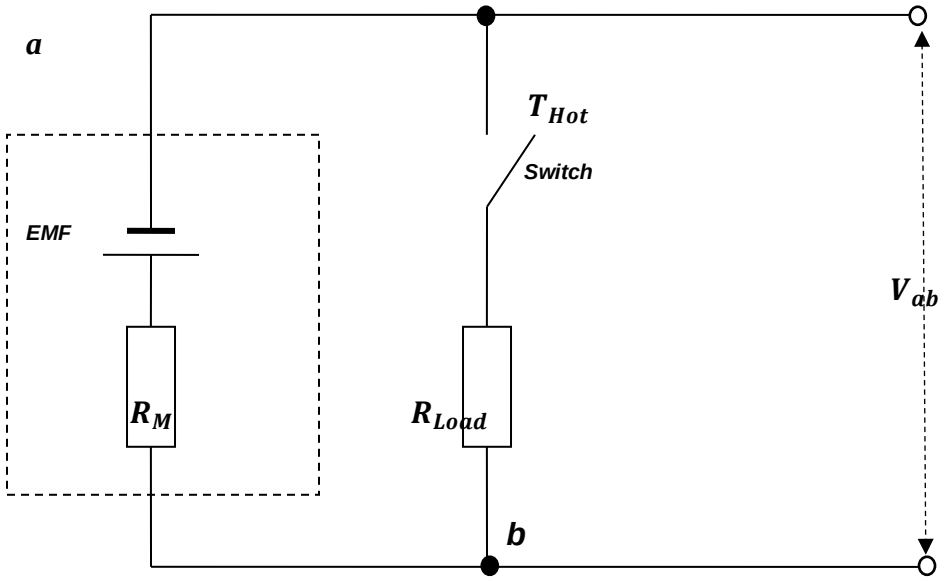

Figure 3.7. Circuit for measuring the maximum power and resistance of thermoelectric modules (www.Tellurex.com, Accessed Jan. 2014).

3.5 VARIABLE PARAMETERS OF THERMOELECTRIC POWER GENERATION MODULES

Figure 3.8 shows the performance curves for the TEG127-50D commercial thermocouple module. These curves deliver a graphical method to design a thermoelectric module using just the hot side temperature (T_h) and cold side temperature (T_c). Optimum efficiency variable (E) and IL / A are established from the T_h and T_c curves once ΔT is established. The amount of heat (Q) required at the hot side of the module is determined by equation 3-19:

$$Q = IV / E \tag{3-19}$$

Electrical power is determined via the heat flow and not only the heat source. Thus a thermoelectric power generation circuit is incomplete without a cooling system such as a heatsink. Heat-sink performance is characterized by the heat-sink resistance (HSR). HSR is a measure of the temperature rise of the sink above ambient temperature (Ta) per watt of power dissipated while T_c is the temperature of the cold side. The heat delivered by a thermoelectric device is determined by equation (3-20) (Bruke and Buist, 1984):

$$T_c = HSR(Q - IV) + T_a \tag{3-20}$$

Thermoelectric generators require a heat source and heat exchanger (Allen *et al*., 2003). A heat exchanger attached needs to dissipate the heat across the module to achieve a considerable ΔT between the hot side and cold side. This directly contributes towards producing maximum power, voltage and current generation from the module (Allen *et al*., 2003).

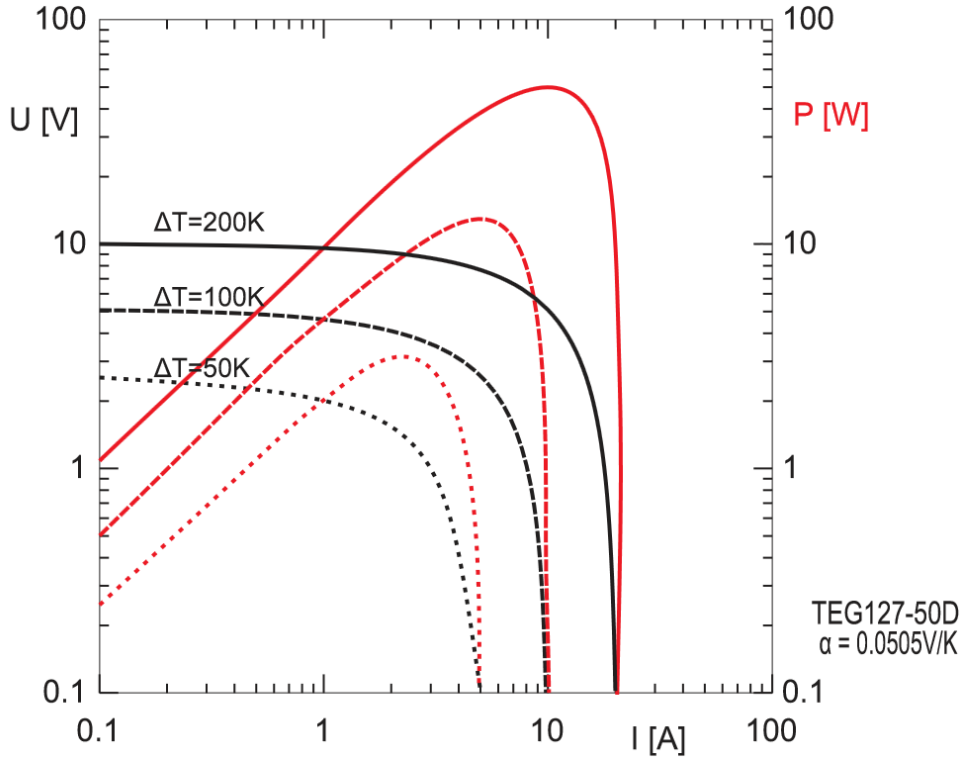

Figure 3.8. Module TEG127-50D temperature curves with Seebeck coefficient (α) (www.everredtronics.com, Accessed Jan. 2014).

3.6 THERMOELECTRIC MODULE COOLING SYSTEMS

TEG modules utilize a heat-sink to cool the device. From Fourier's law of heat conduction, the rate of heat transfer through a material is proportional to the negative gradient in the temperature and to the area, at right angles to that gradient through which the heat is flowing.

A thermoelectric conversion system with a module and heat-sink is illustrated in Figure 3.9. The ceramic thermoelectric module is in direct contact with the heat energy source and the heat-sink. The cold side of the module, which forms the top ceramic plate is fixed to the heat-sink while direct current flows through the load. Heat energy radiates from the bottom ceramic plate which is the hot side of the module to the top ceramic plate and is transported into the heat-sink. This results in the cold side (top plate) cooling.

To generate thermoelectric energy, the module allows heat from the source to flow through it; the heat is dissipated via the heat-sink into the surrounding atmosphere. A large temperature difference between the plates of the module needs to be sustained to generate electrical energy power. Thermoelectric modules are commonly manufactured by substituting the direct current source with a load while exposing the hot side to a heat source (Min and Rowe, 2011; Bruke *et al*., 1984).

3.6.1 Heat-sink Material

The common heat-sink material of choice would be aluminium alloys 6061 and 6063 which have thermal conductivity amounts of 166 W/mK and 201 W/mK (Kordyban, 1998). An alternative material to consider would be copper. Copper has double the conductivity of aluminium alloys although copper is a lot heavier than that of aluminium alloys and expensive. Aluminium alloys also have an advantage of being able to be extruded unlike that of copper. Figure 3.9 gives an example of an aluminum fin heat-sink.

Figure 3.9. Aluminum fin heat-sink.

3.6.2 Heat-sink fin arrangement

A thermoelectric system uses a straight fin arrangement heat-sink for efficient cooling of the modules. Straight fin arrangement heat-sinks are flat surface plates that allows for unidirectional heat dissipation into the atmosphere. As heat flows through the heat fins, a combination of the thermal resistance of the heat-sink impeding the flow plus the heat lost from convection, lowers the temperature of the fins (Sergent and Krum, 1998). A flat base heat-sink arrangement is ideal for mounting the TEG modules onto so as to cover the entire area of the module's cold side. This improves the heat dissipated from the module and aids cooling. Figure 3.10 shows an example of how a TEG module is fixed onto a straight finned heat-sink.

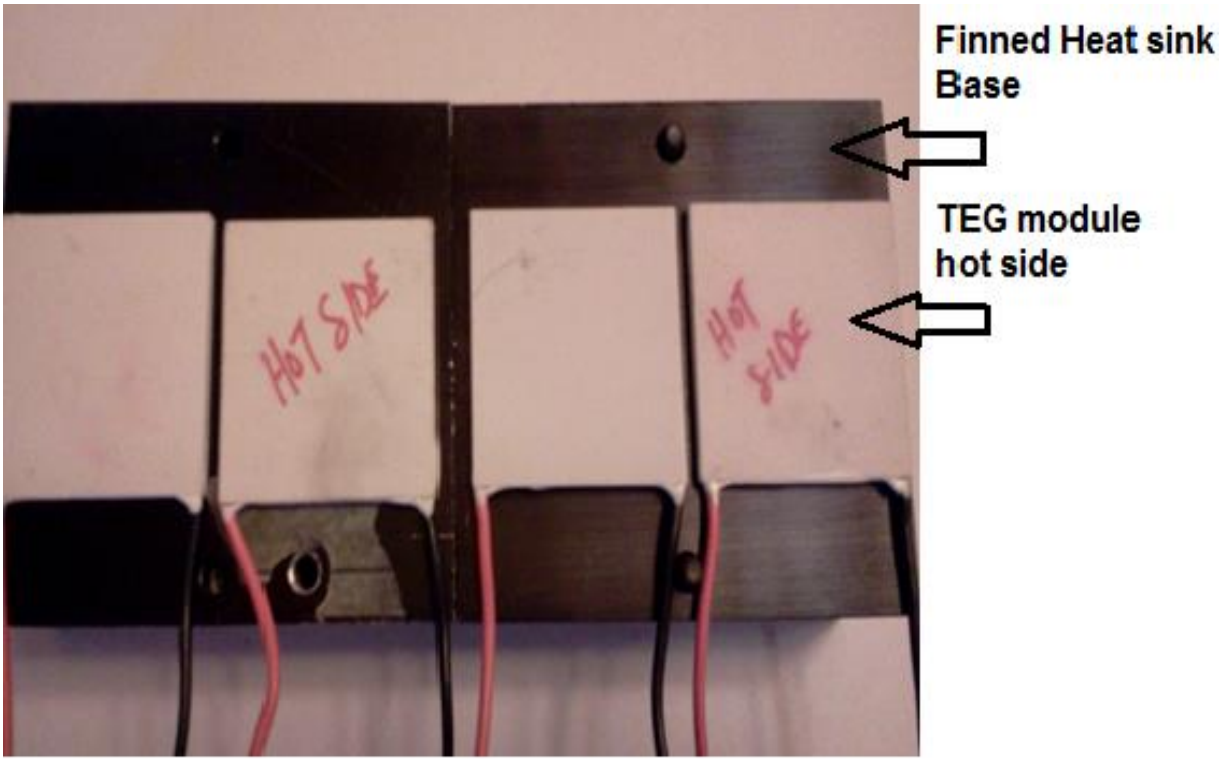

Figure 3.10. TEG module mounted onto heat-sink.

3.6.3 Spreading Resistance of a Heat-sink

Spreading resistance influences thermal conductivity of the heat-sink material. It is described as the thermal energy conveyed from a small region to a larger region within a material with finite thermal conductivity properties (Sergent and Krum, 1998). Hence heat energy will not be distributed uniformly through the base of the heat-sink. The resolution is to improve the heat-sink base thickness while using good thermal conductivity material (Sergent and Krum, 1998).

3.6.4 Heat-sink Surface Colour

The emissivity of a heat-sink is highly influenced by its surface. Metals that are shiny tend to absorb and radiate a smaller amount of heat whereas black (matte) absorbs more heat. In coolant mediated heat-sinks the contribution of radiation is small, and a thin coating on the heat-sink can impair heat flow from the fins to the coolant due to the thermal resistances from the coating.

3.6.5 Forced Convection Cooling using Fan plus Heat-sink Combination

The size of the heat-sink used to dissipate heat from the TEG module can be decreased considerably if forced convection cooling is used to aid the heat-sink. Reducing the size of the heat-sink will also help reduce the cost factor. A heat-sink's performance while attached to the cold side of a thermoelectric module can be enhanced with proper air circulation. A fan mounted on the heat-sink will help improve the ventilation and achieve a larger ΔT that would aid the module's P_{out}. Thermoelectric modules that are customarily constructed for cooling purposes are best suited for this type of application using a heat-sink (Bruke and Buist, 1984). Thermoelectric power generation occurs when DC passes through the various pairs of N-type and P-type semiconductor materials.

The heat absorbed by a cooling heat sink can be removed from the system by a fan (Tan, 2015). By coupling an axial fan to the heat-sink, the heat energy from the heat-sink and surrounding air will dissipate quicker, cooling the heat-sink whilst also aiding in cooling the cold side (T_c) of the TEG module faster. Integrating a fan to assist the heat-sink during cooling will create a temperature differential between the hot side (T_h) and cold side (T_c) of the TEG module at a faster rate. Figure 3.11 is an example of a fan coupled onto a heat-sink.

3.6.6 TEG cooling using the Peltier Effect for heat extraction

A Peltier module is a semiconductor based thermoelectric cooling device (TEC). Peltier modules are reliable, noiseless and environmentally friendly (Min and Rowe, 1999). The Peltier effect occurs when electrical energy passes through the dissimilar materials and creates a heat flux between the semiconductor junctions. The TEC device transfers heat energy from the cold side to the hot side.

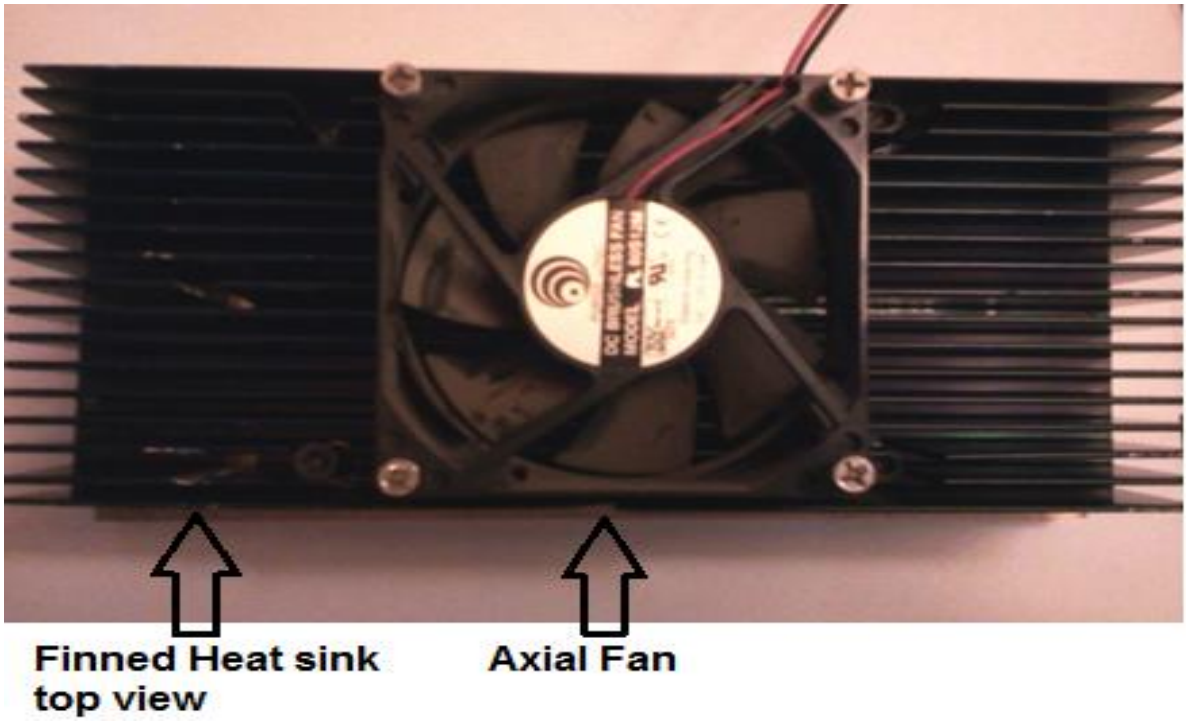

Figure 3.11. Fan plus heat-sink combination.

3.7 THERMOELECTRIC MODULE RELIABILITY: TEG127-50D

The integrity of the thermoelectric modules is dependent on the operation and mean time between failure's (MTBFs). Thermoelectric modules operate at approximately 200,000 hours at ambient temperature before MTBF occurs (Thermoelectric Handbook, 2013). Thermoelectric modules function at a steady state with constant power, heat load and temperature. However, applications involving thermal cycling show a significantly worse MTBFs. Thermoelectric modules exposure to high temperatures must be minimized as much as possible to increase their reliability. Commercial high-temperature modules (TEG127-50D) are rated for 200 °C at normal operating temperature and a maximum temperature of 210°C (www.TeTechnology.com, Accessed Jan. 2014).

Thermoelectric modules are affected by operations at high temperatures above their specifications and the surrounding environment. The module is constructed with nickel-plated copper conductors to electrically connect the thermoelectric pellets to each other as shown in Figure 3.4. The copper has a tendency to diffuse into the thermoelectric material, and this would then degrade the performance of the thermoelectric module. The nickel plating is added to serve as a diffusion barrier to the copper but the nickel is not a perfect barrier, and copper atoms will still diffuse albeit at a much slower rate than if there were no nickel barrier at all. The rate of diffusion typically increases exponentially with temperature. The higher the operating temperature, the more quickly will diffusion occur along with a corresponding degradation in performance. However, in particular with the 80°C module, at 85 °C the solder constituents can begin migrating along cleavage plains of the thermoelectric material due to a theorized minor eutectic reaction (www.TeTechnology.com, Accessed Jan. 2014). This leads to a mechanically weak solder joint and physical expansion of the pellet.

The temperature ratings for the modules are derived from their construction technique. The 80°C module uses solder that melts at 140°C. It has excellent electrical contacts. The 200°C module (TEG127-50D) also has two nickel barriers, a layer of nickel on the copper tab and a layer of nickel on the ends of the pellet. The solder melts at 232 °C for the TEG127-50D modules (www.TeTechnology.com, Accessed Jan. 2014).

3.8 SUMMARY AND CONCLUSION

This chapter has discussed the basic principles of thermoelectric cogeneration. Thermoelectric modules are constructed using semiconductor materials and abide by thermoelectric laws. The dimensions of the module and the number of junctions in the module determined the power output of the module. The following chapter will discuss the performance of the TEG module using different heat sources.

CHAPTER 4

THERMOELECTRIC MODULE CONFIGURATION

4.1 INTRODUCTION

The focus of this chapter is to discuss different cooling methods for thermoelectric modules. We will first establish a suitable heat source for conducting the tests with the TEG modules. For this study, four heat sources, namely an electric cooker plate, LPG cooking gas, biomass in the form of wood and bio-gel heating fuel were tested. The TEG modules is configured in three different configurations and is driven by the heat source. Different cooling systems are also investigated in the following discussions. This chapter is arranged as follows:

Part A discusses the different TEG cooling methods:

Part B looks at how the module can be configured for obtaining maximum efficiency;

Part C discusses the performance of the TEG unit when different heat sources are used.

PART A: TEG COOLING METHODS

4.2 THERMOELECTRIC MODULE COOLING

An adjustable heat source in the form of an electric stove plate was used to heat the TE modules considered in this study. This allowed the tests to be conducted within the TE module's specified thermal operating limits. The following TE cooling methods are utilised during this test:

i) heat sink-blower fan cooling, (ii) heat sink-extractor fan cooling and (iii) heat sink-blower fan combined with Peltier cooling. The most effective and efficient thermoelectric cooling method from the three methods tested will be incorporated as the standard cooling method for further developments in this study. A brief description of these three cooling methods is provided in the following discussions.

4.2.1 TEG cooling with heat sink and blower fan

An axial-flow blower fan was attached to the TEG heat sink to assist the heat sink in dissipating heat away from the reference junction of the TEG module (cf. Figure 4.1). This ensured a greater temperature differential between the hot junction and the cold junction to improve the output of the device. The performance of the TEG module using the heat sink and blower fan cooling combination was monitored over a range of temperatures. The output voltage and current for a range of temperatures are documented in Table 4.1. During these tests the module generated a maximum output voltage V_{TEG} of 3.45V at a maximum current I_{TEG} of 3.070A after 5 seconds, for an average ΔT of 92.37°C.

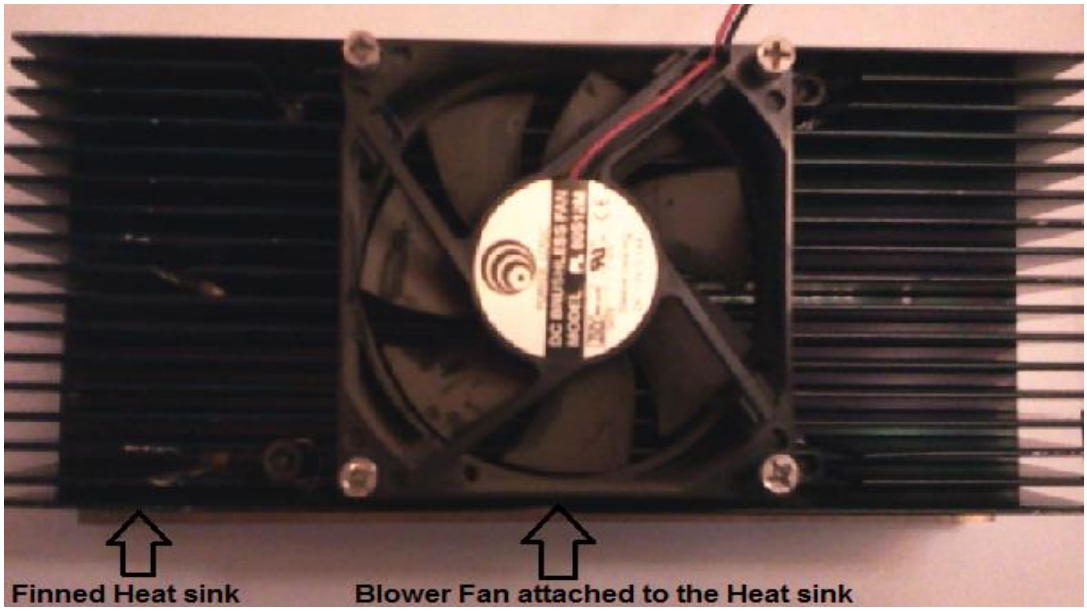

Figure 4.1. Heat-sink blower fan combination.

Table 4.1. Single stage TEG127-50D output currents and voltages using heat sink-blower fan combination (heat source: electric cooker plate).

$T_{hot\ side}$[°C]	$T_{cold\ side}$[°C]	ΔT[°C]	I_{TEG}[A]	V_{TEG}[V]	Time[hh:mm:ss]
26.0	26.0	0.0	0.01	0	*Time 1*: 12:10:30
28.6	26.1	2.5	0.213	0.09	*Time 2*: 12:12:10
44.2	28.6	15.6	0.559	0.54	*Time 3*: 12:13:50
75.1	35.1	40.0	1.693	1.43	*Time 4*: 12:15:30
119.5	48.9	70.6	2.894	2.64	*Time 5*: 12:17:10
144.6	58.0	86.6	3.009	2.99	*Time 6*: 12:18:10
164.7	66.1	98.6	3.061	3.18	*Time 7*: 12:18:50
181.0	73.7	107.3	3.070	3.34	*Time 8*: 12:19:10
196.7	80.8	115.9	3.070	3.44	*Time 9*: 12:20:10
203.0	82.7	120.3	3.070	3.45	*Time 10*: 12:20:30

4.2.2 TEG cooling with heat sink and extractor fan

The blower fan is reconfigured as an extractor fan by reversing the DC polarities. The extractor fan was attached to the heat sink and the TEG module was then exposed to the heat source. The performance of the TEG module over a range of temperatures was monitored. The module's ΔT, V_{TEG} and I_{TEG} is recorded in Table 4.2. The maximum V_{TEG} of the TEG module was recorded at 2.69V at a maximum current I_{TEG} of 2.881A, at an average ΔT of 79.65°C. The maximum safe operating I_{TEG} of 3.070A was not reached due to the inadequate cooling by the heat-sink and extractor fan cooling system.

4.2.3 Comparison of cooling methods: Heat sink-blower fan combination versus heat sink-extractor fan combination

From the Table 4.1 and Table 4.2, we observe that the blower fan provides improved cooling and contributes to an increasing ΔT between the devices hot and cold junctions. This is evident from an analysis of Table 4.1 and Table 4.2 which shows that the cold junction temperature is much lower for the blower fan-heat sink combination than for the extractor fan-heat sink combination.

The average ΔT for the heat sink-blower fan combination is much greater than that of the heat sink-extractor fan combination. This data is illustrated in the graph in Figure 4.2. From Figure 4.2 we observe that faster cooling is provided by the blower fan than the extractor fan cooling system. Figure 4.3 illustrates the currents produced by the heat sink-blower fan combination and the heat sink-extractor fan combination. The maximum I_{TEG} of 3.070A of the module was achieved using the heat sink-blower fan combination after approximately 5 minutes. It is evident that the blower fan cooling system achieves I_{TEG} at a faster rate than the extractor fan cooling system whilst simultaneously maintaining a stable V_{TEG} and I_{TEG} output throughout the duration of the test

procedure. The temperature of the TEG device's cold side $T_{COLD-SIDE}$ was also monitored in order to observe the efficiency of the two cooling systems. The responses are given in Figure 4.3 and illustrate that the heat sink-blower fan combination provides better cooling than the extractor fan cooling system.

Table 4.2. TEG127-50D output currents and voltages using heat sink-extractor fan combination (electric cooker heat source).

$T_{hot\ side}$[°C]	$T_{cold\ side}$[°C]	ΔT[°C]	I_{TEG}[A]	V_{TEG}[V]	Time[hh:mm:ss]
26.5	26.5	0	0.090	0	*Time 1:* 8:57:10
33.4	26.5	6.9	0.159	0.25	*Time 2:* 8:58:10
56.0	37.6	18.4	0.728	0.82	*Time 3:* 8:57:10
84.9	39.4	45.5	2.256	1.38	*Time 4:* 9:02:10
114.9	49.7	65.2	2.607	2.00	*Time 5:* 9:03:50
142.0	60.6	81.4	2.734	2.20	*Time 6:* 9:05:30
165.5	71.3	94.2	2.809	2.40	*Time 7:* 9:07:10
177.8	77.0	100.8	2.848	2.52	*Time 8:* 9:08:10
192.7	84.1	108.6	2.881	2.65	*Time 9:* 9:09:30
202.1	89.1	113.0	2.851	2.68	*Time 10:* 9:10:30

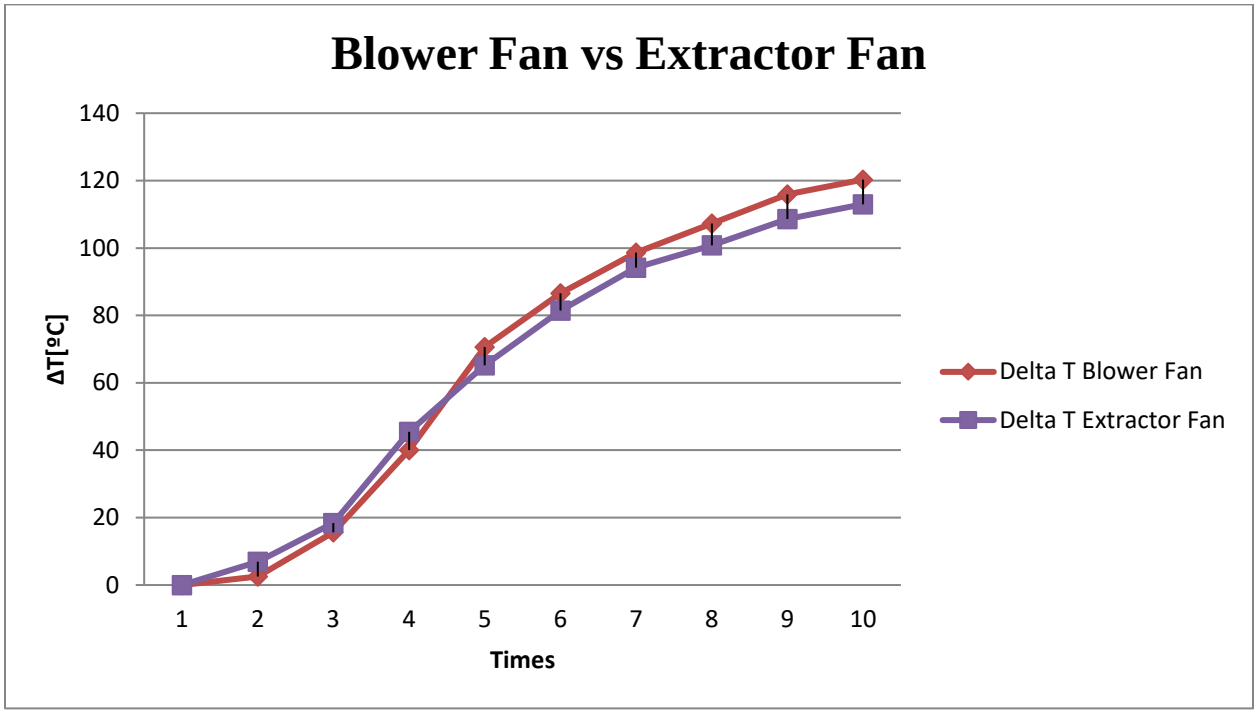

Figure 4.2. Heat sink- blower fan and heat sink-extractor fan cooling systems (cf. Table 4.2).

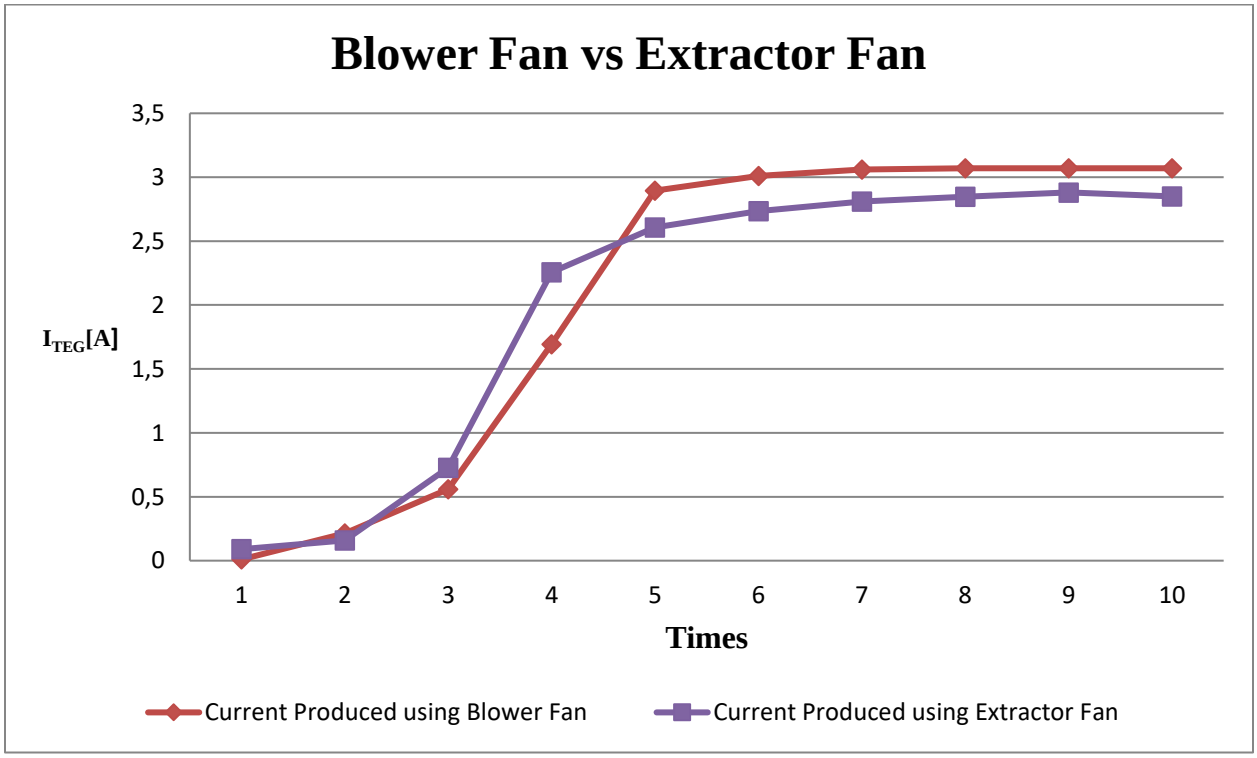

Figure 4.3. TEG currents with heat sink-blower fan and heat sink-extractor fan cooling system (cf. Table 4.2).

4.2.4 TEG cooling using heatsink and blower fan combined with Peltier cooling

The TEG127-50D module can also be used for cooling when connected in the Peltier mode. The device acts as a generator and cooler, depending on how it is configured. The conditions under which the TEG behaves as a generator and cooler is discussed here for convenience to aid the reader.

TEG generator: The TEG acts as a generator when it is operated under forward bias conditions. The device is forward biased when it provides energy to an external device such as a battery under charging conditions. Under these conditions, the negative terminal of the battery is connected to the negative terminal (N-material) and the positive terminal is connected to the positive terminal (P-material). For this connection, the virtual battery existing between the PN sandwich is opposed, leading to a reduction in the physical dimensions of the depletion layers. For the TEG to generate current, a heat source can be applied to the 'hot side' and the opposite side temperature should be maintained constant in order to ensure a large temperature gradient between the hot and cold side. Under these conditions a charging current will be generated to charge a battery or power any other suitable device.

TEG as a Peltier Cooling Device: A TEG device acts as a Peltier cooler when its polarities are reversed. Under reverse polarity conditions the device is reverse biased. This reverse bias increases the strength of the virtual battery and the depletion region, leading to an increased differential within the PN junction. For this configuration no heat source or cooling system is required, unlike in the generator mode. Given this reversed polarity, there is a substantial reduction in current flow through the device, causing it to cool. The module behaves as a source of cooling when connected in this mode.

At an atomic level, within the PN materials itself, electrons will travel from a lower energy stage within the P-type material, through the interconnecting conductor, to a higher energy stage within the N-type material. The heat energy absorbed is conveyed through the semiconductor materials to the hot junction where it is released as the electrons return to a lower energy stage in the P-type material (Min and Rowe, 2001). This is described as the Peltier cooling effect and is a method that can be utilised for module cooling.

Figure 4.4 shows the configuration for the Peltier cooling of a TEG module. With regards to Figure 4.4, the stage 1 module is connected as a generator and a stage 2 module acts as a Peltier cooler to conduct heat from the hot side of the TEG generator. At the Peltier cooler, an external 15 VDC, 1A direct current is injected into the TEG127-50D module to cool the hot side of stage 1. Cooling for the Peltier-heat sink configuration in Figure 4.5 occurs as follows:

The TEG Peltier module conducts heat away from the cold side of stage 1 and the heat absorbed by the Peltier cooler is dissipated by the heat sink.

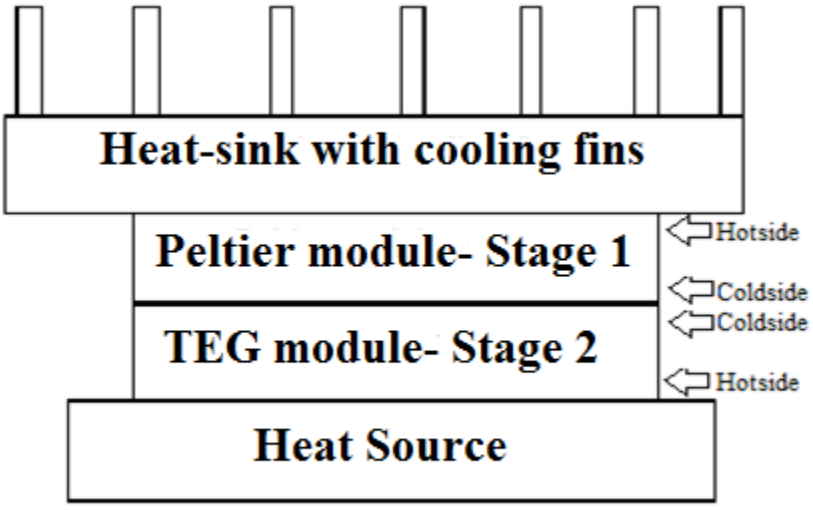

Figure 4.4. Peltier and heat sink-blower fan combination.

Table 4.3 documents the test results from the Peltier cooling system used to improve the temperature differential between the hot and the cold junctions of the TEG. The maximum I_{TEG} produced by the thermoelectric generator is approximately 1.900A at a maximum V_{TEG} of 2.01V. From Figure 4.5, Peltier cooling is more effective at the start of the test. Under Peltier cooling, the modules' cold side cools quicker than with the heat sink-blower fan combination. However, Peltier cooling does not effectively dissipate thermal energy at a rapid enough rate to sustain itself. The heat sink-blower fan cooling system maintains a lower temperature differential than the Peltier and heat sink-blower fan combination as in Figure 4.5. From Figure 4.6, we observe that the faster cooling achieved with the heatsink-blower fan combination allows the module to begin generating electricity faster than with Peltier cooling system. The heatsink-blower fan cooler enables a quicker stable output response for the TEG module to produce stable maximum I_{TEG} of 3.070A; whilst Peltier cooling only produces a maximum I_{TEG} of 1.900A.

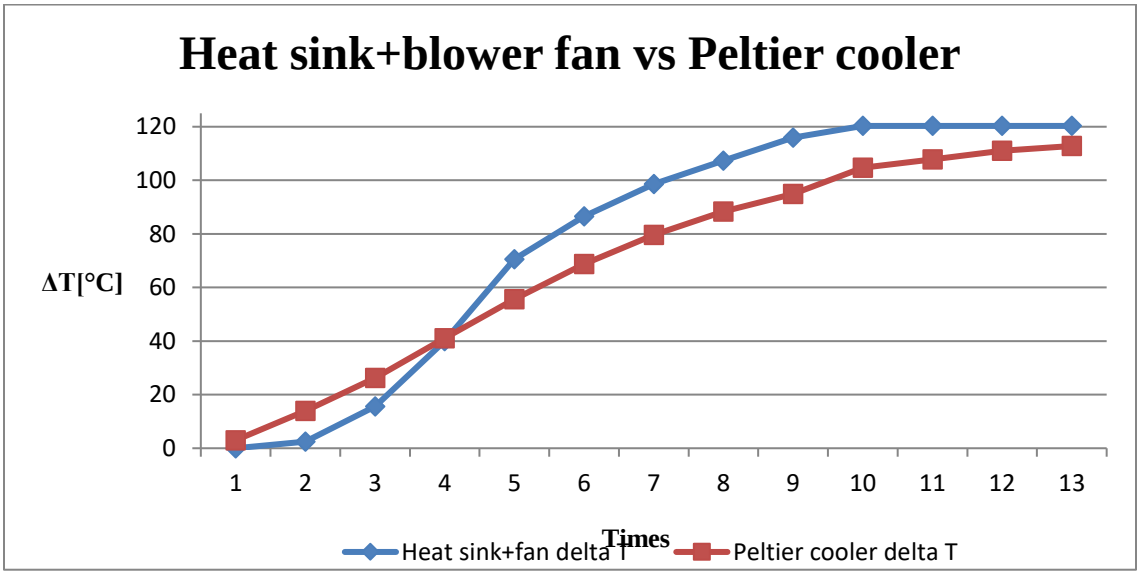

Figure 4.5. Heatsink and blower fan versus Peltier cooler (cf. Table 4.3).

Table 4.3. Peltier cooling values with an injected current of 1 A.

$T_{hot\ side}$[°C]	$T_{cold\ side}$[°C]	ΔT[°C]	I_{TEG}[A]	V_{TEG}[V]	Time[hh:mm:ss]
28.5	25.5	3	0.096	0	*Time 1*: 13:37:02
46.9	33.0	13.9	0.447	0.18	*Time 2*:13:38:42
64.2	38.0	26.2	0.823	0.65	*Time 3*:13:40:22
86.1	45.0	41.1	1.119	0.98	*Time 4*:13:42:02
108.2	52.6	55.6	1.305	1.20	*Time 5*:13:43:42
128.2	59.4	68.8	1.488	1.49	*Time 6*:13:45:22
144.7	65.1	79.6	1.672	1.71	*Time 7* :13:47:02
159.3	71.0	88.3	1.674	1.79	*Time 8*:13:48:42
170.7	75.8	94.9	1.795	1.90	*Time 9*:13:50:22
184.1	79.4	104.7	1.900	2.01	*Time 10*:13:52:47
191.4	83.6	107.8	1.788	1.83	*Time 11*:13:54:27
197.3	86.3	111	1.793	1.88	*Time 12*:13:56:07
200.7	87.9	112.8	1.715	1.72	*Time 13*:13:57:47

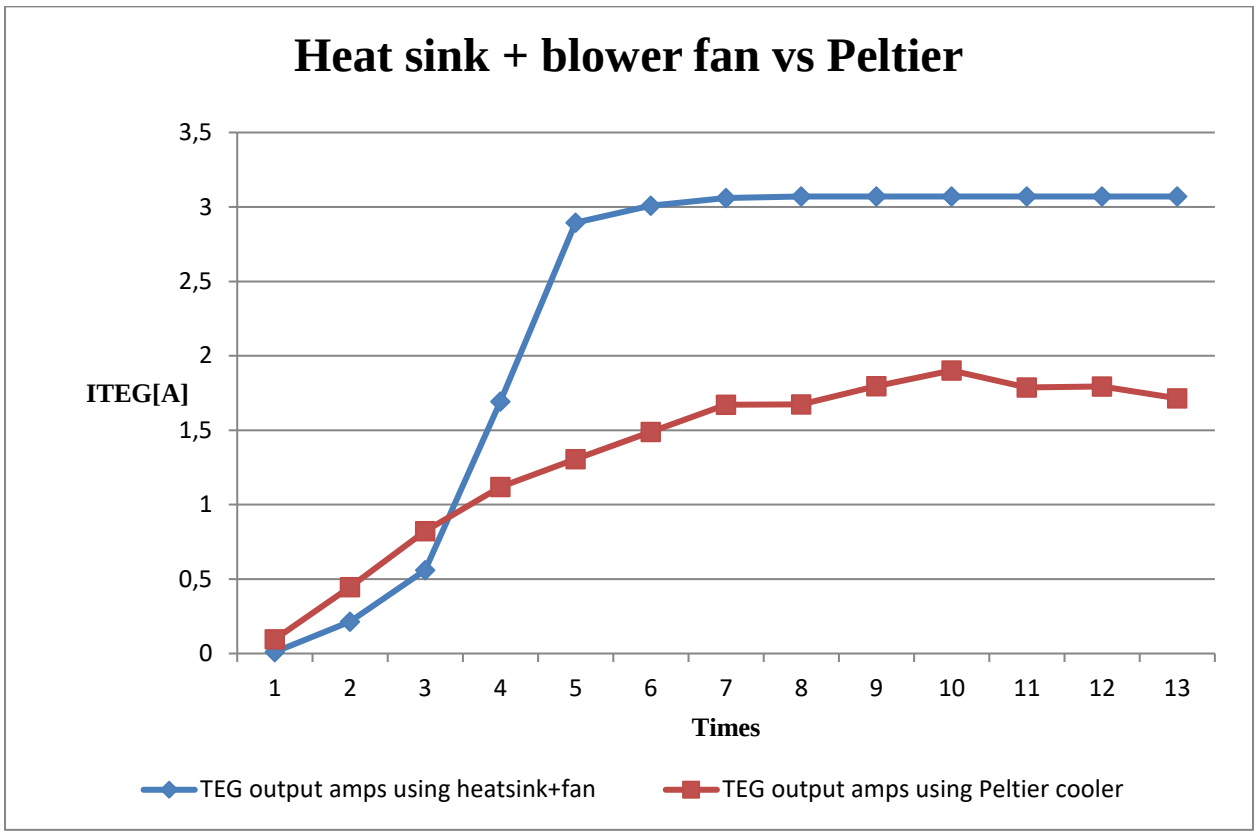

Figure 4.6. Heatsink and blower fan versus Peltier cooler current output (cf. Table 4.3).

PART B: TEG CONFIGURATION

4.2.5 TEG module configuration connection

4.2.5.1 Two-stage TEG module

Two TEG127-50D modules were connected in series as shown in Figure 4.7 to form a two- stage thermoelectric generator. Figure 4.8 illustrates the configuration of the 2-stage modules, including the external power supply that was used to operate the cooling fan. The performance of this 2-stage TEG generator was tested by applying heat from the electric stove cooker plate to the hot side of the TEG127-50D modules. The heat sink-blower fan method of cooling was used to cool the cold side of the TEG127-50D modules. This cooling method was described in section 4.2.1

and was seen to be an efficient method. The test results of the currents and voltages generated by the two-stage TEG127-50D modules are documented in Table 4.4. From Table 4.4 we observe that the two-stage TEG127-50D modules produce a maximum output I_{TEG} of 3.069A. This result is similar to the maximum current produced by the single TEG127-50D module of 3.070A documented in Table 3.1 in chapter 3.

Figure 4.9 illustrates the current curves of a single TEG127-50D module versus that of the two-stage TEG127-50D modules. From Figure 4.10 we observe that the single module cools faster than the 2-stage device and hence generates its maximum current much quicker than the two-stage device. Given that the same cooling system that was used for both devices, the faster cooling of the single stage device is made possible by its smaller surface area of 50mm x 50mm compared to the 2-stage device's larger surface area of 100mm x 100mm.

From Table 4.4, we observe that the maximum V_{TEG} output produced from the 2-stage connected TEG127-50D modules is 6.10V for a temperature difference of 102.5^0C . These results show that the two stage generator produces nearly twice the output voltage for a similar temperature differential shown in Table 4.1.

The current and voltage data given in Table 4.1 and Table 4.4 is illustrated graphically in Figure 4.9 and Figure 4.10, respectively. From Figure 4.10, we can observe that the voltages produced from a single TEG127-50D module increases by ≈75.94% when it is electrically connected in series with another TEG127-50D module to form a two-stage thermoelectric generator. It is important to note that the I_{TEG} of the two-stage connected TEG127-50D modules remain the same as the single TEG127-50D module when the TEG127-50D modules were operated within its manufacturers specified limitation of 210°C on the hot side due to the thermoelectric modules series connection (www.everredtronics.com, Accessed Jan. 2014). This is so because when we

connect these modules in series, the output voltage represents the algebraic sum of the voltage generated by each module; the current remains relatively unchanged because the surface area of the PN junctions do not change.

Figure 4.7. 2-stage modules connected in series.

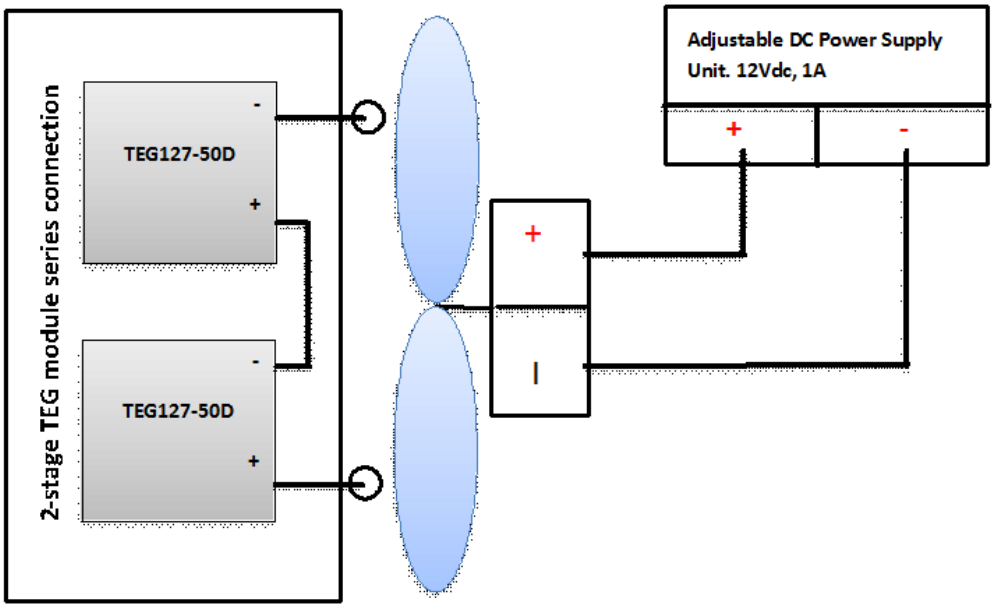

Figure 4.8. 2-stage series connected TEG modules using electric heat source.

Table 4.4. Currents and Voltages produced with the two stage TEG127-50D module and heatsink-blower fan cooling.

$T_{hot\ side}$[°C]	$T_{cold\ side}$[°C]	ΔT[°C]	I_{TEG}[A]	VTEG[V]	Time[hh:mm:ss]
26.4	24.6	1.8	0.010	0.47	*Time 1:* 11:10:44
40.1	29.0	11.1	1.014	1.31	*Time 2:* 11:12:44
73.4	42.6	30.8	1.683	2.13	*Time 3:* 11:14:04
90.6	47.7	42.9	2.212	2.83	*Time 4:* 11:15:44
107.2	54.5	52.7	2.550	3.39	*Time 5:* 11:17:24
122.0	61.8	60.2	2.731	3.79	*Time 6:* 11:19:04
135.2	68.1	67.1	2.859	4.52	*Time 7:* 11:20:44
164.9	83.3	81.6	3.069	5.40	*Time 8:* 11:22:24
186.2	90.5	95.7	3.069	5.83	*Time 9:* 11:24:04
200.0	97.5	102.5	3.070	6.10	*Time 10:* 11:27:24

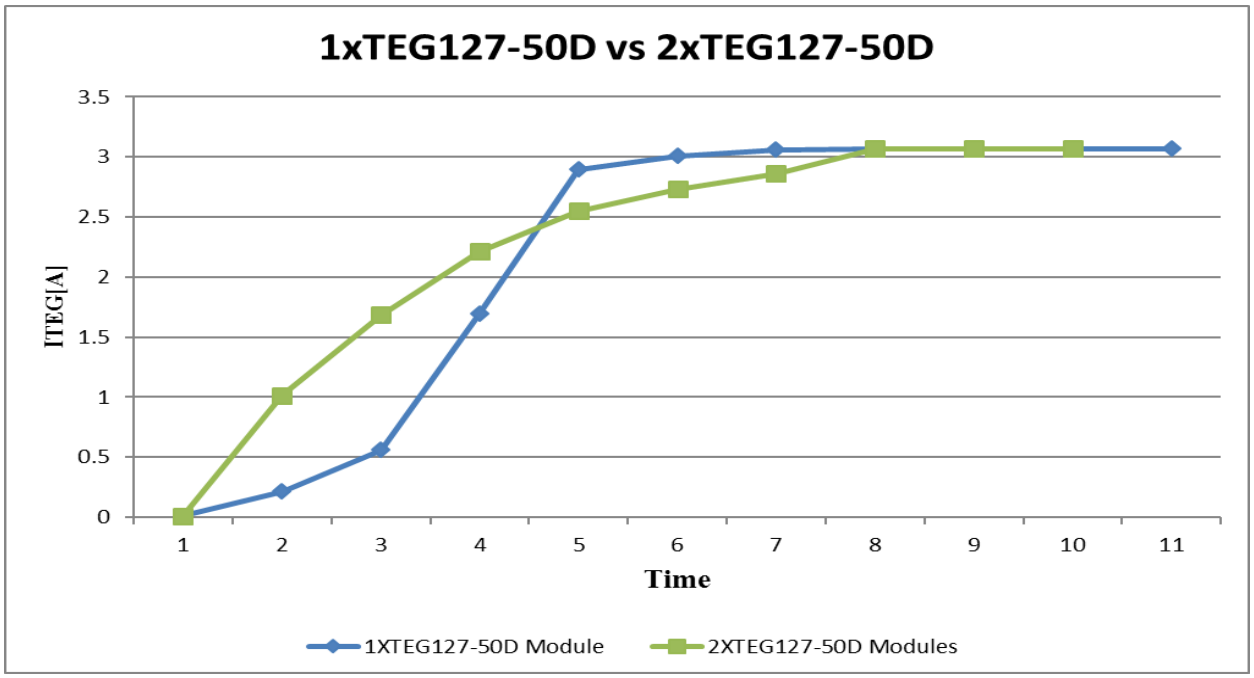

Figure 4.9. Current curves: Single-stage vs two-stage TEG modules (cf. Table 4.1 and Table 4.4) using blower fan and heat-sink cooling combination.

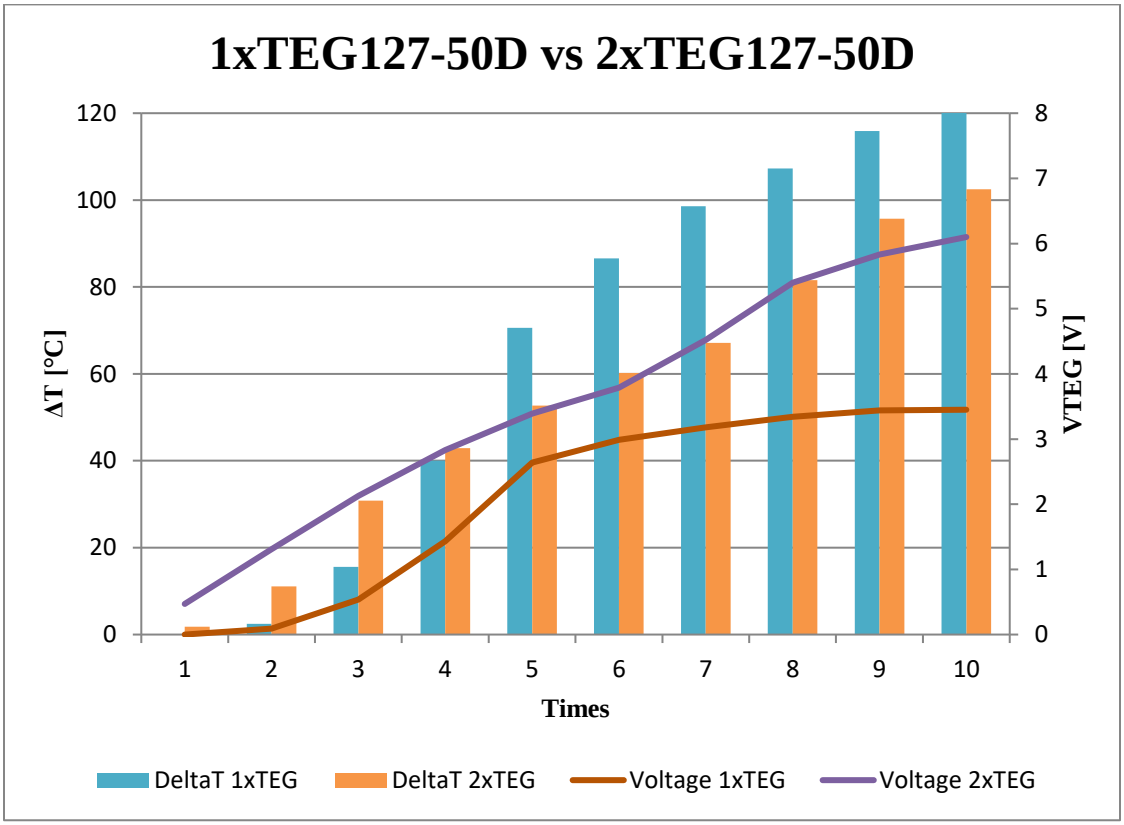

Figure 4.10. Voltage Curves: Single stage modules vs Two-stage modules (cf. Table 4.1 and Table 4.4).

4.2.5.2 Four-stage TEG module

For this experiment four TEG127-50D modules were connected in series as shown in Figure 4.11 to form a 4-stage TEG module. The TEG unit was wired using a 4-stage series connection as shown in Figure 4.12. The four thermoelectric modules charge the 2 sets of rechargeable battery banks (battery bank 1 and battery bank 2) within the circuit. The both batteries are connected in series with each other while they are connected to the input of the buck-boost convertor unit. Both the batteries supply the buck-boost convertor with an input voltage of 7 VDC. This voltage of 7VDC is converted to 13VDC at the output of the buck-boost convertor. The both batteries are also responsible for the powering of the direct current fan used in the cooling system of the thermoelectric modules.

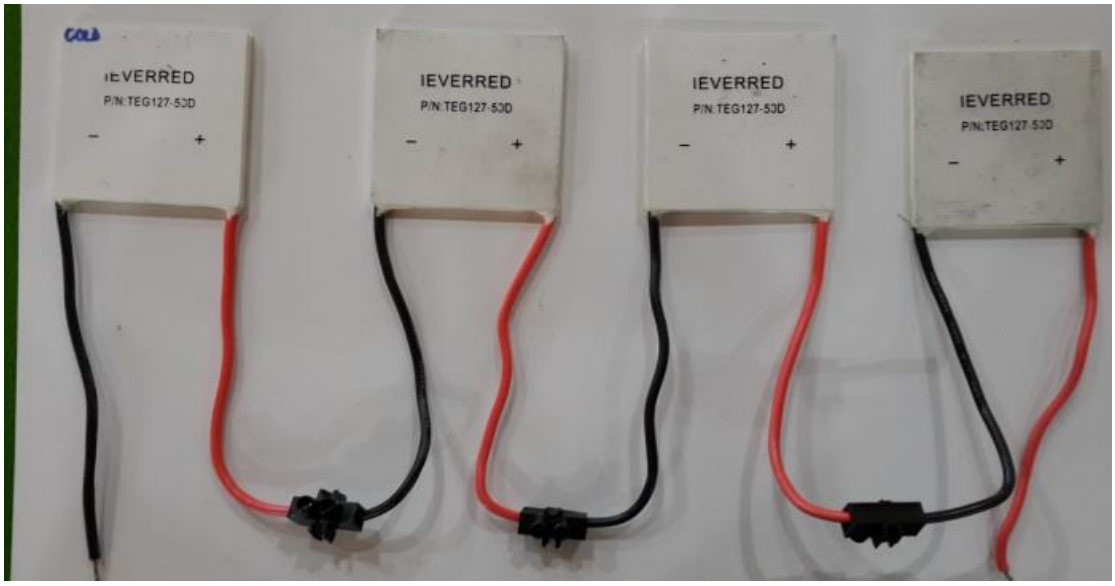

Figure 4.11. 4-stage modules connected in series.

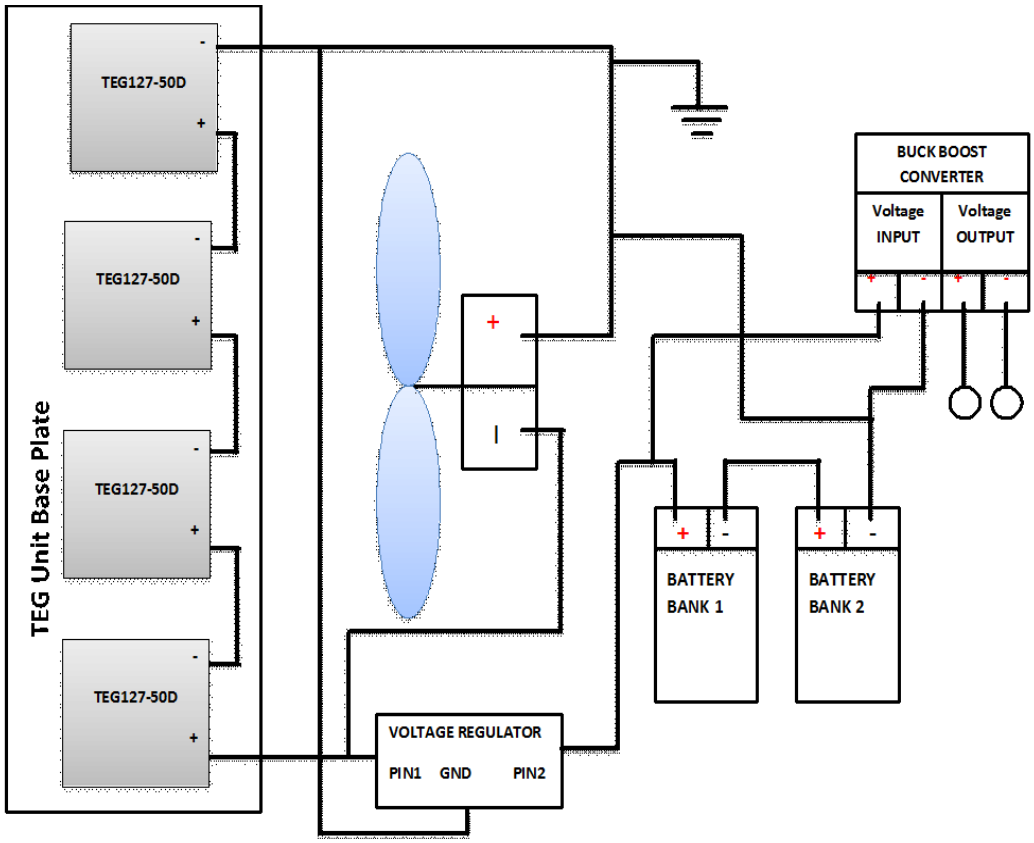

Figure 4.12. Schematic layout of the TEG unit with a 4-stage connection using electric heat source.

The thermal generating performance of this 4-stage device was tested using an electric stove plate as a heat source within an ambient temperature controlled environment. The 4-stage generator is tested under similar conditions that were described for the 2-stage generator mentioned in the previous discussions. The currents and voltages generated by the 4-stage connection TEG modules are shown in Table 4.5 and the corresponding current and voltage graphs are given in Figure 4.13 and Figure 4.14, respectively. From these graphs we observe the following:

The maximum I_{TEG} output produced by the two-stage and the four-stage TEG modules is 3.070A for the 2–stage unit and 3.069A for the 4-stage device. This constant I_{TEG} is a result of the series connection between the thermoelectric modules. The current curve shows that the two-stage connected TEG127-50D modules has a quicker response time than the four-stage modules due to the increased cooling effect of the blower fan over its smaller hot surface area. This allows the two-stage modules to cool at a more rapid rate and begin thermoelectric generation much quicker.

From Table 4.5, a maximum V_{TEG} output of 7.55V occurs at 205.0°C at the hot side of the 4-stage modules. The maximum V_{TEG} output of the 2-stage modules described in Table 4.4 was 6.10V at 200.0°C. The maximum V_{TEG} output increase from the 2-stage connected TEG127-50D modules to the 4-stage connected TEG127-50D is 1.42V, corresponding to ≈ 23.39%. This was achieved by electrically connecting four TEG127-50D modules in series. The I_{TEG} output of the 4-stage device remains unchanged at 3.069A (cf. Table 4.1 for 1-stage and Table 4.5 for 2-stage). This constant current is attributed to the size of the PN junction surface area remaining unchanged when the device is connected in series.

Table 4.5. Currents and voltages produced in the 4-stage series arrangement.

$T_{hot\ side}$ [°C]	$T_{coldside}$ [°C]	ΔT [°C]	I_{TEG}[A]	V_{TEG}[V] (modules)	V_{OUT}[V] (BuckBooster)	Time[hh:mm:ss]
20.5	20.4	0.1	0.10	0.02	0	*Time 1:*15:02:11
24.9	21.0	3.9	0.38	0.20	0	*Time 2:*15:02:51
36.0	22.5	13.5	0.778	0.68	0	*Time 3:*15:03:51
45.6	24.5	21.1	0.987	1.10	0	*Time 4:*15:04:31
70.1	31.9	38.2	1.649	2.16	0	*Time 5:*15:06:11
91.5	40.7	50.8	2.249	3.16	0	*Time 6:*15:07:51
125.6	51.5	74.1	2.854	4.66	0	*Time 7:*15:09:31
168.5	66.7	101.8	3.039	6.43	0	*Time 8:*15:11:11
205.0	86.0	119	3.069	7.55	11.59	*Time 9:*15:12:51
202.0	99.1	102.9	3.069	7.49	11.48	*Time 10:*15:14:31

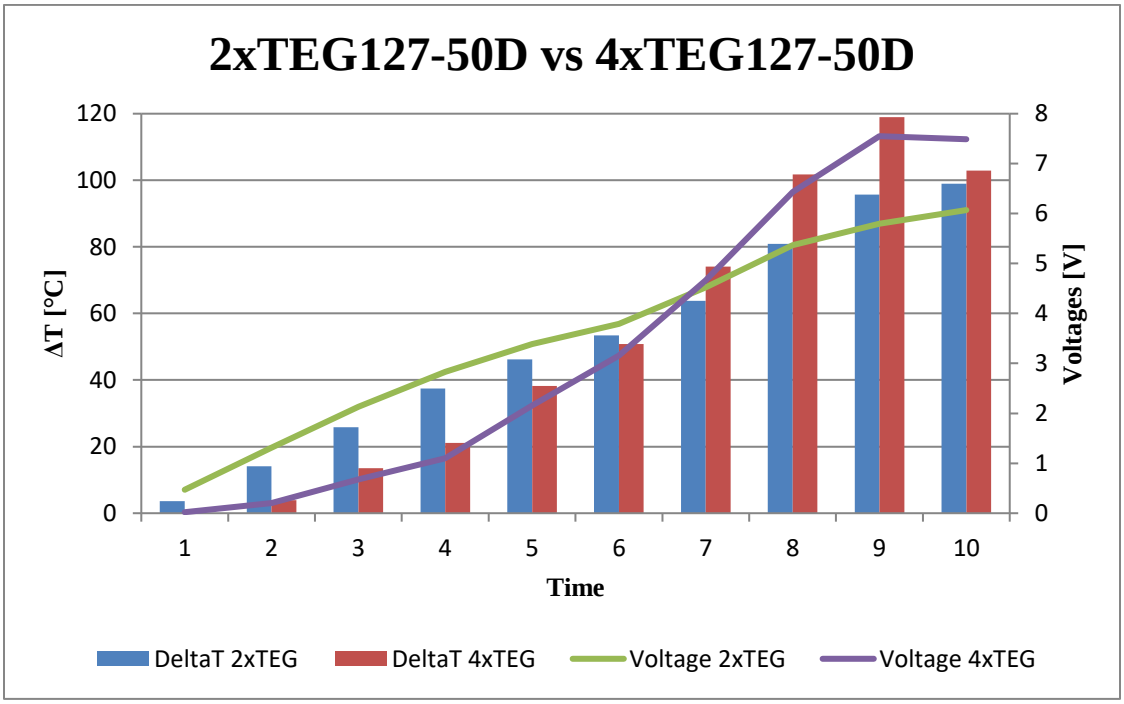

Figure 4.13. Voltage vs temperature responses for 2 stage and 4 stage units (cf. Table 4.5).

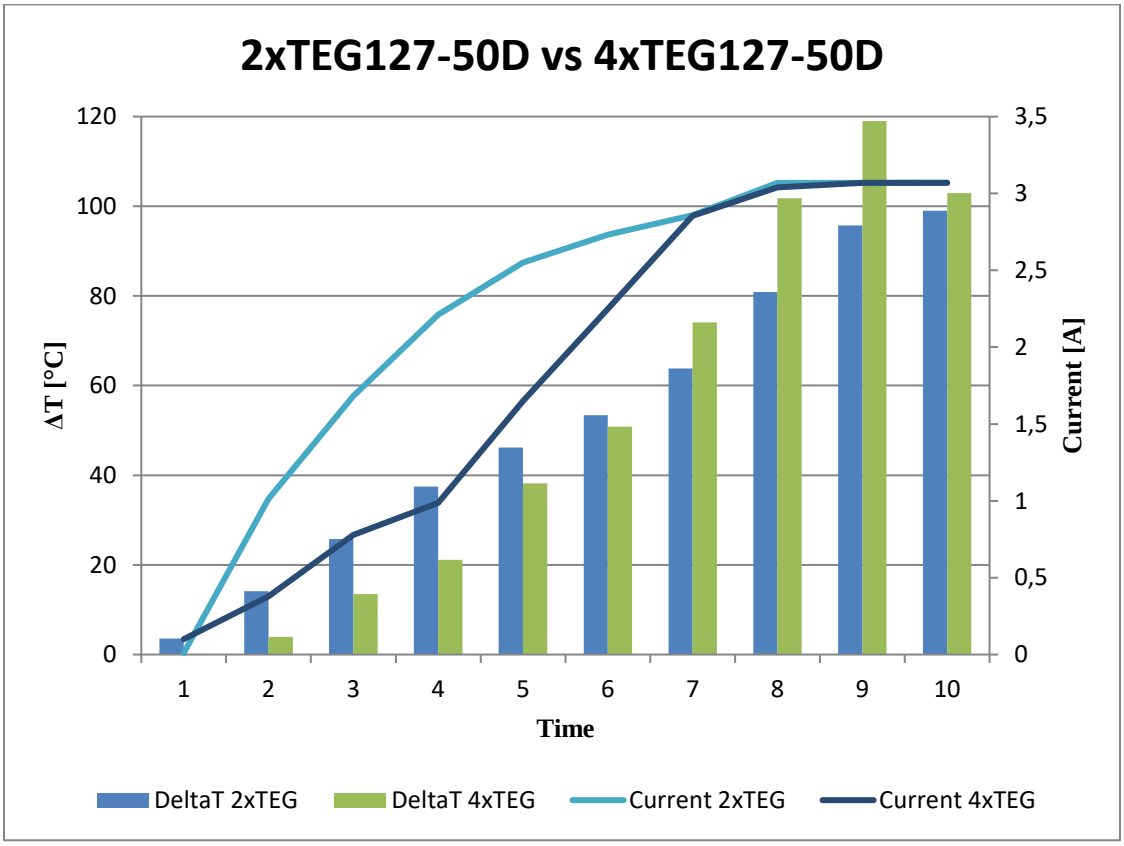

Figure 4.14. Current vs temperature responses for 2 stage and 4 stage units (cf. Table 4.5)

PART C: HEAT SOURCES

4.4 GEL FUEL TEG UNIT TEST

Combustible gel fuel (cf. Figure 4.15) was used to test the thermal generating properties of the 4-stage TEG unit. Gel fuel is an alternative fuel source to paraffin and LPG for cooking in South Africa (Lloyd and Visagie, 2009). Gel fuel is made from renewable agricultural sources rather than fossil fuels and burns clean with very low CO_2 emissions (Greenheat, 2014).

Figure 4.15. Greenheat Gel (www.Greenheat.co.za, Accessed Jan. 2014).

For these tests, we powered a bioheat stove in Figure 4.17 with the gel fuel (cf. Figure 4.16). The bioheat stove is manually adjustable with 4 settings to control the size of the flame. The Greenheat gel fuel is spontaneously combustible with a flame source and the blue flame generated from the Greenheat gel is smokeless but not odourless. The TEG unit was placed over the bioheat stove plate with the manual adjustment set on maximum flame. A paperless recorder in Figure 4.17 monitors and records the temperatures, voltages and currents produced by the TEG module.

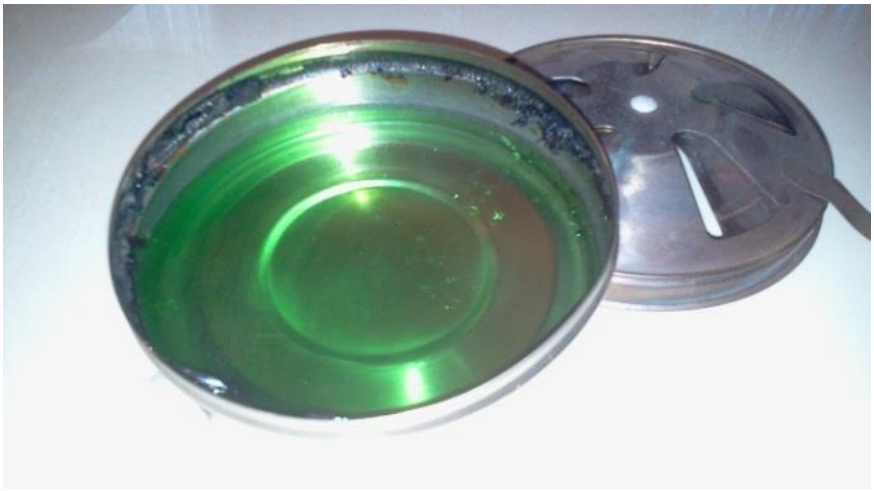

Figure 4.16. Greenheat gel fuel inserted within a bioheat plate.

Figure 4.17. TEG unit on the bioheat stove test.

The graphs in Figure 4.18 and Figure 4.19 represent the measureable variables from the TEG unit during the bioheat gel fuel test. The measureable variables from Figure 4.18 and Figure 4.19 were extrapolated from Table 4.6. From these graphs, we observe that although the thermoelectric

module cooling system remains stable, the heat generated by the gel fuel produced 2.23VDC and is insufficient to drive the buck-boost converter.

Table 4.6. Measureable variables of the TEG unit bioheat gel test.

$T_{hot\ side}$ [°C]	$T_{cold\ side}$ [°C]	ΔT [°C]	I_{TEG}[A]	V_{TEG}[V] (Modules)	V_{OUT}[V] (buck-boost)	Time[hh:mm:ss]
36.8	24.7	12.1	0.15	0.68	0	*Time 1:*13:08:31
71.5	29.5	42.0	0.29	2.15	0	*Time 2:*13:10:11
82.4	37.7	44.7	0.654	2.16	0	*Time 3:*13:11:51
88.1	43.4	44.7	0.801	2.17	0	*Time 4:*13:13:31
90.2	47.2	43.0	1.345	2.17	0	*Time 5:*13:15:11
93.8	49.7	44.1	1.480	2.17	0	*Time 6:*13:16:51
96.1	51.0	45.1	1.559	2.17	0	*Time 7:*13:18:31
101.3	51.7	49.6	1.619	2.18	0	*Time 8:*13:20:11
101.4	52.1	49.3	1.759	2.23	0	*Time 9:*13:20:31
108.3	53.7	54.6	1.549	2.17	0	*Time 10:*13:29:25

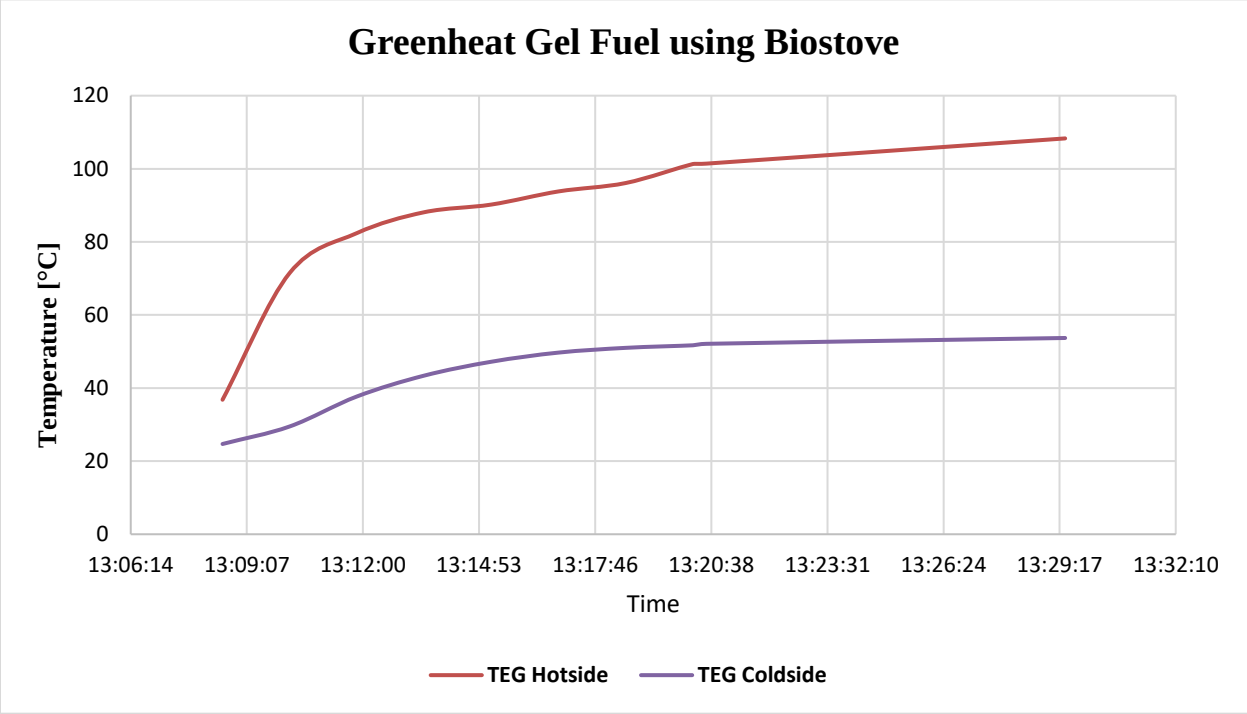

Figure 4.18. Temperature of the TEG unit bioheat gel test (cf. Table 4.7).

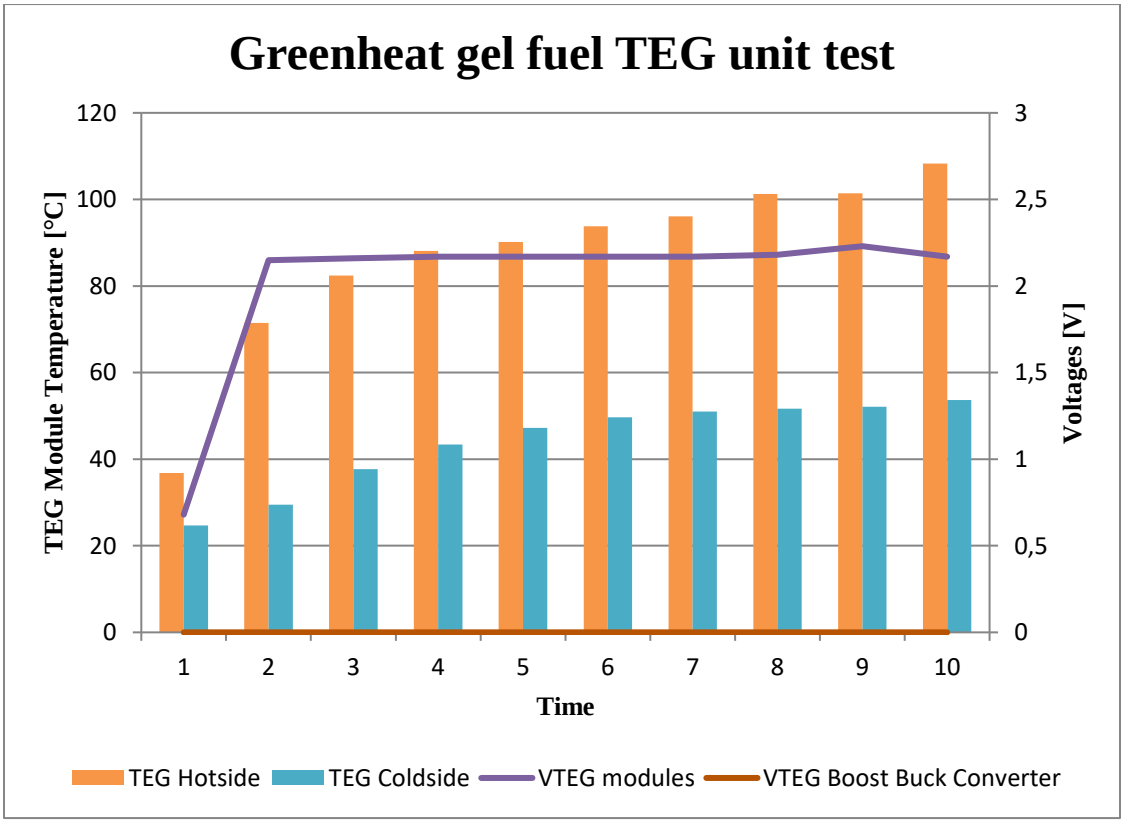

Figure 4.19. The voltages produced by the 4-stage unit (cf. Table 4.7).

The tests using the gel stove has shown that the heat energy produced using the gel fuel is inadequate for producing sufficient thermal energy for conversion into electrical energy. This conclusion is drawn from Table 4.6 and Figure 4.18 which show the maximum temperature produced by the gel was 108.3ºC. The maximum temperature of 108.3ºC was also recorded at the 'hot side' of the thermoelectric modules, with a corresponding temperature of 53.7ºC at the cold side. The ΔT of the TEG module reached 54.6ºC. Figure 4.19 draws comparison between the hot side and cold side of the TEG modules. From Figure 4.19, the cold side illustrates an efficient cooling system under the lower heat energy test conditions. The line graph in Figure 4.19 shows a steep voltage response at the beginning of the test while settling into a steady response as the heat energy emitted from the gel fuel reaches its maximum temperature at a medico 108.3ºC. The maximum V_{TEG} produced by the TEG unit during the test was only 2.23VDC. This value is insufficient for activating the buck-boost convertor circuit which has been calibrated at 7VDC at its input to produce a constant V_{TEG} output of 13.8VDC. Therefore, a 0 VDC at the TEG unit output was achieved since the buck-boost convertor was not activated. The results obtained from the test conducted using the Greenheat gel fuel have provided evidence that the gel fuel does not generate adequate heat energy for thermoelectric generation. The gel fuel has very little energy and requires a large quantity of gel fuel to produce a small amount of heat energy (Lloyd and Visagie, 2009).

4.5 TEG UNIT TESTING USING LPG POWERED HEAT SOURCE

In this section the discussion is based on the performance of the 4-stage TEG unit when LPG gas is used as to heat the hot side of the generator. Only the 4-stage unit is discussed from this point onwards because it generated sufficient voltage to operate the boost-buck converter.

A test was conducted using a single plate LPG stove as shown in Figure 4.20. The flame is controlled by a manual hand ball valve. The temperature and size of the flame was increased gradually until the manufacturer specified temperatures were reached. With regards to Figure 4.20, a fin heat sink radiates thermal energy away from the cold side of the thermoelectric modules and a direct current axial-flow fan supplements the cooling system.

The test result of the currents and voltages generated by the 4stage unit with LPG gas as the heat source is shown in Table 4.7.

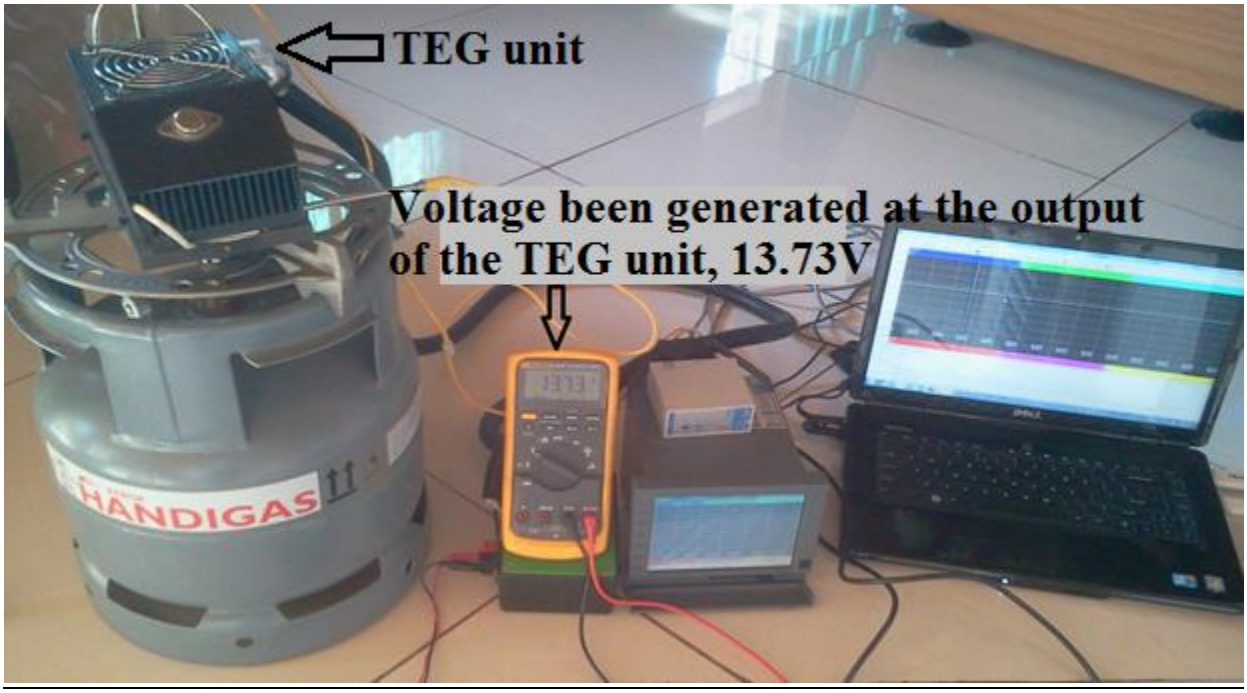

Figure 4.20. TEG unit setup with test equipment.

Table 4.7. Measureable variables of the TEG unit with the LPG heat source.

$T_{hot\ side}$ [°C]	$T_{cold\ side}$ [°C]	ΔT [°C]	I_{TEG}[A]	V_{TEG}[V] (modules)	V_{OUT}[V] (buck-boost)	Time[hh:mm:ss]
80.4	68.8	11.6	0.690	5.20	0	*Time 1:*10:00:06
170.4	71.4	99.0	3.021	7.19	0	*Time 2:*10:00:46
254.7	74.4	180.3	3.069	8.33	7.29	*Time 3:*10:01:46
298.2	76.8	221.4	3.070	9.15	9.98	*Time 4:*10:02:06
308.8	78.7	230.1	3.070	9.45	10.83	*Time 5:*10:03:26
340.8	80.3	260.5	3.070	9.65	13.74	*Time 6:*10:04:06
291.3	79.1	212.2	3.070	8.41	11.85	*Time 7:*10:04:46
225.6	75.6	150.0	3.069	6.09	0	*Time 8:*10:05:06
198.7	72.6	126.1	3.058	3.97	0	*Time 9:*10:05:26
169.1	69.4	99.7	3.018	2.20	0	*Time 10:*10:05:46

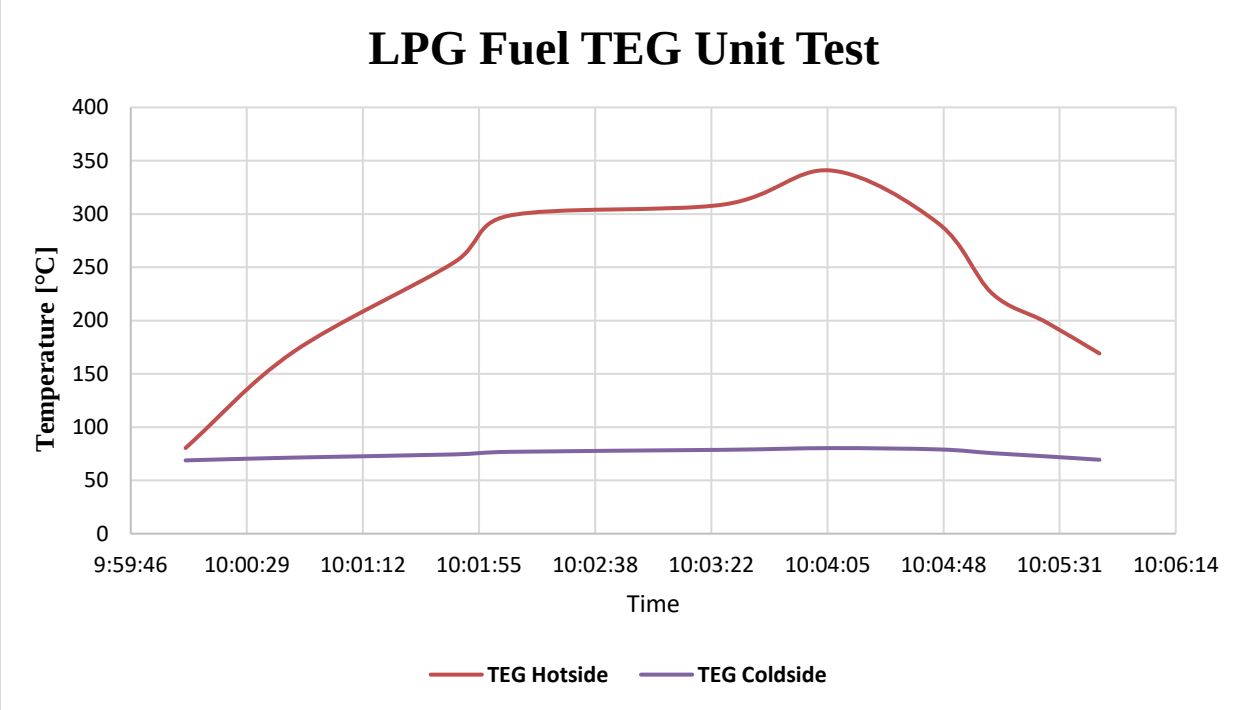

Figure 4.21. 4-Stage unit temperatures with LPG heat source.

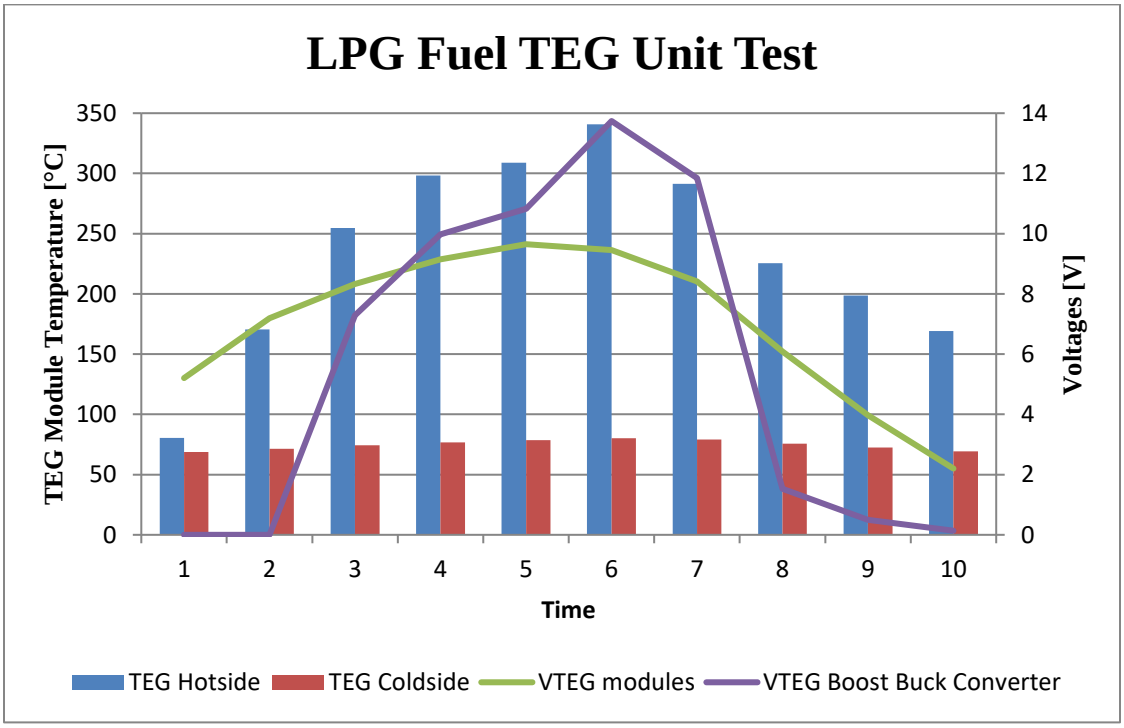

Figure 4.22. The voltages produced by the TEG modules and output of the unit.

The responses in Figure 4.21 represent the comparison of the temperatures of the hot side and cold side of the 4-stage connected TEG modules. A maximum hot side temperature of 340.1°C is reached within four minutes. This temperature produced a voltage (V_{TEG}) of 9.65V generated by the 4-stage connected TEG modules and the final output from the buck-boost converter (V_{OUT}) 13.74V. From Figure 4.22, we observe that the steep hot side temperature slope indicates the LPG provides sufficient heat energy to reach the desired operating temperatures. The gentle horizontal slope response of the cold side illustrates an efficient cooling system aided by the cool surroundings temperatures. Figure 4.22 draws a comparison between the line graph representing the voltages (V_{TEG} and V_{OUT}) generated by the 4-stage TEG modules as the final output from the buck-boost converter and the bar graph representing the hot side and cold side temperatures. The TEG unit demonstrated positive results using LPG as a thermal source of energy.

4.6 WOOD FUEL TEG UNIT TEST

There is an intensifying plea to use biomass as an energy source to moderate the emissions of greenhouse gases as well as to introduce biomass as a renewable energy source (Moser *et al*., 2006). Within the recent years, small scale pellet boilers and pellet stoves have made advances within the European states (Moser *et al*., 2006). They provide CO_2-balanced heat in a comfortable and environment-friendly way (Moser *et al.,* 2006). Wood is an excellent and cheap alternate source of industrial as well as domestic fuel. Wood is available in many forms such as firewood, pellets and sawdust. They have been used for centuries by humans for both cooking, sources of heating and lighting in households.

Firewood in Figure 4.23 was used as a source of fuel for the test with the TEG unit. The firewood was placed into a mild steel metal base stove as in Figure 4.23. The TEG unit was placed over the firewood stove as shown in Figure 4.23. The TEG unit was exposed to the open flame of the fire. The flame temperature was not adjusted during the test and the maximum heat energy of the fire was exerted onto the TEG unit. The measured variables such as the module's temperatures, voltages and currents were documented during the testing procedure.

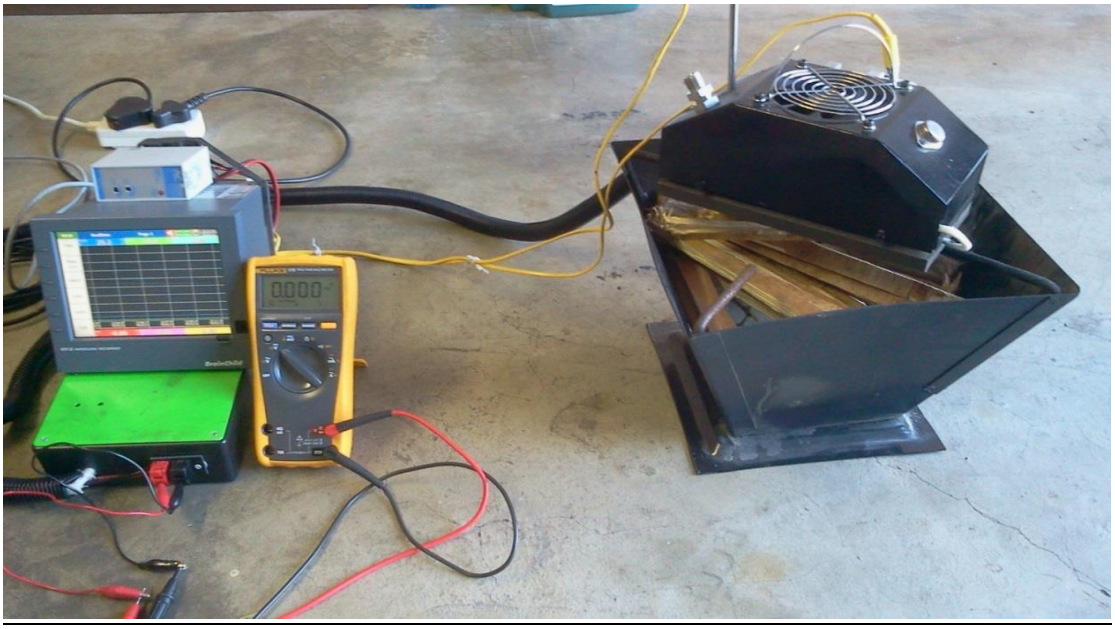

Figure 4.23. TEG unit test on firewood stove.

Table 4.8. Measurable variables for the TEG unit.

$T_{hot\ side}$[°C]	$T_{cold\ side}$ [°C]	ΔT [°C]	I_{TEG}[A]	V_{TEG}[V] (modules)	V_{OUT}[V] (Boost-buck)	Time[hh:mm:ss]
52.3	28.5	23.8	0.768	1.09	0	*Time 1:*13:47:21
154.6	31.2	123.4	1.654	2.27	0	*Time 2:*13:48:41
203.1	39.4	163.7	3.069	9.26	10.00	*Time 3:*13:49:21
228.1	50.1	179.7	3.069	12.16	13.72	*Time 4:*13:50:21
232.1	48.4	183.7	3.069	12.15	13.72	*Time 5:*13:50:41
167.3	53.4	113.9	3.069	9.55	13.72	*Time 6:*13:51:21
136.6	55.1	81.5	3.012	6.69	4.45	*Time 7:*13:51:41
123.8	55.7	68.1	2.289	3.42	1.07	*Time 8:*13:52:01
113.2	56.0	57.2	1.598	2.22	0.38	*Time 9:*13:52:21
112.2	56.0	56.2	1.594	2.21	0.35	*Time 10:*13:52:41

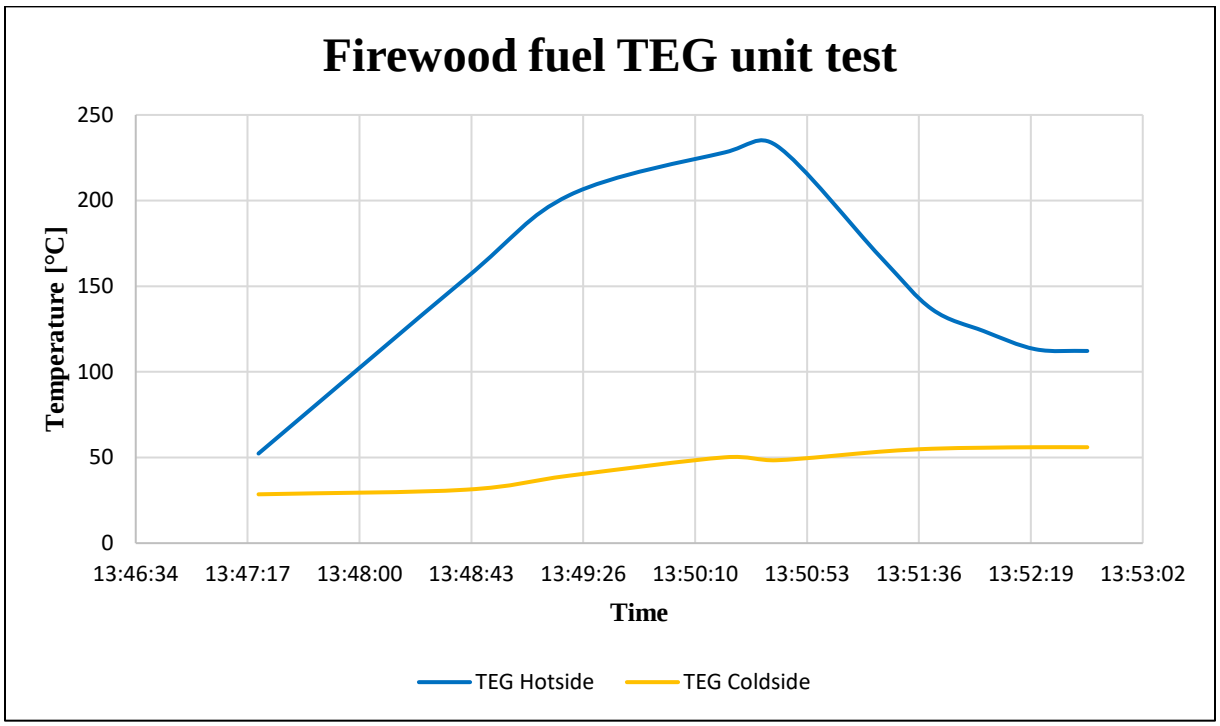

Figure 4.24. TEG temperatures with biomass heat-source (cf. Table 4.8).

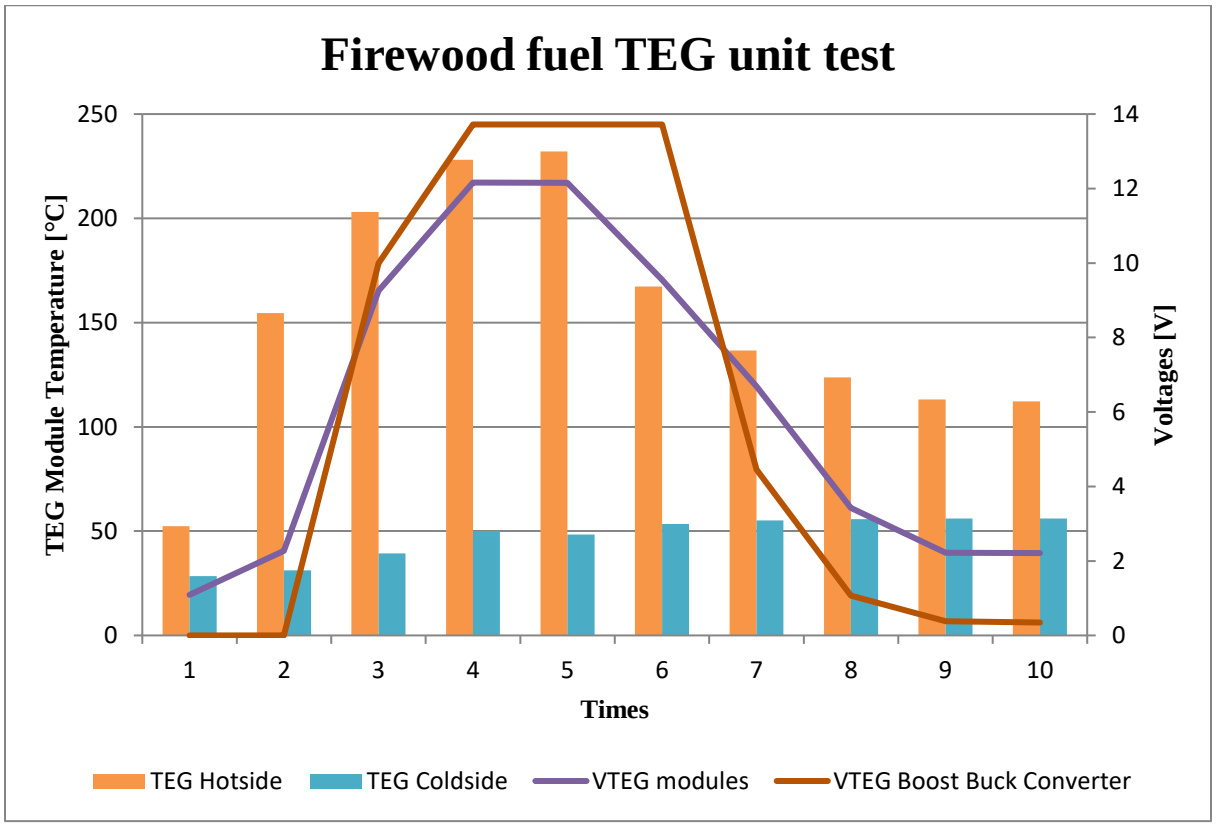

Figure 4.25. The voltages produced at the TEG unit (cf. Table 4.8).

From studying the firewood fuel test results, we observe that the heat energy generated from the firewood fuel produced adequate thermal energy for conversion into usable electrical energy. The measurable variables in Table 4.8 shows a maximum temperature of 228.1°C was reached within 3 minutes. A voltage (V_{OUT}) of 12.16V was generated by the 4-stage TEG modules (V_{TEG}) and 13.72V was generated at the output of the buck-boost converter. With reference to Figure 4.24, from the gradual vertical increase in the hot side graph, it is evident that the wood fuel produces adequate heat energy for the hot side of the TEG modules. A gentle horizontal slope response of the cold side illustrates an efficient cooling system aided by the cool surroundings temperatures (cf. Figure 4.27). Figure 4.25 draws a comparison between the 4-stage TEG modules as the final output from the buck-boost converter and the bar graph representing the hot side and cold side temperatures. The rapid vertical response curves from the TEG unit output voltages (V_{TEG} and V_{OUT}) confirms wood fuel to be an adequate source of heat energy for powering the TEG unit and converting the heat energy into electrical energy under these test conditions.

4.7 SUMMARY AND CONCLUSION

From the discussions on the experiments described in this chapter, it was found that the most challenging aspect of the design is the cooling of the TEG unit. Following from the experiments, we found that the heatsink and blower fan cooling combination has achieved the most efficient differential temperatures, and produced the manufacturer's specified current and voltage outputs.

Besides the cooling, another focus area of the study was to increase the module's output voltage, whilst simultaneously maintaining a stable current. To this end, we configured the modules in series as single-stage, two-stage and four-stage connections. These series connections achieved the objective of increasing the TEG voltage output whilst maintaining a constant output current.

Various household fuels were also investigated to explore the potential of the TEG unit for domestic applications. The results of these tests are as follows:

i. *Gel fuel:* Gel fuel has a low calorific value and did not generate sufficient thermal energy for thermoelectric conversion. The TEG unit failing to produce sufficient current to drive the boost-buck converter.

ii. *LPG and Biomass*: These fuels produced maximum output currents and voltages from the TEG module, irrespective of the configuration.

The study described in this chapter has provided sufficient proof that if a suitable heat source is used, the TEG module has the potential to generate sufficient electrical energy to power a suitable low energy device.

CHAPTER 5

PROTOTYPE

5.1 INTRODUCTION

Emissions such as hot exhaust gases from boilers and furnaces, and excess steam are commonly found in modern industrial installations. These emissions are potential heat sources to drive a TEG module. However, careful consideration should be exercised when utilizing a TEG module for applications like these that have the potential for driving the module beyond its safe operating parameters.

TEG units are available in two variants, namely a commercial unit and an industrial type. This chapter will describe the tests that were first performed with a commercial TEG device and then with an industrial type.

5.2 COMMERCIAL MODULE TEG 127-50D TEST

A commercial TEG unit (127-50D) was tested within a boiler environment of a sugar mill situated in Kwazulu-Natal, South Africa. The boiler environment is a harsh environment for a commercial TEG module, as was evident from the high ambient temperature of approximately 60^0C to 70^0C that persisted during the tests.

Boiler-Environment Test 1: A 4-stage commercial TEG module (previously described in detail in section 4.3.5.2 of Chapter 4) with the buck-boost converter shown in Figure 4.12 was mounted

on the boiler drum. The buck-booster converter is calibrated to switch on at 7.0 VDC. For this test the module is mounted onto the boiler drum and the performance of the device under these conditions is given in Table 5.1. From Table 5.1 we observe the following:

- The buck-booster is calibrated to switch over a range of 7VDC to 13VDC. It produces an output voltage for V_{TEG} above 7VDC and remains inactive for any V_{TEG} lower than 7VDC.
- The TEG output decreases for $\Delta T > 100^0C$. This could be attributed to the failure of the semiconductor junction caused by poor cooling (cf. Table 5.1 and Figure 5.1).

Table 5.1. TEG 127-50D voltage test within the boiler house at Illovo Sugar, Eston Mill.

$T_{hot\ side}$ [°C]	$T_{coldside}$ [°C]	ΔT [°C]	I_{TEG}[A]	V_{TEG}[V] (Modules)	V_{OUT}[V] (buck-boost)	Time[hh:mm:ss]
70.1	46.0	24.1	0.765	2.16	0	*Time 1:* 18:46:20
74.8	58.2	16.6	0.669	2.15	0	*Time 2:* 18:46:45
77.6	70.0	7.6	0.401	2.19	0	*Time 3:* 18:47:45
86.9	71.7	15.2	0.660	2.16	0	*Time 4:* 18:48:25
110.5	75.1	35.4	1.459	2.20	0	*Time 5:* 18:49:20
159.8	84.5	75.3	1.325	6.20	0	*Time 6:* 18:51:05
174.4	89.0	85.4	1.199	8.34	7.31	*Time 7:* 18:51:45
196.7	89.3	107.4	0.985	5.34	0	*Time 8:* 18:52:20
206.4	89.0	117.4	0.852	2.24	0	*Time 9:* 18:53:20
209.0	88.0	121.0	0.652	2.22	0	*Time 10:* 18:53:45

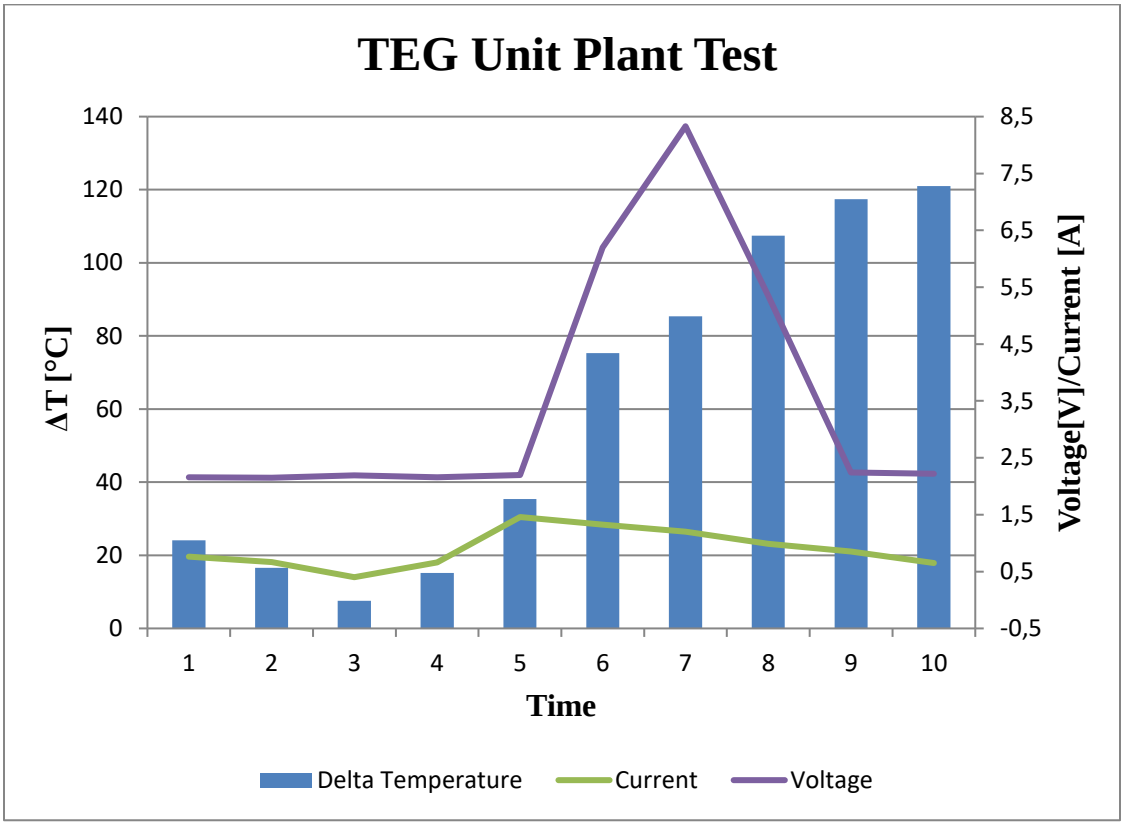

Figure 5.1. TEG 127-50D voltages and currents reproduced from Table 5.1.

5.3 PROTOTYPE COMMERCIAL TEG MODULE 'COLLAR' UNIT

5.3.1 Design and development of a prototype commercial TEG module 'collar' unit

The prototype TEG 'collar' unit was designed and developed with due consideration to the harsh industrial environment within which it is intended to work. For a boiler environment, a large portion of waste heat lies within the numerous steam lines transporting high pressure superheated steam from the boiler to steam driven plant equipment (Magasiner, 1966). The TEG 'collar' unit was fabricated as follows:

A pipe 'collar' having a diameter of 13.5cm (6 inches) was manufactured from mild steel pipe for mounting around the steam line. A base mounting plate is then fixed onto the collar. The TEG 127-

50D is then mounted onto the base plate. The collar serves as a thermal coupler for the waste heat to transfer from the steam pipes to the module's base plates.

Collar construction: The collar is divided into three equal portions of 4.5cm. Heavy duty industrial barrel hinges were used to couple the three portions together over the pipe making it safe and easy to attach to the steam lines as is shown in Figure 5.2.

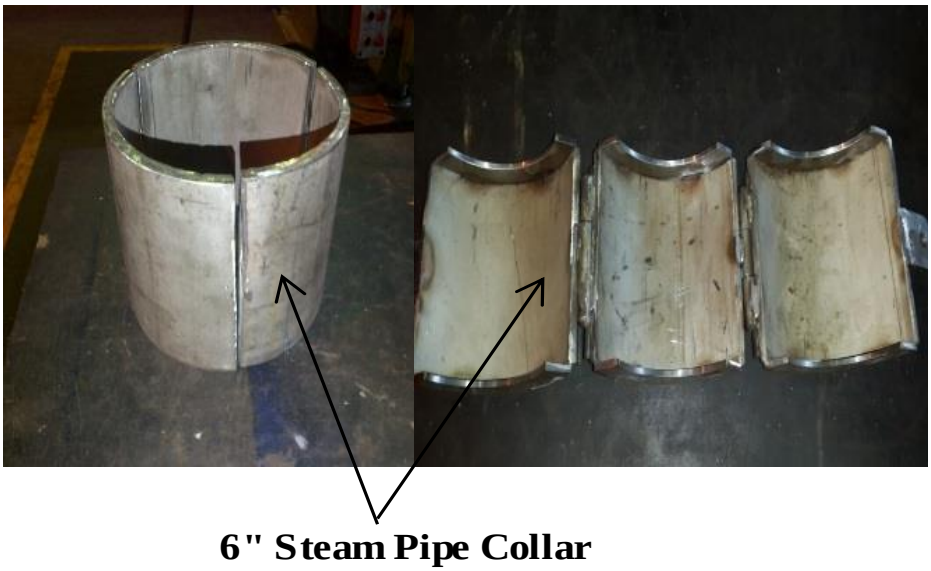

Figure 5.2. A 13.5cm (6 inches) mild steel pipe divided into three portions.

Construction of the module mounting plate: Stainless steel was used to machine six 70mm x 120mm mounting plate segments as shown in Figure 5.3. Stainless steel is used because of its excellent conducting properties. These plates assist with the thermal conduction of waste heat from the thermal collar to the TEG modules. Figure 5.4 shows the base plates welded onto the mild steel collar which in turn fits over the steam line (cf. Figure 5.7).

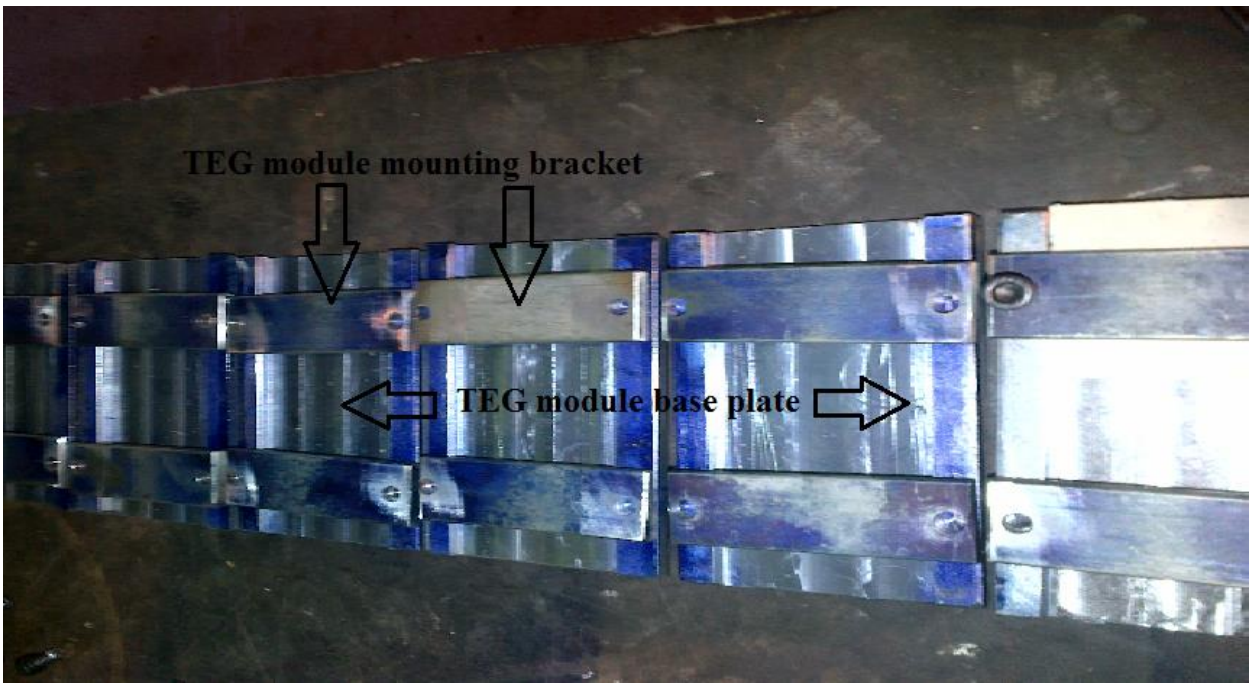

Figure 5.3. Thermoelectric module stainless steel base plates.

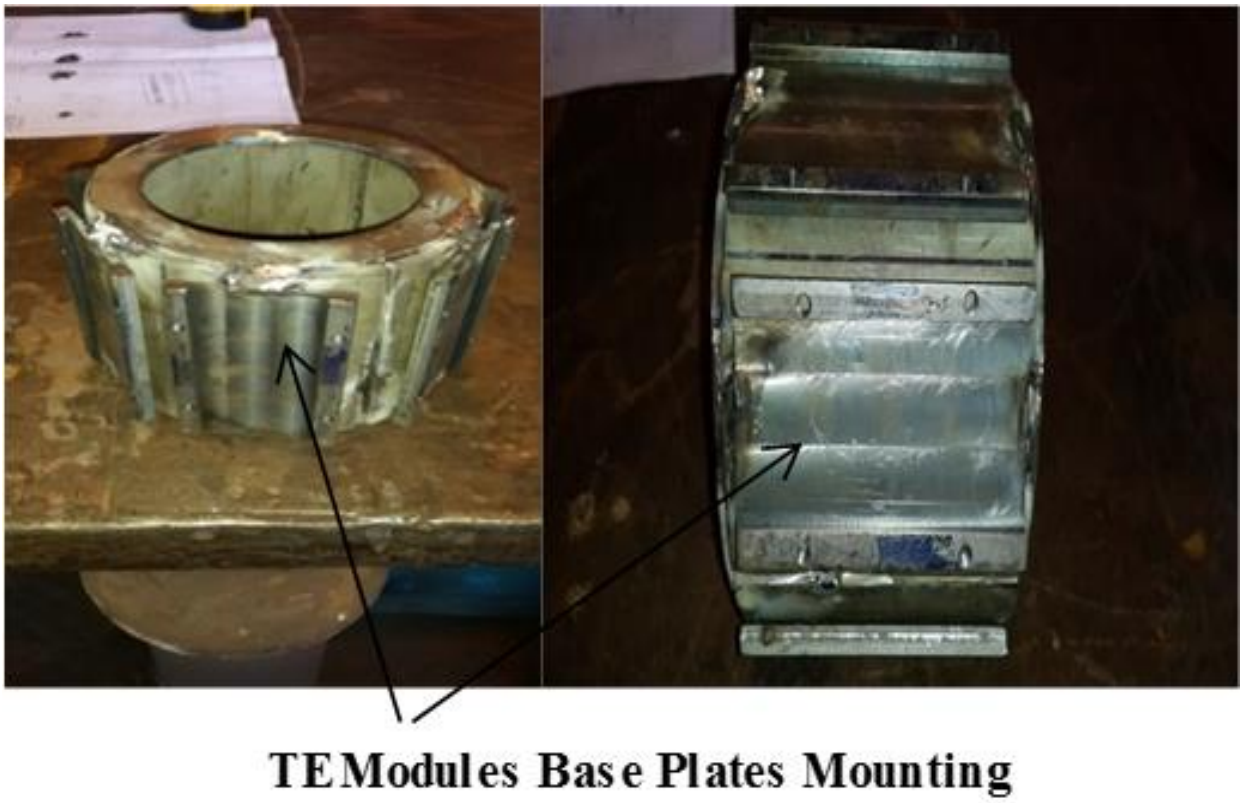

Figure 5.4. Thermoelectric module base plates attached to the pipe.

Each 50mm x 120mm TEG 127-50D module is fixed to the stainless steel plate with a mounting bracket. A maximum of two modules can be mounted per stainless steel plate as shown in Figure 5.5. A fin-type aluminum heat sink with dimensions of 65mm x 100mm is used to maintain the cold-side temperature of each module as shown in Figure 5.6. Thermal coupling paste to facilitate cooling is used to ensure maximum heat transfer from the cold side to the heat sink.

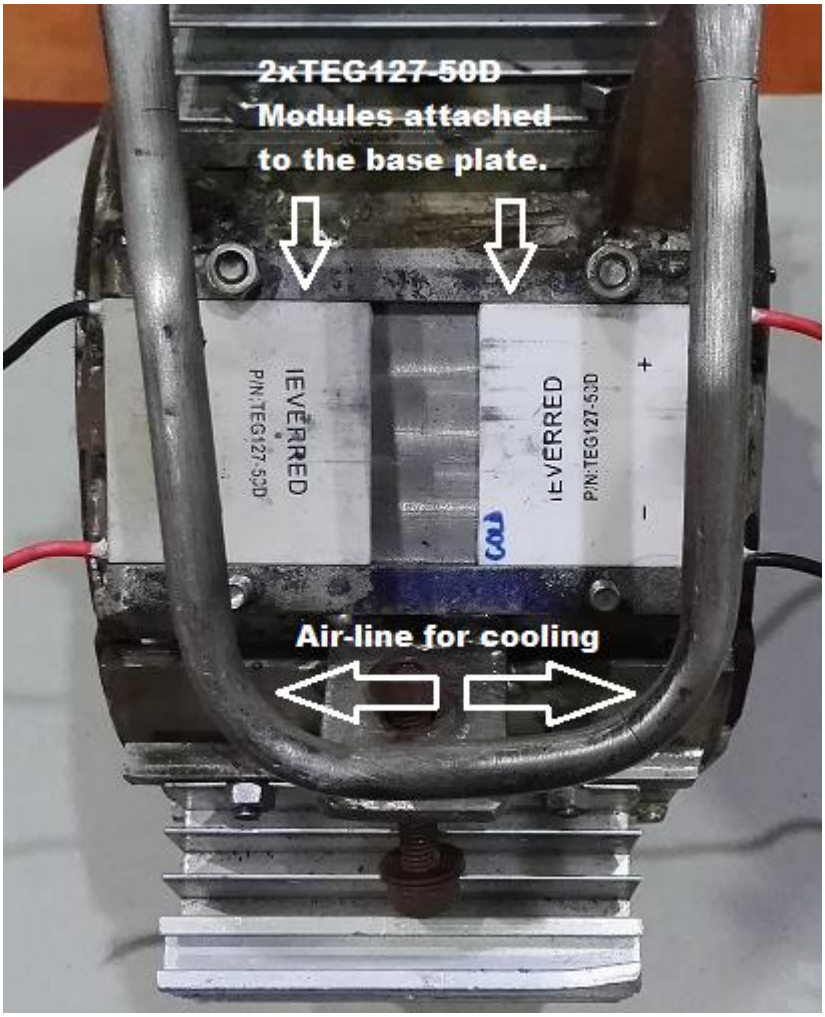

Figure 5.5. Thermoelectric module attached to the base plate.

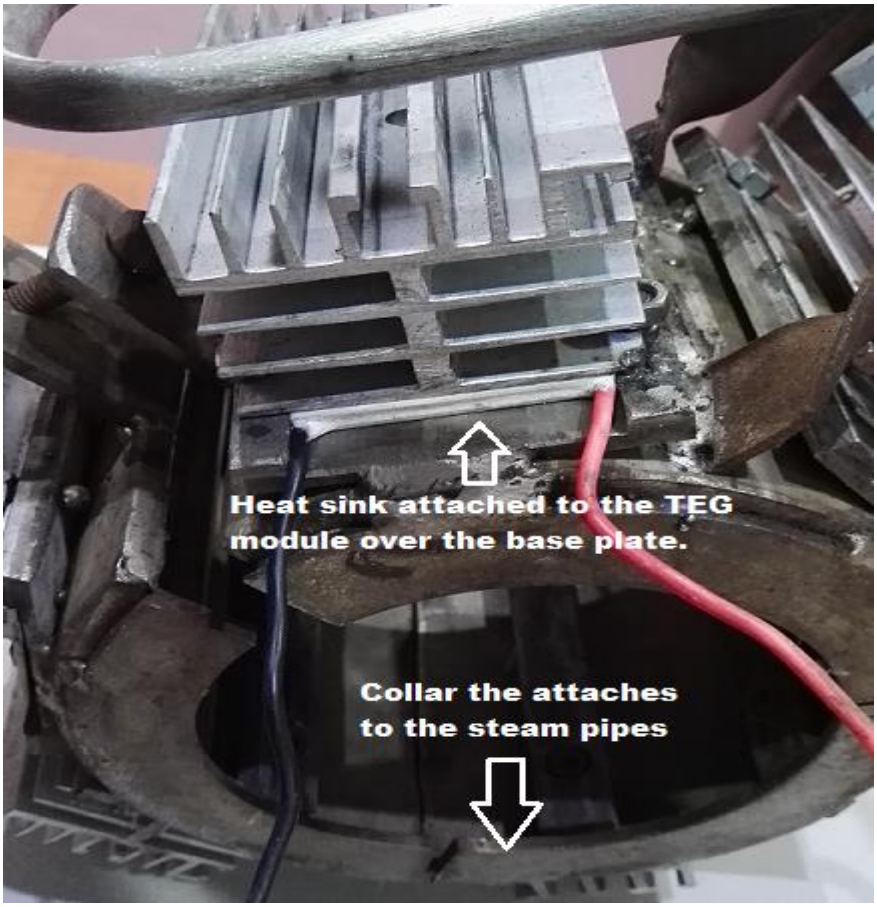

Figure 5.6. Aluminum heat sink mounted onto the stainless steel base plate.

The aluminum heat sinks did not provide sufficient cooling for the cold side of the modules. This is attributed to the high ambient temperatures within the boiler plant environment. To improve cooling, we used readily available compressed air to dissipate the heat away from the heat sink. *Compressed air:* Stainless steel pipe is used to supply cold compressed air to aid with the dissipation of heat away from the heat sink (See Figure 5.7). Multiple 3mm holes were drilled into the stainless steel pipe to blow directly onto the aluminum fins to facilitate cooling. A 12mm quick shut off ball valve is used to throttle and control the 6 bar compressed air as shown in Figure 5.7.

Figure 5.7. Prototype TEG 'collar' unit attached to a steam pipe.

5.3.2 4-module prototype collar simulation tests using the TEG 127-50D commercial device

For this test four TEG 127-50D thermo-electric devices are fixed to the prototype collar described previously. The four TEG modules are electrically connected in series as shown in Figure 5.8. This four module prototype device was tested under managed conditions in a 'workshop' having a stable ambient temperature of approximately 25^0C. The prototype TEG unit was attached to a 13.5 cm (6-inch) mild steel steam pipe to simulate the process pipe where the prototype unit would be eventually used.

As previously mentioned, the workshop environment has a stable ambient temperature of about 25^0C. We still took the added precaution of using approximately 150kPa of compressed air to supplement the heat sinks for cooling. This was done in order to reduce the possibility of the TEG module exceeding its temperature operating parameters that would cause it to enter into thermal runaway and then destruction.

LPG gas was used to heat the pipe as shown in Figure 5.9. The heat was evenly distributed throughout the 13.5cm pipe to simulate the steam temperature conditions expected in the boiler plant. The range of temperatures, voltages and currents produced during this test is recorded in Table 5.2. Table 5.3 shows a voltages and currents for the commercial TEG module.

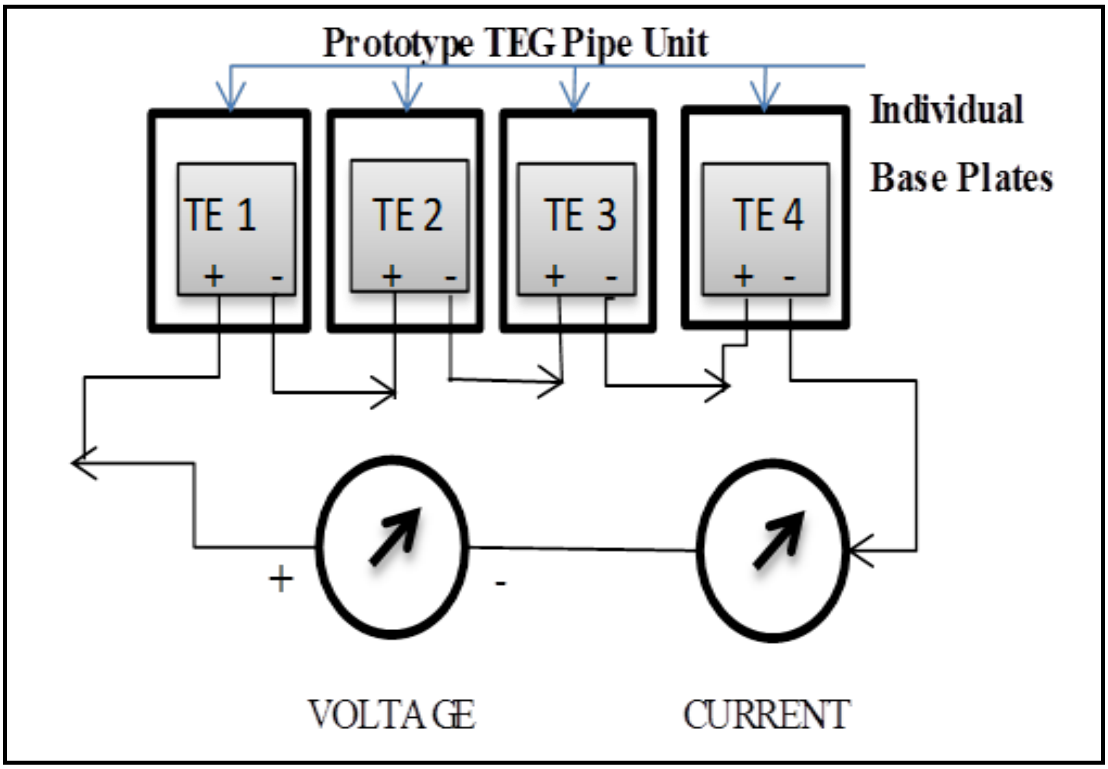

Figure 5.8. Prototype 4-module commercial TEG connection.

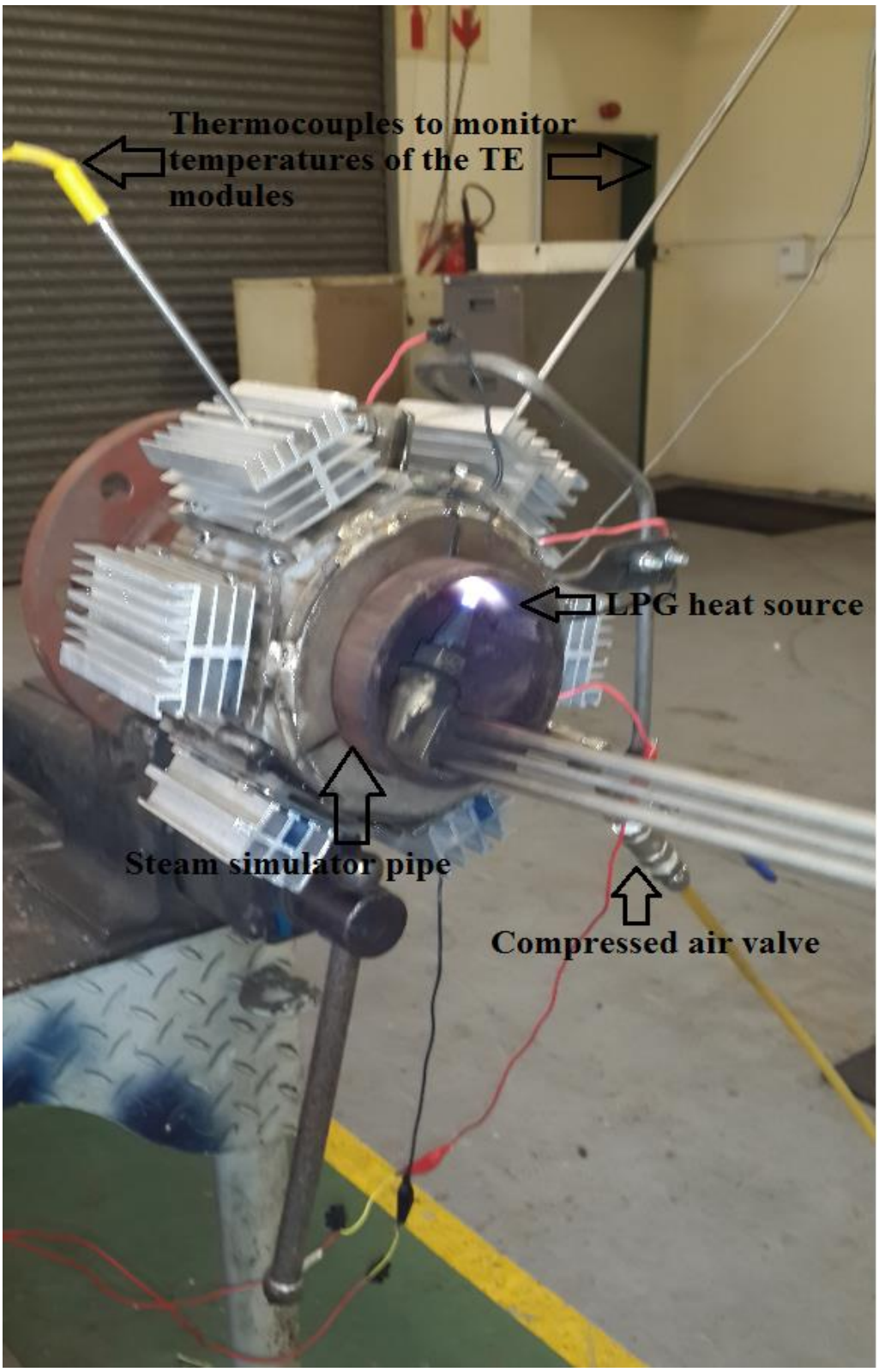

Figure 5.9. Prototype TEG collar unit test at Eston sugar mill.

Table 5.2. Prototype 4-module commercial TEG output currents and voltages.

$T_{hot\ side}$ [°C]	$T_{coldside}$ [°C]	ΔT [°C]	I_{TEG}[A]	V_{TEG}[V] (Modules)	Time[hh:mm:ss]
85.5	50.3	35.2	5.23	1.65	*Time 1:* 10:17:43
163.4	55.8	107.6	7.43	1.79	*Time 2:*10:20:03
190.1	63.6	126.5	8.61	2.49	*Time 3:*10:23:03
197.7	65.9	131.8	8.59	2.93	*Time 4:*10:24:23
199.2	68.5	130.7	8.72	3.21	*Time 5:*10:50:03
200.1	71.6	128.5	9.50	3.25	*Time 6:*10:51:03
201.8	72.9	128.9	9.59	3.28	*Time 7:*11:17:43
201.0	73.9	127.1	9.99	3.40	*Time 8:*11:28:43
202.0	75.3	126.7	10.01	3.42	*Time 9:*11:41:43
206.1	75.5	130.6	10.21	3.45	*Time 10:*11:55:20

Table 5.3. Voltages and currents for a commercial (non-industrial) TEG module.

TEG Module Type	TE Module Connection	V_{TEG} [V]	I_{TEG} [A]
Single module with hot side fixed to a base plate and then placed on a cooker plate.	Single stage connection (Chapter 4, Table 4.1)	3.45	3.070
TEG hot-side fixed on a flat metal surface and then mounted onto steam drum.	Four stage series connection (Chapter 4, Table 4.5)	7.49	3.069
Prototype commercial TEG 'collar' unit with the hot side fixed onto a base plate and then mounted onto a steam pipe collar.	Four Stage series connection (Chapter 5, Table 5.2)	3.45	10.21

5.3.3 Discussion about the results of the workshop environment test

From Table 5.2 and Table 5.3 we observe the following for the TEG 'collar' unit:

- The prototype 4-stage commercial unit produced 3.45V at a differential temperature of 130.6°C. This value is similar to the voltage output of a single thermoelectric module.
- A maximum current of 10.21A at a differential temperature of 130.6°C is produced. This current is approximately 332% more than the current produced by the 4-stage TEG unit discussed in chapter 4. This high current flowed when the module failed following thermal overloading. A brief discussion of what occurred during failure is mentioned below.

  TEG failure: Table 5.2 demonstrates the reliability of the commercially produced modules operating at its peak limit within high temperature environments. The corresponding graphs for the data given in Table 5.2 is shown in Figure 5.10. From Table 5.2 and Figure 5.10, we observe that for temperatures above 200°C the copper connections coupling the N and P semiconductor materials within the module starts to diffuse into the semiconductor material at an accelerating rate as junction temperature increases. Copper has 11 valent electrons which contributes towards improving the conduction characteristics of the semiconductor pellets. This is evident from the large currents that flowed at hot-side temperatures beyond 200^0C (cf. Table 5.2). At these temperatures the large currents cannot be sustained because of the large quantity of heat being generated at the junctions, causing the module to slide into thermal runaway and eventual destruction. The cooling systems used in the tests were inadequate for providing adequate cooling at these high hot-side temperatures.

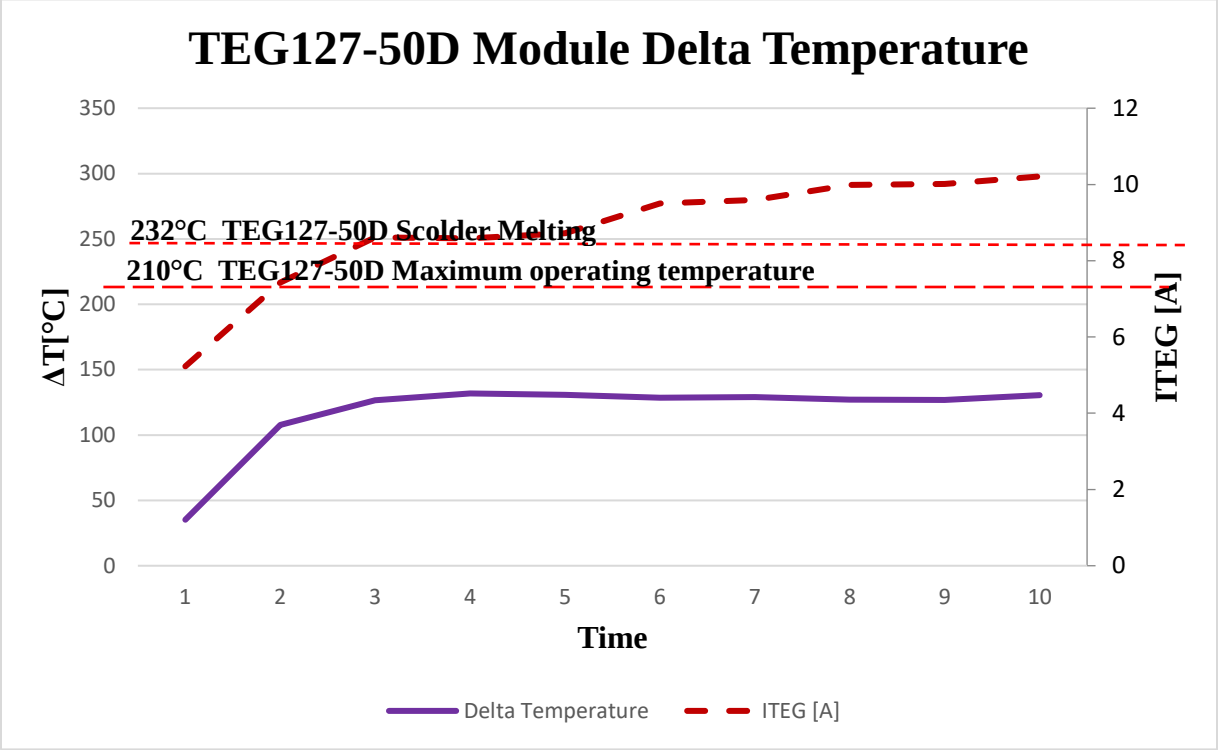

Figure 5.10. TEG127-50D (commercial module) 4-stage module temperature difference and current output with the LPG heat source.

5.4 TESTS USING AN INDUSTRIAL TEG MODULE 'COLLAR' UNIT

Sub-section 5.3.3 discussed the tests that were conducted with the commercial TEG device, and we observed the shortcomings and failure of the device at high operating temperatures. To overcome the shortcomings of the commercial device, we selected an industrial TEG unit (TEG1B 12610-5.1) and conducted similar tests that were conducted with the commercial TEG unit. A cross –section of an industrial TEG device is shown Figure 5.11 and the device is shown in Figure 5.12.

RTV Silicone Coating Protective Layer
Ceramic plate
PN semiconductor materials
Ceramic plate
RTV Silicone Protective Layer

Figure 5.11. Cross section of industrial TEG module (TEG1B 12610-5.1) having maximum hot side temperature of 320^0C.

Figure 5.12. TEG1B 12610-5.1 module.

With regards to Figure 5.12, the construction of the industrial unit is similar to that of the commercial unit. At a physical level the only difference is the RTV (room temperature vulcanization) silicone coating bonded to the ceramic plate for increasing the range of temperatures over which the module can operate. RTV silicone is stable at high temperatures and has superior heat resistance properties. RTV silicone has good dielectric properties, ultraviolet durability, excellent chemical and thermal degradation resistance when applied as a coating (Seyedmehdi *et al.*, 2011). The silicone coating acts as a heat shield between the heat source and the PN junction.

In this way the PN junction is protected from thermal runaway (Seyedmehdi *et al.*, 2011). The downside of this arrangement is that lesser heat is applied to the PN junction, leading to a decrease in the module's power output. The manufacturer's specifications for the TEG1B 12610-5.1 industrial modules used in the boiler-room tests is given in Table 5.4 (www.tecteg.com, Accessed Jan. 2014).

Table 5.4. TEG1B 12610-5.1 data sheet.
(www.tecteg.comgenerator, Accessed Jan 2014)

Hot side Temperature (^{0}C)	300
Cold side Temperature (^{0}C)	30
Open circuit voltage (V)	7.2
Matched Load Resistance (Ω)	1.8
Matched Load Output Voltage (V)	3.6
Matched Load Output Current (A)	2.0
Matched Load Output Power (W)	7.1
Heat Flow Across the Module (W)	148

For this study, we configured four industrial TEG modules (TEG1B 12610-5.1) into electrical series connections in order to assess their dynamic performance. This configuration is similar to the commercial unit tests discussed in section 5.3. Two tests were performed. These tests are described in the following sections.

5.4.1 Test 1: Prototype industrial thermoelectric 'collar' unit test using LPG heat source

Methodology: Test 1 is performed in an industrial workshop and used a LPG heat source. The conditions under which this test is conducted are similar to those conducted with the commercial unit as discussed in section 5.3.2. The conditions pertaining to this test, and the results, are

summarized in Table 5.5. The temperatures, voltages and currents produced during the tests are given in Table 5.6. A graphical representation of these results is shown in Figure 5.13.

Table 5.5. Prototype industrial TEG 'collar' unit test details.

	TEST1	**TEST2**
LOCATION	Workshop	Boiler
module connection	4-stage series	4-stage series
cooling method	Heat –sink and compressed air	Heat –sink and compressed air
heat source	LPG	'Live' high pressure steam
maximum hot-side temperature	206.9 [^{0}C]	154.7 [^{0}C]
maximum temperature difference	117.8 [^{0}C]	77.5 [^{0}C]
maximum voltage produced	13 [V]	12.95 [V]
maximum current produced	2.11 [A]	2.01 [A]
maximum power produced	27.43 [W]	26.0295 [W]
reference figure	Figure 5.9	Figure 5.16

Table 5.6. Test 1 results using industrial TEG collar device and LPG heat source.

$T_{hot\ side}$ [°C]	$T_{coldside}$ [°C]	ΔT [°C]	I_{TEG}[A]	V_{TEG} [V] (Modules)	Time[hh:mm:ss]
25.1	24.9	0.2	0.0	0.7	*Time 1*: 10:02:02
45.2	42.1	3.1	0.58	5.32	*Time 2*: 10:10:26
97.3	59.0	38.3	0.91	8.45	*Time 3*: 10:18:06
125.7	62.8	62.9	1.52	10.41	*Time 4*: 10:25:56
133.8	65.4	68.4	1.68	11.42	*Time 5*: 10:33:18
143.1	69.3	73.8	1.97	12.78	*Time 6*: 10:42:26
159.8	77.1	82.7	2.03	12.98	*Time 7*: 10:50:42
178.7	81.9	96.8	2.09	12.99	*Time 8*: 10:59:02
191.2	85.3	105.9	2.10	12.99	*Time 9*: 11:08:26
206.9	89.1	117.8	2.11	13.00	*Time 10*: 11:15:02

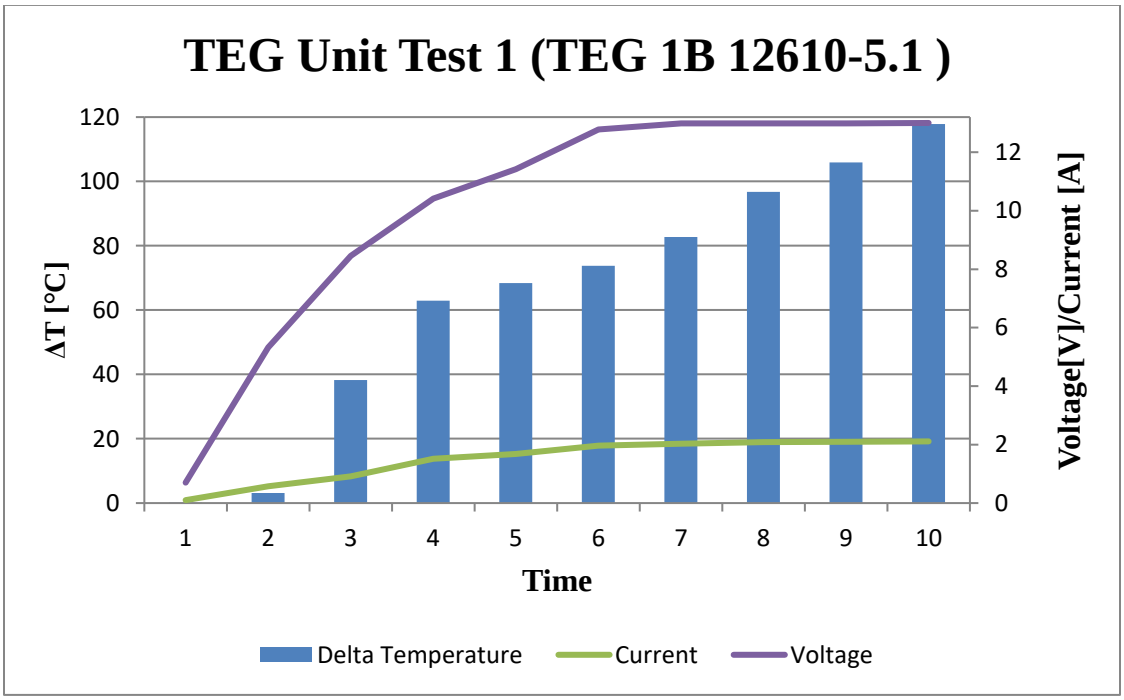

Figure 5.13. Representation of the TEG unit (TEG1B12610-5.1) test.

Observations and Analysis: From Figure 5.13 we observe that the output response of the prototype industrial TEG 'collar' device produces stable voltages and currents which changes as the temperature changes. The device response is linear for ΔT up to 82.7^0C. For temperatures differences beyond 82.7^0C the change in current output is small for changes in temperature. This is due to the charge carriers within the semiconductor materials approaching saturation.

The voltage output produced by the 'collar' unit is sufficient to activate a buck-boost converter. The operation of the buck-boost converter was discussed in Chapter 4, section 4.3.5.2. The application of the buck-boost converter in a battery charging system is discussed later in this chapter.

5.4.2 Test 2: Prototype industrial thermoelectric 'collar' unit test with steam heated source

Methodology: For this test we attached the prototype TEG 'collar' device to a steam turbine's high pressure steam pipe at the sugar mill where the tests were conducted (cf. Figure 5.14). Readily available heat from the boiler steam pipes are used to heat the hot-side of the module. The cooling system is the same as that was used for *Test 1* (section 5.4.1), namely plant compressed and an aluminum heat sink. The electrical configuration used in the modules is similar to that described in section 5.3.2, Figure 5.8.

Observations and Analysis: The temperatures, voltages and currents produced during the tests are recorded in Table 5.7. From Table 5.7, Figure 5.15 and Figure 5.16 we observe that the output of the 'collar' unit is linear for the temperature ranges considered in this study. The tests were conducted for temperature differences that fall within the devices linear region of operation. For this test we observe that the current saturates at a differential temperature of approximately 77.5^0C, which produces a current of about 2A. This current corresponds to the manufacturers

specifications for this device (cf. www.tecteg.com, Accessed Jan. 2014). A graph of the data given Table 5.7 is given in Figure 5.15.

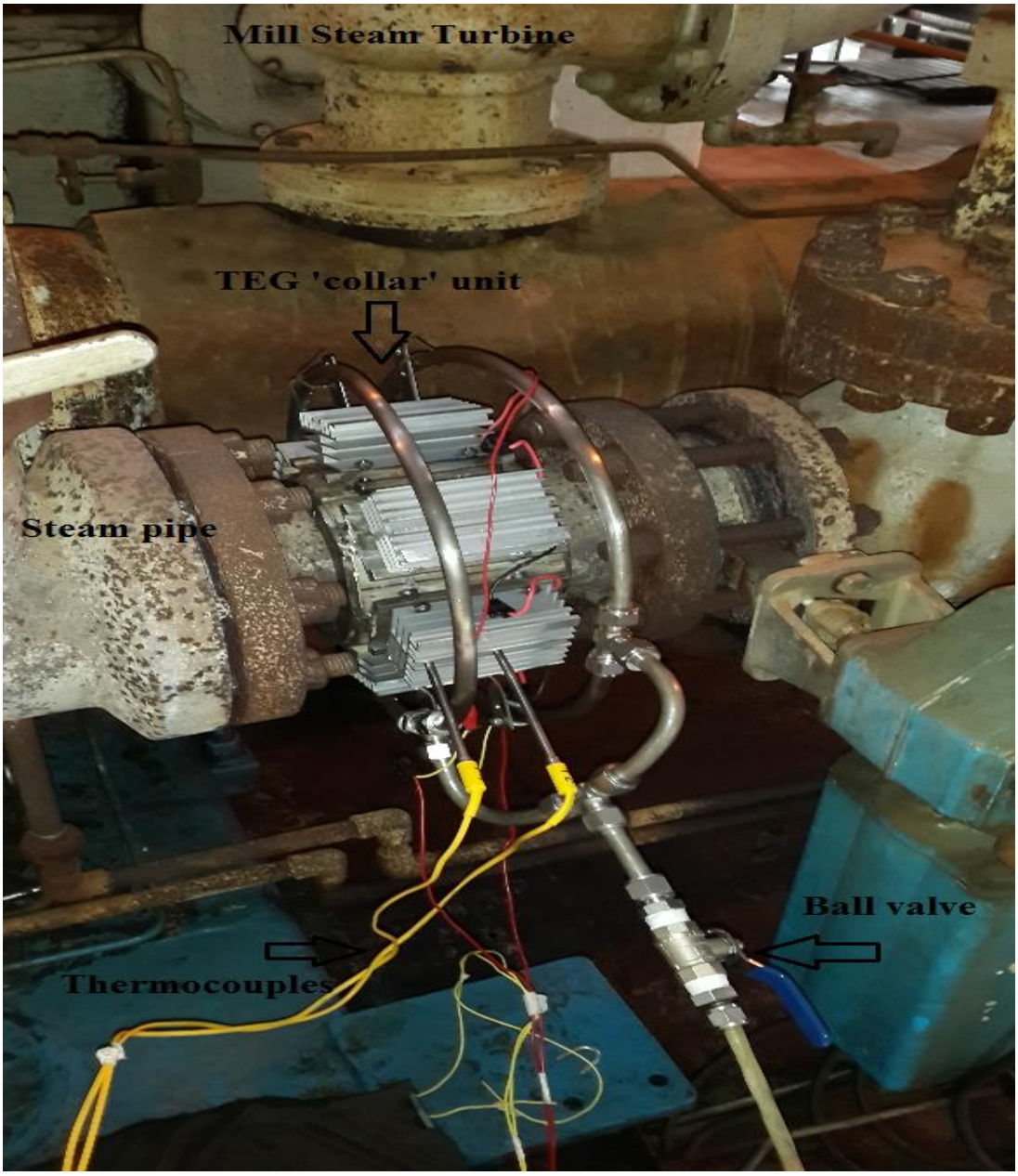

Figure 5.14. The prototype TEG 'collar' unit coupled to a steam pipe.

Table 5.7. Test 2 results using industrial TEG collar device and 'live' steam heat source.

$T_{hot\ side}$ [°C]	$T_{coldside}$ [°C]	ΔT [°C]	I_{TEG} [A]	V_{TEG} [V] (Modules)	Time[hh:mm:ss]
32.4	30.6	1.8	0.08	0.86	*Time 1:*13:02:02
43.1	34.5	8.6	0.42	6.32	*Time 2:*13:10:26
92.2	51.5	40.7	0.84	7.98	*Time 3:*13:18:06
113.8	53.1	60.7	1.09	8.94	*Time 4:*13:25:56
120.5	60.2	60.3	1.18	10.29	*Time 5:*13:33:18
125.1	63.5	61.6	1.41	11.09	*Time 6:*13:42:26
134.1	66.6	67.5	1.59	11.34	*Time 7:*13:50:42
142.3	72.4	69.9	1.79	11.99	*Time 8:*13:59:02
147.9	75.3	72.6	1.91	12.51	*Time 9:*14:08:26
154.7	77.2	77.5	2.01	12.95	*Time 10:*14:15:02

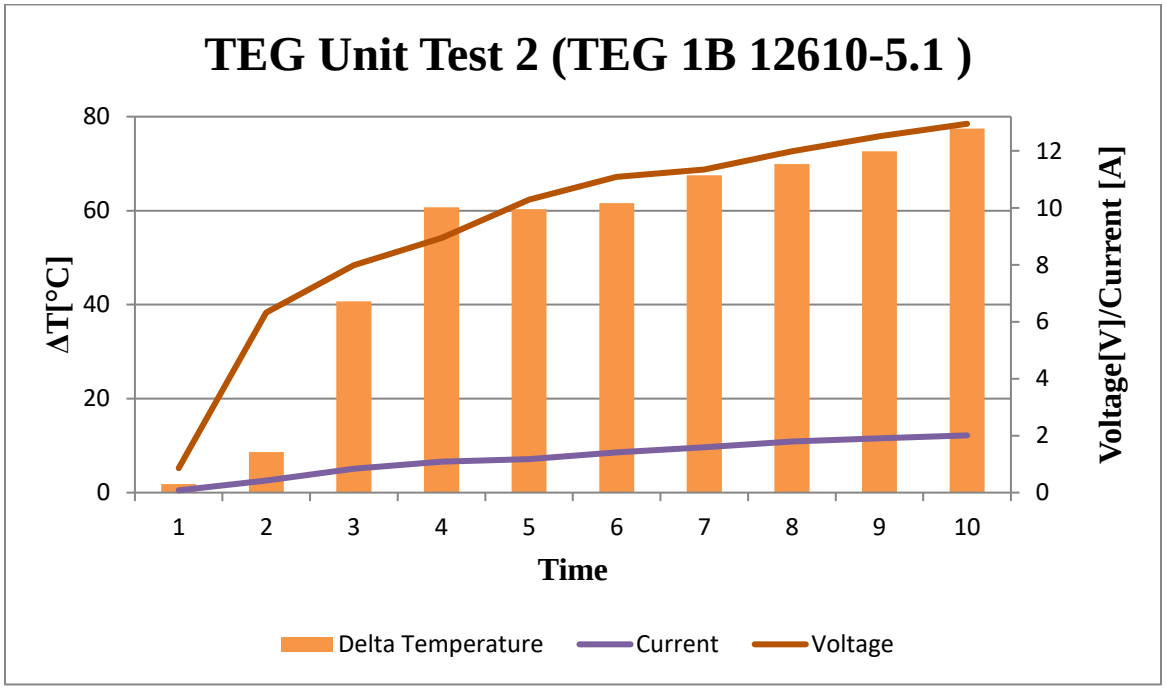

Figure 5.15. Representation of the TEG unit (TEG1B12610-5.1) test.

Figure 5.16 and Figure 5.17 summarizes the results of Test 1 and Test 2.

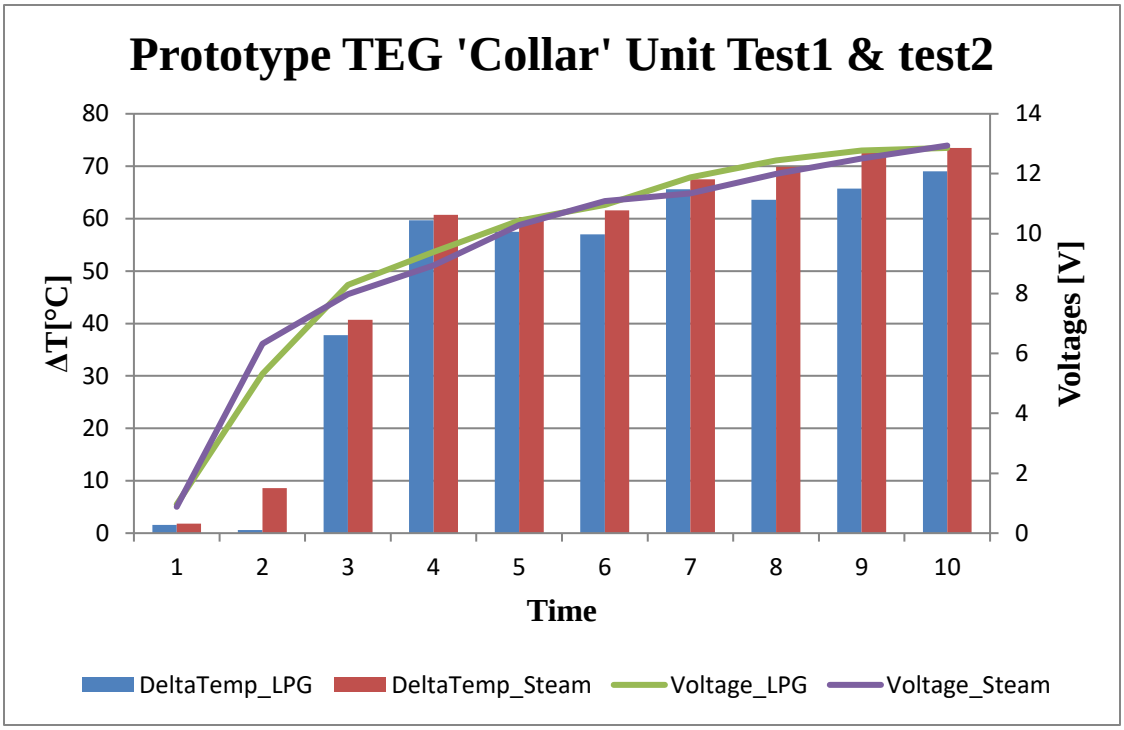

Figure 5.16. Voltages generated by the prototype TEG 'collar' unit Test1 and Test2.

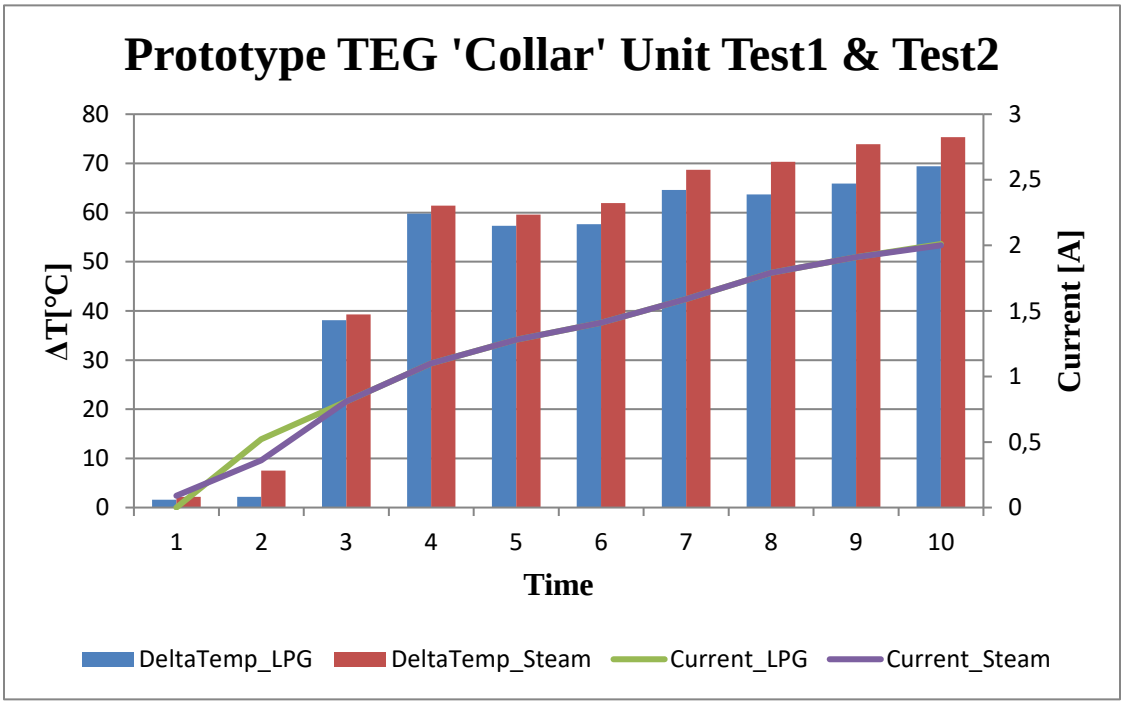

Figure 5.17. Currents generated by the prototype TEG 'collar' unit Test1 and Test2.

5.5 BATTERY CHARGING SYSTEM UTILIZING THE STEAM OPERATED 'COLLAR' UNIT

The prototype TEG 'collar' unit output was connected to a power supply battery as shown in the circuit schematic in Figure 5.18. The battery used in the test is given in Figure 5.19. The battery is connected via the buck-boost converter of the prototype TEG 'collar' unit. The buck-boost converter was calibrated to produce 13Vdc at 2A at its output. The buck-boost converter was connected to charge the power supply battery rated at 8.6Ah and 12Vdc.

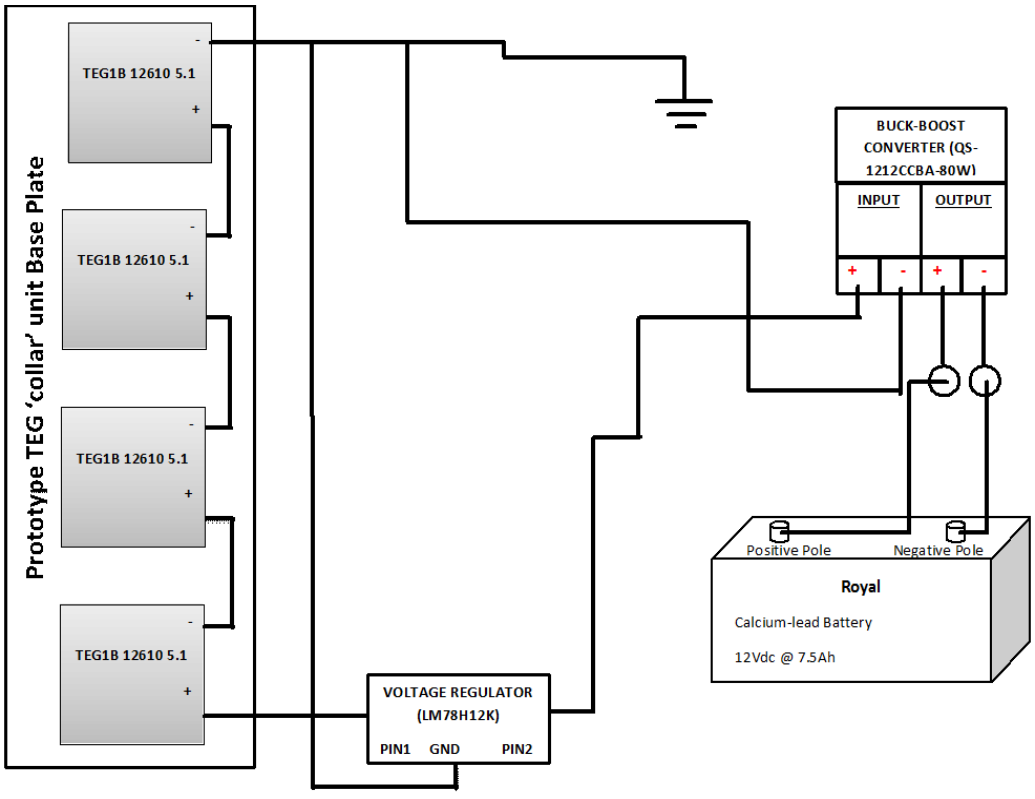

Figure 5.18. Schematic of the prototype TEG collar device with buck-boost converter charging a UPS battery. (cf. Appendix B)

Figure 5.19. Sealed lead-acid battery used for charging by the prototype TEG 'collar' unit.

5.5.1 Battery charging

Ideal conditions for battery charging: The 'ideal' charging time of a lead acid sealed battery is calculated as follows:

Charging Time of battery (T) = Battery Ah (Ah) / Charging Current (A)

A minimum of 10% of a battery's Ampere-hour rating is required for a battery to charge efficiently. For our battery we calculated a charging current of *8.6Ah x (10/100) = 0.86 Amperes* to fully charge the 8.6Ah battery over a 10-hour period.

To compensate for a 1% loss in charging current due to the battery losses, we increased the minimum charging current to *8.6Ah x (1/100) + 0.86Ah = 0.946Ah*.

Battery charging under real-life conditions: Factors such as operating environment temperature will influence the charge and discharge times of a battery. For this reason, we increased the ideal charge current by 40% as follows:

8.6Ah x (40/100) + 0.86Ah = 4.3Ah

Under these conditions the charging required for the 8.6Ah battery becomes:

8.6Ah + 4.3Ah = 12.9Ah

Taking the internal losses into consideration, the total charge time required for the 8.6Ah battery under practical conditions is determined as follows:

Ampere hour / Charging current = 12.9Ah / 0.946A = 13.64 hours

5.5.2 Battery charging with the steam driven prototype TEG 'collar' unit

The prototype TEG 'collar' unit was attached to a steam turbine's high pressure inlet steam pipe within the sugar mill. The turbine's speed depends on the steam flow-rate and the steam-pipe surface temperature is proportional to the speed of the turbine.

A power supply battery was connected to the output of the buck-boost converter of the prototype TEG 'collar' unit as per the schematic in Figure 5.17. The objective of the test was to charge the battery to its full capacity. The battery was initially discharged to a residual charge of 1.22Ah. The results of the test are documented in Table 5.8 and illustrated graphically in Figure 5.19. From Table 5.8, we observe that fluctuations in steam turbine speed will affects the temperatures of the TEG unit. The buck-boost converter is activated by the TEG unit's output and maintains a constant output battery charge current. The TEG unit's output current was able to charge the battery with a constant 2A supply. The battery took 6 hours and 33 minutes to charge from 1.22A to its maximum charging capacity of 8.55A. Since battery charge and discharge is inversely proportional to temperature, the harsh temperature of the boiler room where the test was conducted accounted for the longer charge time of the lead-acid battery.

Table 5.8. Steam driven battery charger data.

Turbine Speed[RPM]	**$T_{hot\ side}$ [°C]**	**$T_{coldside}$ [°C]**	**ΔT [°C]**	**I_{TEG} [A]** (Charge current from Boost-Buck)	**V_{TEG} [V]** (Boost-Buck)	**I_{Bat}[A]** (Battery)	**Time[hh:mm:ss]**
3509	155	78.4	76.6	2.02	12.88	1.22	*Time 1:*09:02:18
3689	158.3	79.1	79.2	2.04	12.89	2.26	*Time 2:*09:50:26
2671	146.5	74.1	72.4	2.01	12.85	3.35	*Time 3:*10:58:06
2403	140.1	69.5	70.6	2.01	12.85	3.91	*Time 4:*11:45:56
3699	168	81.6	86.4	2.04	12.96	4.81	*Time 5:*12:33:18
3989	175.6	82	93.6	2.06	12.97	5.72	*Time 6:*13:10:02
4221	187.7	88.2	99.5	2.07	12.99	6.54	*Time 7:*13:50:42
2500	144.4	72.6	71.8	2.00	12.85	7.42	*Time 8:*14:35:26
3589	159.9	79.5	80.4	2.04	12.90	8.11	*Time 9:*14:58:02
3488	154.7	77.2	77.5	2.01	12.89	8.55	*Time 10:*15:35:02

Figure 5.20 illustrates the TEG's constant output current (I_{TEG}) in spite of fluctuations in the temperatures from the heat source (live steam pipe). From the graph, we observe that the battery charge current increases at a constant rate from for the entire duration of the charge. The constant rate of charge curent is attributed to the excellent requlating characterisitcs of the buck-boost converter. The battery charging current curve has a linear response, given the constant charge current provided by the 'collar' unit.

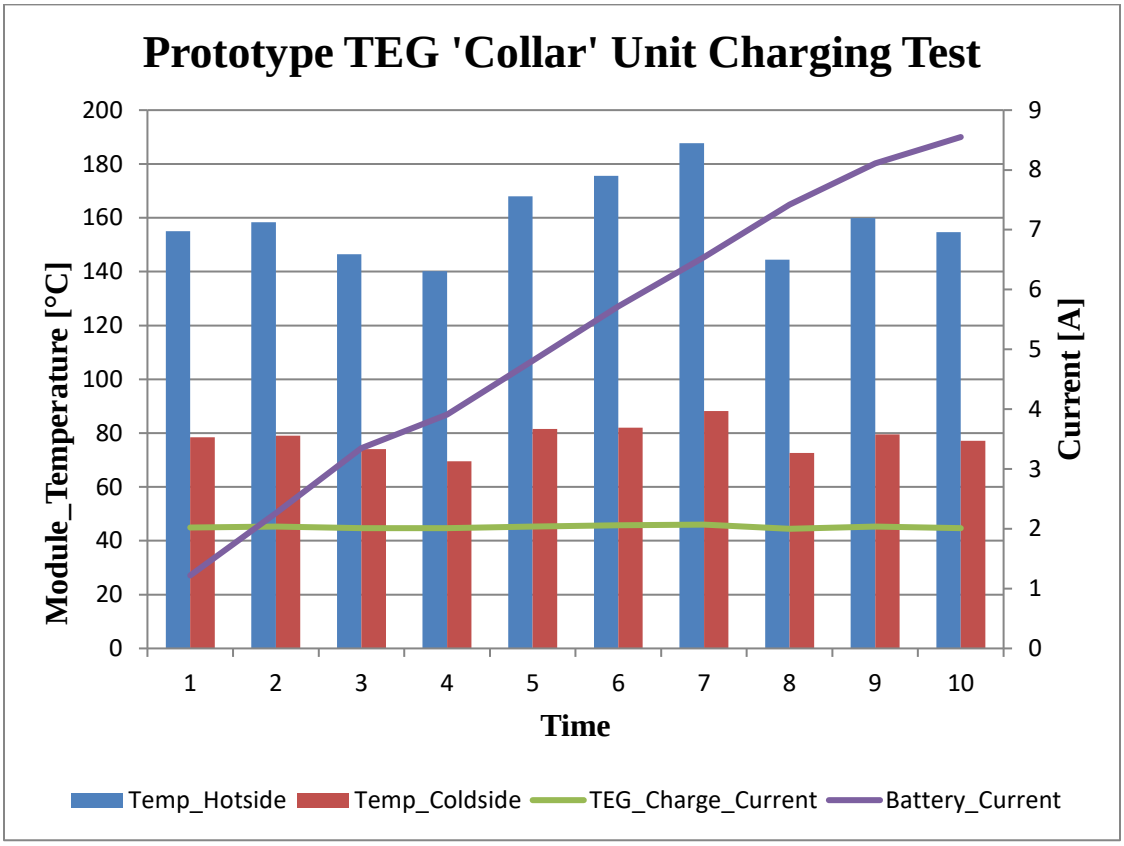

Figure 5.20. Prototype TEG 'collar' unit module temperatures, charge currents and power supply battery currents.

5.5 SUMMARY, CONCLUSION AND RECOMMENDATIONS

A battery charge circuit comprising of a buck-boost converter was designed to charge a 12V lead acid battery. Cooling of the TEG prototype modules was achieved by using a heat sink and compressed air combination. The prototype industrial TEG unit was powered from two sources namely:

- under managed conditions in the workshop using LPG gas and
- in the steam boiler room from the expended heat generated by a turbine steam pipe.

The tests showed that the non-industrial TEG unit performed well under managed temperature conditions in the workshop but failed in the harsh temperature environment of a steam boiler room. The failure of the commercial (non-industrial) unit is due to the absence of a protective heat retarding layer over the ceramic coating of the device. The industrial TEG unit on the other hand performed well in all the tests. The current produced by the industrial TEG device was sufficient to fully charge a 12V lead acid battery.

CHAPTER 6

ANALYSIS OF EXPERIMENTS

6.1 INTRODUCTION

This chapter provides an analysis of the experiments that were described in Chapter 4 and Chapter 5. The experiments focused on the following aspects of the energy harvesting TEG module:

- Module cooling
- Output power maximization
- Identification of suitable heat sources

Each of the above-mentioned aspects will be discussed in detail in the following sections.

6.2 THERMOELECTRIC COOLING

Three different cooling combinations were assessed on the TEG127-50D commercial module. The data from these experiments (discussed in Chapter 4 and Chapter 5) is given in Table 6.1. The efficacy of the cooling combinations was assessed based on their ability to ensure a maximum temperature gradient between the hot side and cold side of the thermo-electric module.

Table 6.1. Summary of tests with the TEG127-50D commercial module.

	COOLING METHODS		
	HEAT-SINK & EXTRACTOR FAN	**HEAT-SINK, BLOWER FAN & PELTIER COOLING**	**HEAT-SINK & BLOWER FAN**
TEST LOCATION	Laboratory	Laboratory	Laboratory
HEAT SOURCE	Electric cooker plate	Electric cooker plate	Electric cooker plate
MODULE MODEL	TEG127-50D	TEG127-50D	TEG127-50D
MODULE TYPE	Commercial (module excludes RTV silicone layer)	Commercial (module excludes RTV silicone layer)	Commercial (module excludes RTV silicone layer)
MODULE CONNECTION	Single-stage	Single-stage	Single-stage
MAXIMUM VOLTAGE GENERATED	2.61 VDC (cf. Chapter 4, Table 4.2)	2.01 VDC (cf. Chapter 4, Table 4.3)	3.45 VDC (cf. Chapter 4, Table 4.1)
MAXIMUM CURRENT GENERATED	2.881A (cf. Chapter 4, Table 4.2)	1.900A (cf. Chapter 4, Table 4.3)	3.070A (cf. Chapter 4, Table 4.1)
MAXIMUM TEMPERATURE GRADIENT	113.0ºC (cf. Chapter 4, Table 4.2)	112.8ºC (cf. Chapter 4, Table 4.3)	120.3ºC (cf. Chapter 4, Table 4.1)
MAXIMUM OUTPUT POWER	7.52W	3.82W	10.59W
RATED POWER PER MODULE	5.4W (cf. Chapter 3, Table 3.1)	5.4W (cf. Chapter 3, Table 3.1)	5.4W (cf. Chapter 3, Table 3.1)

6.2.1 Analysis and Discussion

Following from our discussions in Chapter 4 which reported on the performance of the TEG device, we arrived at the following conclusions with regards to the performance of the cooling systems utilised in this study:

6.2.1.1 Heat sink and extractor fan cooling:

Based on the relatively low maximum temperature gradient existing between the module's hot side and cold side (cf. Table 6.1), we deduced that this type of cooling is inefficient. The poor cooling is due to the inability of the extractor fan to dissipate sufficient thermal energy away from the heat sink. A direct consequence of this poor cooling is the reduction in the generated current. The cumulative effects of poor cooling resulted in the output power (current and voltage) decreasing over time (cf. Chapter 4, Figure 4.2). Under these conditions, the modules maximum output power rating of 10.59W as per the manufacturers specification was not achieved (cf. Chapter 3, Figure 3.8).

6.2.1.2 Heat sink, blower fan and Peltier cooling:

With Peltier cooling, a Peltier cooling module is created by connecting an external power source to oppose the current flowing through the module's junction. This is achieved by connecting the positive polarity of the power source to the negative polarity of the module, and the module's negative polarity to the positive polarity of the source power. The heat sink is attached to the cold side of the Peltier module (cf. Chapter 4, Figure 4.4) to dissipate heat from the module. A blower fan supplements cooling by conducting the heat away from the heat sink. The poor cooling is a combination of the inability of the Peltier module to efficiently dissipate sufficient heat away from the module itself, plus inadequate cooling by the heat sink. The insufficient cooling experienced

by the device reduces the temperature gradient across the module. For these reason the module's maximum power output was not achieved.

6.2.1.3 Heat sink and blower fan cooling:

From the results achieved (cf. Table 6.1), we can observe that this cooling method is the most efficient method of cooling. From Table 6.1, we observe that the maximum output current and voltage (and hence the power) is the largest when the heat-sink and blower fan combination was used to cool the thermo-electric module's hot-cold junction. This large power is due to the fact that much of the heat is dissipated away from the heat sink by the blower fan. Greater heat dissipation resulted in a larger temperature gradient between the device's hot and cold junctions.

6.3 CHANGING THERMOELECTRIC CONNECTIONS

Three different module connections were tested on the TEG127-50D module (cf. Chapter 4). The main objective of the tests was to maximise the power output from the module for each respective configuration. Three modules connections were tested, namely a 1-stage connection (using a single TEG), a 2-stage connection (using 2 modules) and a 4-stage connection (using 4 modules). The objective of each test was to maximise the power output from the module/s. A summary of the conditions that existed during the test with different number of modules is given in Table 6.2.

Table 6.2. Summary of the TEG127-50D tests with additional modules.

	MODULE CONFIGURATION			
	SINGLE MODULE		**TWO MODULES**	**FOUR MODULES**
TESTING LOCATION	Laboratory		Laboratory	Laboratory
HEAT SOURCE	Electric cooker plate		Electric cooker plate	Electric cooker plate
MODULE MODEL	TEG127-50D		TEG127-50D	TEG127-50D
MODULE TYPE	commercial		commercial	commercial
MODULE CONNECTION	1-stage series 		2-stage series 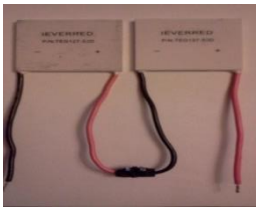	4-stage series 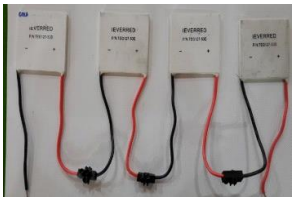
COOLING CONFIGURATION	Heat-sink and blower fan combination		Heat-sink and blower fan combination	Heat-sink and blower fan combination
VOLTAGE	Produced: 3.45VDC (cf. Chapter 4, Table 4.3)	Rated per module: 2.5VDC (Cf. Chapter3, Table 3.1)	6.10VDC (cf. Chapter 4, Table 4.4)	7.55VDC (cf. Chapter 4, Table 4.5)
CURRENT	Produced: 3.070A (cf. Chapter 4, Table 4.3)	Rated per module: 2.15A (Cf. Chapter3, Table 3.1	3.070A (cf. Chapter 4, Table 4.4)	3.069A (cf. Chapter 4, Table 4.5)

Continued from Table 6.2. Summary of the TEG127-50D tests with additional modules.

	MODULE CONFIGURATION			
	SINGLE MODULE		TWO MODULES	FOUR MODULES
POWER	10.59W	Rated per module: 5.4W (Cf. Chapter3, Table 3.1	18.73W (no rated power information is available from the manufacturer)	23.17W (no rated power information is available from the manufacturer)

6.3.1 Analysis and Discussion

Single module:

The single module produced a maximum power output that exceeded the manufacture's specifications for a single module (cf. Chapter 3, Table 3.8). The power produced during the tests were nearly twice that specified by the manufacturer. This improvement can be attributed to the efficient cooling provided by heat sink and blower fan combination.

Two module:

The output from the 2-stage series connected modules produced an increase in voltage of 75.94% while maintaining a constant current output equivalent to that of a single module (cf. Chapter 4, Table 4.3). These results are possible because when the modules are connected in series, the output voltage represents the algebraic sum of the voltage generated by each module; the current remains relatively unchanged because the surface area of the PN junctions do not change. The power

produced has nearly doubled, and some losses were inevitable due to limitations of the cooling system.

Four modules:

The output voltage from the 4-stage series connected modules increases by 23.39%, when compared to that of the 2-stage device, while consistently maintaining the current output of that of a single module (cf. Chapter 4, Table 4.3). Once again the current remains unchanged due to the surface area of the PN junctions not changing. The power produced has nearly tripled, and some losses were inevitable due to limitations of the cooling system. The four modules produced sufficient output for the powering of low current devices such as a cellular telephone charger circuit and LED lights.

6.4 TEST USING DIFFERENT FUELS

Four different fuels were used to heat the hot side of the TEG127-50D commercial module. Each fuel was tested with a view to determine whether it could generate adequate heat energy for efficient thermoelectric conversion. The heat-sink and blower fan cooling system was chosen for these tests because of its efficient cooling. A summary of the test is given in Table 6.4.

Table 6.3. Summary of the TEG127-50D tests with different fuels.

	HEAT SOURCES			
	GEL FUEL	**ELECTRICITY**	**LP GAS**	**BIOMASS**
TESTING LOCATION	Laboratory	Laboratory	Laboratory	Laboratory
FUEL	Greenheat gel fuel	Electricity to heat an electric cooker plate	Liquid petroleum gas	Wattle Wood
CALORIFIC VALUE	16.1 MJ/kg	N/A	46.3 MJ/kg	19 MJ/kg
MODULE MODEL	TEG127-50D	TEG127-50D	TEG127-50D	TEG127-50D
MODULE TYPE	Non-industrial	Non-industrial	Non-industrial	Non-industrial
MODULE CONNECTION	4-stage series	4-stage series	4-stage series	4-stage series
COOLING CONFIGURATION	Heat-sink and blower fan combination	Heat-sink and blower fan combination	Heat-sink and blower fan combination	Heat-sink and blower fan combination
MAXIMUM VOLTAGE	2.23VDC (cf. Chapter 4, Table 4.6)	7.55VDC (cf. Chapter 4, Table 4.5)	9.65VDC (cf. Chapter 4, Table 4.7)	12.16VDC (cf. Chapter 4, Table 4.8)
MAXIMUM CURRENT	1.759A (cf. Chapter 4, Table 4.6)	3.069A (cf. Chapter 4, Table 4.5)	3.069A (cf. Chapter 4, Table 4.7)	3.069A (cf. Chapter 4, Table 4.8)
SURROUNDING TEMPERATURE	25 ºC	25 ºC	25 ºC	25 ºC
MAXIMUM MODULE HOT-SIDE TEMPERATURE	108.3ºC (cf. Chapter 4, Table 4.6)	205.0 ºC (cf. Chapter 4, Table 4.5)	340.8 ºC (cf. Chapter 4, Table 4.7)	232.1 ºC (cf. Chapter 4, Table 4.8)
TEMPERATURE CHANGE	54.6 ºC (cf. Chapter 4, Table 4.6)	102.9 ºC (cf. Chapter 4, Table 4.5)	260.5 ºC (cf. Chapter 4, Table 4.7)	183.7 ºC (cf. Chapter 4, Table 4.8)
MAXIMUM POWER	3.92W	23.17W	29.62W	37.32W

6.4.1 Analysis and Discussion

Gel fuel:

This fuel produced 3.92W. The maximum temperature generated by the combustion of gel fuel was 108.3ºC, with a calorific value of 16.1 MJ/kg (Lloyd and Visagie, April 2014). This temperature was not able to produce sufficient heat energy for thermoelectric conversion by the modules. The calorific value of gel fuel is greater than that of biomass, but its cost offsets this benefit.

Electricity:

Electric energy provided constant and sufficient heat energy for thermoelectric conversion by the modules. The modules generated an operable amount of power at 23.17W. However, this source of energy is not recommended, as the intention of the study is to develop an alternate energy source.

LPG fuel:

LPG fuel provided a constant and sufficient amount of heat energy for thermoelectric conversion by the modules. LPG generated the highest amount of heat energy during the combustion process. This can be attributed to its high calorific value of 46.3 MJ/kg (www.biomassenergycentre.org.uk, Accessed April 2014) which contributed to the module's high power output. Although LPG is an excellent source for heat energy, the advantage that it offers is offset by its relatively high cost when compared to biomass.

Biomass fuel:

Wattle wood fuel produced the greatest amount of power during our tests. These excellent results can be attributed to the high calorific value (19 MJ/kg) of the biomass used in the tests (www.biomassenergycentre.org.uk, Accessed April 2014). Biomass is inexpensive and yields excellent power when used in conjunction with the TEG modules.

6.5 PERFORMANCE OF A COMMERCIAL TEG VERSUS THAT OF THE PROTOTYPE 'COLLAR' UNIT

In this section we compared the performance of the prototype commercial TEG unit to that of an industrial TEG unit. Both these devices were connected to a collar and then applied to a steam pipe in the boiler environment at a sugar mill. The tests with the so-called 'collar-unit' were described in Chapter 5. The main difference between the industrial TEG module and a commercial TEG device is its high temperature handling capacity. Improvements in temperature handling capacity is due to the RTV silicone layer which the industrial module is coated with. The test conditions and results are summarised in Table 6.4.

Table 6.4. Commercial TEG versus Industrial TEG 'collar units'.

	COMMERCIAL TEG UNIT				**PROTOTYPE TEG 'COLLAR' UNIT**			
TESTING LOCATION	Workshop		Boiler room		Workshop		Boiler room	
HEAT SOURCE	LPG		'Live' high pressure steam		LPG		'Live' high pressure steam	
MODULE MODEL	TEG127-50D		TEG127-50D		TEG1B 12610-5.1		TEG1B 12610-5.1	
MODULE TYPE	Commercial		Commercial		Industrial		Industrial	
MODULE CONNECTION	4-stage series		4-stage series		4-stage series		4-stage series	
COOLING CONFIGURATION	Heat-sink & blower fan		Heat-sink & blower fan		Heat-sink & compressed air		Heat-sink & compressed air	
MAXIMUM VOLTAGE	9.65VDC (cf. Chapter 4, Table 4.7)		*8.34VDC (Very unstable)* (cf. Chapter 5, Table 5.1)		13VDC (cf. Chapter 5, Table 5.5)		12.95VDC (cf. Chapter 5, Table 5.6)	
MAXIMUM CURRENT	3.069A (cf. Chapter 4, Table 4.7)	Rated per module: 2.15A (Cf. Chapter3, Table 3.1	*1.459A (Very unstable)* (cf. Chapter 5, Table 5.1)	Rated per module: 2.15A (Cf. Chapter3, Table 3.1	2.11A (cf. Chapter 5, Table 5.5)	Rated per module: 2.0A (cf. Chapter 5, Table 5.4)	2.01A (cf. Chapter 5, Table 5.6)	Rated per module: 2.0A (cf. Chapter 5, Table 5.4)
SURROUNDING TEMPERATURE	24ºC		62 ºC		24ºC		60ºC	
MAXIMUM MODULE HOT-SIDE TEMPERATURE	340.8 ºC (cf. Chapter 4, Table 4.7)		209.0ºC (cf. Chapter 5, Table 5.1)		206.9 ºC (cf. Chapter 5, Table 5.5)		154.7ºC (cf. Chapter 5, Table 5.6)	
MAXIMUM MODULE DELTA TEMPERATURE	260.5 ºC (cf. Chapter 4, Table 4.7)		121.0 ºC (cf. Chapter 5, Table 5.1)		117.8 ºC (cf. Chapter 5, Table 5.6)		77.5 ºC (cf. Chapter 5, Table 5.6)	
MAXIMUM POWER	29.62W		12.17W		27.43W		26.03W	

6.5.1 Analysis and Discussion

TEG unit:

The TEG units output was stable within a controlled environment (cf. Chapter 4, Table 4.7). The non-industrial modules generated sufficient power within the lower ambient temperature environment of the workshop. The device's output was unstable in the boiler-room due to the high ambient temperature present in this environment. An unstable output in the boiler-room is due to the high ambient temperatures which reduced the efficacy of the cooling system.

The prototype TEG 'collar' unit:

The 'collar' units output was stable in both environments. The cooling system consisting of the aluminium heat sink collars and compressed air proved to be efficient when the device operated in the harsh temperature environment of an industrial boiler room. The industrial modules generated its maximum power output and matched the manufacturer's specifications (cf. Appendix A).

6.6 CONCLUSION

The analysis provides the following valuable insight into the requirements for efficient thermo-electricity generation, namely:

i. *Thermoelectric module type:* Industrial and non-industrial TEG modules provide best performance under different operating conditions.

ii. *Cooling system:* An efficient cooling system for a TEG module is vital for maintaining a stable temperature gradient across the device's hot and cold junctions. Under these conditions the device will yield optimal or near-optimal performance, depending on the configuration used.

iii. *Module configuration:* The amount of power generated by a TEG device is also dependent on how the modules are configured (either as single stage units, 2-stage units or 4-stage (cf. Table 6.2)).

iv. *Heat source:* The fuel burnt to generate the heat also has an impact on the amount of power delivered by a TEG module. TEG industrial modules have a greater heat tolerance than their non-commercial counterparts.

With sufficient cooling and a proper configuration, the TEG device will provide an excellent initiative for harvesting energy that would otherwise have been wasted.

Traditional renewable energy sources such as solar and wind only supply a minute quantity of the South Africa's energy demand. Research into the feasibility of investing capital into other alternate energy sources such as hydro, geothermal and tidal energy sources is ongoing. The South African government, through the Department of Science and Technology, also provides seed funding for projects of this nature. Most of the research and applications of thermo-electric energy is currently in space science and medical science.

No great effort is being made to investigate the feasibility of using thermo-electric energy for low power industrial applications. The efficiency of thermoelectric conversion is significantly low compared to the relatively high cost, therefore it has mainly been used for deep space satellites and remote power generation for units where the application outweighs the cost (Yazawa and Shakouri, 2011, Yee *et al.*, 2013).

The positive aspect of harvesting waste heat from industrial applications is that the heat source fuel is 'free', unlike many conventional methods of electricity generation were the major cost is attributed to the fuel. The energy conversion efficiency of modern thermoelectric generators is much lower than that of conventional mechanical engines. However, thermo-electric devices do have considerable potential because they provide us with a simple means of recovering energy that would otherwise be wasted (Yazawa and Shakouri, 2011). Thermoelectric costing is divided into three areas:

1. *The heat source:* The waste heat emitted from industrial applications that would be otherwise lost to the environment. These waste heat sources are free.

2. *The conversion from heat energy to electric energy:* An industrial thermoelectric module TEG1B 12610-5.1 was used for this application. The financial cost of the industrial modules is relatively high due to the nature of the materials and the specialization of the process.

3. *The cooling system:* The cooling of the industrial thermoelectric modules TEG1B 12610-5.1 was achieved using a heat sink and compressor air combination. The cost of aluminium heat-sinks are expensive due to the demand for alloy materials in industrially manufacturing.

With such huge potential, it is not surprising that there is also significant interest in finding cost-effective technologies for generating electricity from waste heat. The cost-efficiency trade-off for thermoelectric power generation is improving steadily with advancements in technology (Yazawa and Shakouri, 2011). The cost of implementing a thermoelectric generation unit into an industry

site is relatively minute compared to the benefits of recycling waste heat that would otherwise be vented into the atmosphere.

REFERENCE

[1] S. B Riffat and X Ma. (2002, Dec.). "Thermoelectrics: A review of present and potential applications." *Institute of Building Technology, School of Built Environment*. [On-line]. 23(1), pp. 913-935. Available: www.sciencedirect.com [Jan. 20, 2013].

[2] W. V Slaton and J.C.H Zeegers. (2005, Oct.). "Thermoelectric power generation in a thermoacoustic refrigerator." *Applied Acoustic*. [On-line]. 67, pp.450-460. Available:www.sciencedirect.com [Jan. 21, 2013].

[3] D. M Rowe. (1999). "Thermoelectrics, An Environmentally-Friendly Source of Electrical Power." *Renewable Energy*. [On-line]. 16(1), pp. 1251-1256. Available: www.sciencedirect.com [Jan. 25, 2013].

[4] G. Min and D.M Rowe. (2002)." Symbiotic application of thermoelectric conversion for fluid preheating/power generation." *Energy conversion and management*. [On-line]. 43(1), pp. 221-228. Available: www.sciencedirect.com [Jan. 30, 2013].

[5] G. Westcott, M. Tacke, N. Schoeman, and N. Morgan. (2007, May). "Impala Platinum Smelter, Rustenburg- an integrated smelter off-gas treatment solution." *The Journal of The Southern African Institute of Mining and Metallurgy*. [On-line]. 107, pp. 281-288 Available: www.saimm.co.za/Journal/v107n05p281.pdf [Jan. 30, 2014].

[6] E. J Bruke and R. J Buist. (1984). "Thermoelectric coolers as power generators." *Marlow Industries Inc. Dallas, Texas*. [On-line]. 17(3), pp. 91-94. Available: www.prog-paradisaea.com/IMG/pdf/reference_4_TE_technology.pdf [Feb. 18, 2013].

[7] D. T Allen, A. S Kushch and J.C Bass. (2003, March). "Thermoelectric Generation for Self-Powered Appliances." *International Appliance Technical Conference*. [On-line]. pp. 1-17. Available: www.hi-z.com [Feb. 19, 2013].

[8] D. M Rowe and G. Min. (1998, June). "Evaluation of thermoelectric modules for power generation." *Journal of power sources*. [On-line]. 73(2), pp. 193-198. Available: www.sciencedirect.com [March 05, 2013].

[9] J. B Fourier. (1955). "Theorieanalytique de la chaleur." *Dover Publications*. [On-line]. pp. 190. Available: http://books.google.co.za/books [March 10, 2013].

[10] J. Sergent and A. Krum. (1998). "Thermal management handbook for electronic assemblies." (1st Edition). [On-line]. (1), pp. 2-9 Available: www.sciencedirect.com [June 07, 2013].

[11] T. Kordyban. (1998). "Hot air rises and heat-sinks – Everything you know about cooling electronics is wrong." (1st Edition). [On-line]. (1), pp. 39. Available: www.asme.org/products/books/hot-air-rises-heat-sinks-everything-know-cooling, [Dec. 15, 2012].

[12] E. Walsh and R. Grimes. (2007, May). "Low profile fan and heat-sink thermal management solutions for portable applications." *International Journal of Thermal Sciences*. [On-line]. 46, pp. 1181-1190. Available: www.sciencedirect.com [Dec. 12, 2012].

[13] G. Destouni and H. Frank. (2010). "Renewable Energy." *Royal Swedish Academy of Sciences.* [On-line]. 39, pp.18-21. Available: www.ncbi.nlm.nih.gov/pubmed/20873681 [June 15, 2013].

[14] C-T Hsu, G-Y Huang, H-S Chu, B Yu and D-J Yao. (2011, Dec.). "An effective Seebeck coefficient obtained by experimental results of a thermoelectric generator module." *Applied Energy*. [On-line]. 88(12), pp. 5173–5179. Available: www.sciencedirect.com [Jan. 19, 2013].

[15] C-T Hsu, G-Y Huang, H-C Chu, B Yu and D-J Yao. (2010, Oct.). "Experiments and simulations on low-temperature waste heat harvesting system by thermoelectric power generators." *Applied Energy*. [On-line]. 88, pp.1291-1297 Available: www.sciencedirect.com [Jan. 26, 2013].

[16] Tellurex. "Frequently Asked Questions about Our Cooling and Heat Technology." Internet: www.tellurex.com/archive.today/c6Kv7, Jan. 5, 2013 [Jan. 13, 2014].

[17] G. Min and D. M Rowe. (1999, May)."Improved model for calculating the coefficient of performance of a Peltier module." *Energy Conversion and Management*. [On-line]. 41, pp. 163-171. Available: www.sciencedirect.com [Jan. 20, 2013].

[18] G. Donev, G.J.H.M Wilfried van Sark, K. Blok, O. Dintchev. (2012, June)."Solar water heating potential in South Africa in dynamic energy market conditions." *Renewable and Sustainable Energy Reviews.* [On-line]. 16(5), pp. 3002-3013. Available: www.sciencedirect.com [Jan. 11, 2014].

[19] Eskom. "Generating Electricity." Internet: www.eskom.co.za/AboutElectricity/ElectricityTechnologies/Pages/Generating_Electricity, Jan. 20, 2013 [Jan. 29, 2014].

[20] L. Wessa. "Renewable Solutions & Reduced Demand." Internet: www.wessa.org.za/focus-areas/energy.htm, April, 2013[Jan. 13, 2014].

[21] M. H Elsheikh, D. A Shnawah, M.F.M Sabri, S.B.M Said, M. H Hassan, M.B.A Bashir and M. Mohamad. (2013, Nov.). "A review on thermoelectric renewable energy: Principle

parameters that affect their performance." *Renewable and Sustainable Energy Reviews*. [On-line]. 30, pp. 337-355. Available: www.sciencedirect.com [June 21, 2014].

[22] M. Edkins, A. Marquard and H. Winkler. (2010, June). "South Africa's renewable energy policy roadmaps." *Energy Research Centre*. [On-line]. (1), pp. 1-48 Available: www.webdav.uct.ac.za/depts/erc/Research/publications/10Edkinesetal-Renewables_roadmaps.pdf [Feb. 19, 2014].

[23] J. R Welty, C. E Wicks, R. E Wilson, and G. L Rorrer. (2008). "Fundamentals of Momentum, Heat and Mass Transfer." (5th Edition). [On-line]. pp. 291-231.Available: http://www.sciencedirect.com [Jan. 24, 2014].

[24] K. Qiu and ACS Hayden. (2008). "Development of a thermoelectric self-powered residential heating system." *Journal of Power Sources*. [On-line]. 180(2), pp. 884–889. Available: www.sciencedirect.com [March 02, 2013].

[25] N. Magasiner. (1966, March). "Boiler design and selection in the cane sugar industry." *Proceedings of The South African Sugar Technologists.* Internet: www.sasta.co.za/wpcontent/uploads/Proceedings/1960s/1966_Magasiner_Boiler%20Design%20And%20Selection.pdf [Jan. 20, 2014].

[26] S Maharaj and P Govender. "A Seebeck System for Wasted Electrical Energy Harvesting." ICCBN, 2013, pp. 534-554.

[27] Everredtronics. "Technical Information." Internet: www.everredtronics.com/EN/TEM/tech.html, Jan., 2013 [Jan. 12, 2014].

[28] Laird Technologies (2010, Jan.). *Thermoelectric Handbook.* (2nd Edition). [On-line]. Available: www.lairdtech.com [Jan. 12, 2014].

[29] PJD Lloyd and E.F Visagie. (2009). "The Testing of Gel Fuels and their comparison to alternative cooking fuels." *Energy Research Centre.* [Online]. 1, pp. 1-6 Available: www.erc.uct.ac.za/Research/publications/07Lloyd%20Visagie%20fuels.pdf [June 17, 2013].

[30] E. Barrett. "Greenheat." Internet: www.Greenheat.co.za, January, 2013 [Jan. 23, 2014].

[31] W. Moser, G. Friedl, and W. Haslinger. (2006, Aug.). "Small-scale pellet boiler with thermoelectic generator." *Bioenergy*. [On-line]. 1(25), pp. 349-353. Available: www.ieeexplore.ieee.org [March 14, 2013].

[32] V. K Pantangi, S. C Mishra, P. Muthukumar and R. Reddy. (2011, Aug.). "Studies on porous radiant burners for LPG (liquefied petroleum gas) cooking Applications." *Energy.* [On-line]. 36(10), pp. 6074-6080. Available: www.sciencedirect.com, [April 28, 2013].

[33] N. Mohlakoana and W. Annecke. (2009, Nov.). "The use of liquefied petroleum gas by South African low income urban households: A case study1." *Journal of Energy in Southern Africa*. [On-line]. 20(4), pp. 1-6 Available: www.erc.uct.ac.za/jesa/volume20/20-4jesa-mohlakoana.pdf, [April 27, 2013].

[34] S. Maharaj and P. Govender. "A Prototype Thermoelectric Co-generation Unit," *Domestic Usage of Energy*, 2014, pp. 197-202.

[35] T. Hendricks and W. T Choate. "Engineering Scoping Study of Thermoelectric Generator Systems for Industrial Waste Heat Recovery." Internet: www1.eere.energy.gov/manufacturing/industries_technologies/imf/pdfs/teg_final_report_13.pdf Nov., 2006 [Jan. 17, 2013].

[36] X. Gou, H. Xiao and S. Yang. (2010, Oct.). "Modeling, experimental study and optimization on low-temperature waste heat thermoelectric generator system." *Applied Energy*. [On-line]. 87(10), pp. 3131-3136 Available: www.sciencedirect.com/science/article [Jan. 27, 2014].

[37] Tetechnology. "FAQ's and Technical Information." Internet: www.tetech.com, Jan. 01, 2011 [Jan. 27, 2014].

[38] Tecteg MFR. "How Thermoelectric TEG Generators Work." Internet: www.tecteg.com/wp-content/uploads/2014/09/1, Oct. 28, 2013 [April 24, 2014].

[39] Current Automation. "Current Automation Power Solution Providers." Internet: www.rectifier.co.za/Batteries/ROYAL/Royal%20spec%20sheets/1150K.pdf, Jan, 2013 [March 02, 2014].

[40] Title 18: Conservation of Power and Water Resources; Part 292—Regulations under Sections 201 and 210 of the Public Utility Regulatory Policies Act of 1978; Subpart A – General Provisions, 292.101 Definitions.

[41] Dr. A.C Thekdi. "Waste Heat Management Options Industrial Process Heating Systems." Internet: www.northwestchptap.org/NwChpDocs/WasteHeatManagementOptions_Thekdi.pdf, Aug. 20, 2009 [Feb. 18, 2014].

[42] Implats Sustainable Development Report 2009. "Smelter upgrade-addressing improved air quality." Internet: www.implats.co.za, Jan., 2009 [April 23, 2014].

[43] Gas Cleaning Technologies. "Electric Smelting Furnace Off-Gas System Design." Internet:www.gcteng.com/marketing/electric-smelting-furnace-off-gas-system-design, Jan. 2, 2014 [April 23, 2014].

[44] R. Viskanta. (1963, Nov.). "Interaction of Heat Transfer by Conduction, Convection, and Radiation in a Radiating Fluid." *Heat Transfer*. [On-line]. 85(4), 318-328 Available: www.heattransfer.asmedigitalcollection.asme.org/article.aspx?articleid=1432979 [Jan. 30, 2014].

[45] C. Li, M. Zhang, L. Miao, J. Zhou, Y Pu Kang, C.A.J Fisher, K. Ohno, Y. Shen and H. Lin. (2014, July). "Effects of environmental factors on the conversion efficiency of solar thermoelectric co-generators comprising parabola trough collectors and thermoelectric modules without evacuated tubular collector." *Energy conversion and management.* [On-line]. 85, pp. 944-951. Available: www.sciencedirect.com, [June 18, 2015].

[46] S. O Tan and H. Demirel. (2015, July). "Performance and cooling efficiency of thermoelectric modules on server central processing unit and Northbridge." *Computers and Electrical Engineering.* [On-line]. Vol. 46, pp. 46-55. Available: www.sciencedirect.com, [Nov. 15, 2015].

[47] M. Jaworski, M. Bednarczyk and M. Czachor. (2015, December). "Experimental investigation of thermoelectric generator (TEG) with PCM module." *Applied Thermal Energy*. [On-line]. Vol. 96, pp. 527-533. Available: www.sciencedirect.com, [Jan. 13, 2016].

[48] J. Chen, J. Yu and M. Ma. (2015, April). "Theoretical study on an integrated two-stage cascade thermoelectric module operating with dual power sources." *Energy conversion and management*. [On-line]. 98, pp. 28-33. Available: www.sciencedirect.com, [Dec. 16, 2015].

[49] F. D Rosi. (1968, Aug.). "Thermoelectricity and thermoelectric power generation." *Solid State Electronics.* [On-line] Vol. 11, Issue 9, pp. 833-868. Available: www.sciencedirect.com [Accessed: January 18, 2015].

[50] K. Yazawa and A. Shakouri (2011, July). "Cost-Efficiency Trade-off and the Design of Thermoelectric Power Generators." *Environmental Science and Technology*. [On-line]. 45(17), pp. 7548-53. Available: www.researchgate.net/publication/51525223_Cost-Efficiency_Trade-off_and_the_Design_of_Thermoelectric_Power_Generators [Jan. 20, 2016].

[51] S. K. Yee, S. LeBlanc, K. E Goodsonb and C. Dames. (2013, June). "$ per W metrics for thermoelectric power generation: beyond ZT." *Energy and Environment Science*. [Online]. 6, pp. 2561–2571. Available: www.pubs.rsc.org/en/content/articlelanding/2013/ee/c3ee41504j#!divAbstract, [Jan. 20, 2016].

APPENDIX A

Manufacturer's specifications for the TEG1B 12610-5.1 industrial module

(www.everredtronics.com, Accessed Jan. 2014)

- Hot Side Temperature - 320ºC
- Cold Side Temperature - 30ºC
- Open Circuit Voltage - 7.2V
- Matched Load Resistance - 1.8Ω
- Matched load output voltage - 3.6V
- Matched load output current - 2.0A
- Matched load output power - 7.1W
- Heat flow across the module - 148W
- Heat flow density - $9.2Wcm^{-2}$
- AC Resistance, Measured under 27ºC @1000HZ - 0.8-1.0Ω

APPENDIX B

SPECIFICATIONS FOR THE BUCK BOOST CONVERTER

Input Voltage: DC 7 ~ 30 V (input Change, Output not Change)

Output Voltage: DC 2 ~ 16 V (auto Buck & Boost; Input change, output constant voltage, adjustable)

Output Current: 0.5~6A (adjustable, Constant current)

Maximum Power: 80W Natural cooling

Efficiency: 94 % (high output voltage, high efficiency)

Module Properties: Non-isolated step-down/UP module (BUCK & BOOST, CC & CV)

Full Load temperature rise: 40 â„ƒ

No load current: 45 mA

Output ripple: 20M bandwidth, 20mV

Load Regulation: ± 2%

Voltage Regulation rate: ± 0.5%

Dynamic response speed: 5% 200uS

Short-circuit Protection: YES, Output current limit protection

Input voltage Protection: 7.7V

Indicator: Yes, the work of normal (Green), the work is extremely or protection (RED)

Input Reverse Protection: YES

Operating Temperature: Industrial (-40 â„ƒ to +85 â„ƒ)

Size: 72 x 42 x 23 mm (L*W*H Installation location: 90mm)

APPENDIX C

WIRING LAYOUT OF THE TEG UNIT WITH A 4-STAGE CONNECTION

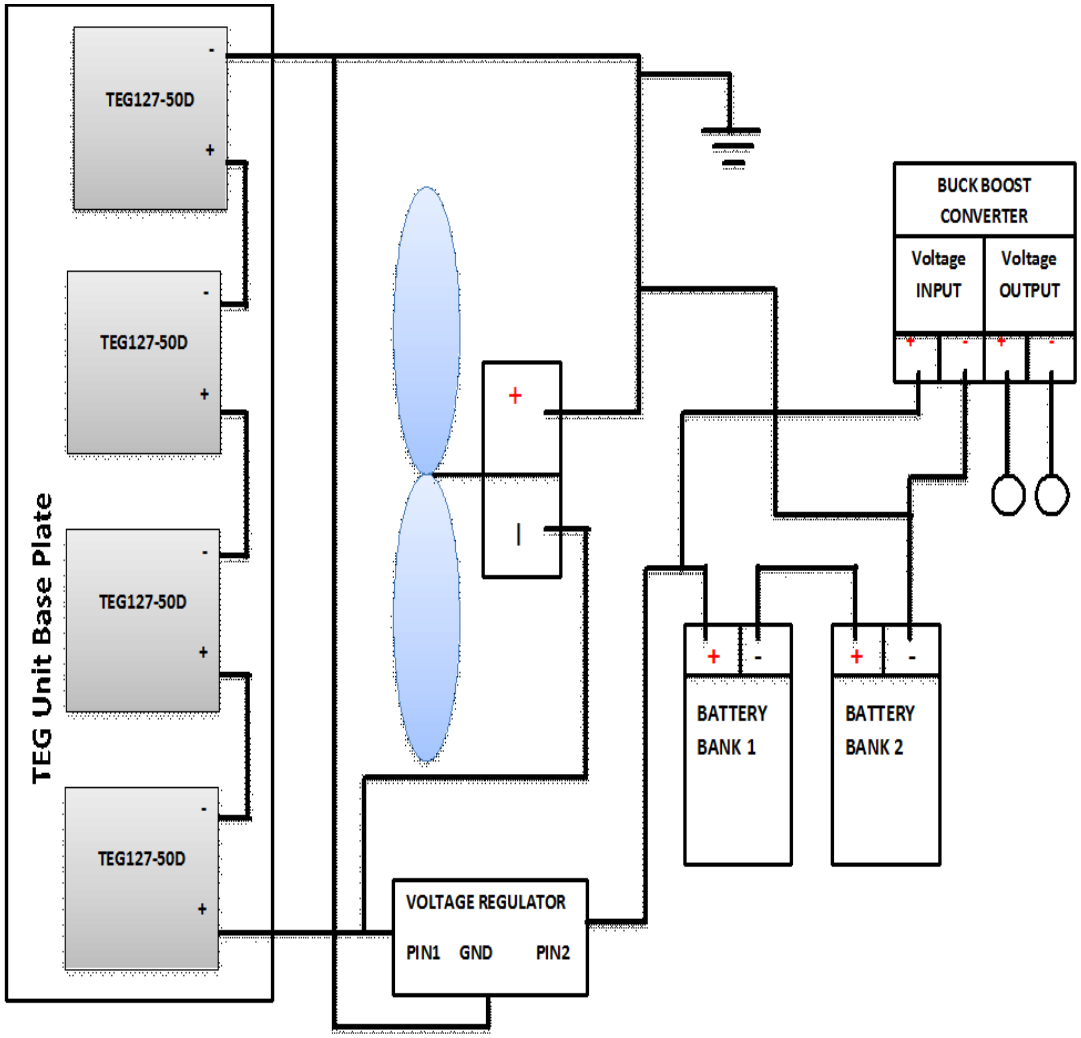

APPENDIX D

PROTOTYPE TEG COLLAR UNIT FRONT VIEW